EANDC(UK) 80 'S'

AERE - PR/NP 10

INDC(UK)*017/R

INDC - 142

AERE - PR/NP 10

UNCLASSIFIED

(Approved for Publication)

Much of the information in this document is intended for publication in a journal and it is made available on the understanding that extracts or references will not be published, prior to the publication of the original, without the consent of the author. Some of the information is of a preliminary nature and should be treated with caution; it must not be quoted in publications nor listed in data compilations.

E MINIMIS MAXIMA

United Kingdom Atomic Energy Authority

RESEARCH GROUP

NUCLEAR PHYSICS DIVISION PROGRESS REPORT

For the period 1st November 1965 to 30th April 1966

Editors: D. L. ALLAN C. F. COLEMAN

Nuclear Physics Division,

Atomic Energy Research Establishment,

Harwell, Berkshire.

1966

000147

U.D.C.
047.1:539.1
539.1

UNCLASSIFIED
(Approved for Publication)

AERE - PR/NP10

N U C L E A R   P H Y S I C S   D I V I S I O N

P R O G R E S S   R E P O R T

For the period 1st November 1965 to 30th April 1966

Editors: D. L. ALLAN
C. F. COLEMAN

Nuclear Physics,
U.K.A.E.A. Research Group,
Atomic Energy Research Establishment,
HARWELL.

September, 1966.

/HMB

HL 66/4706 (C 17)

CONTENTS

Project No.		Page No.
	Fellows, Temporary Research Associates and Attached Staff in Nuclear Physics Division	(v)
	List of Groups in Nuclear Physics Division	(vi)
2/5/50	NUCLEAR DATA FOR FAST REACTORS	1
	Elastic and inelastic neutron scattering from ^{239}Pu	1
4	GENERAL REACTOR TECHNOLOGIES AND STUDIES	1
	4/11 GENERAL NUCLEAR DATA FOR REACTORS - I	1
	Fission cross section measurements:	1
	I - ^{239}Pu (a) Assessment of error	1
	(b) Fluctuation analysis	2
	(c) Multi-level resonance analysis	3
	II - ^{241}Pu	4
	III - ^{235}U	4
	Total neutron cross section measurements:	5
	I - ^{93}Nb	5
	II - ^{10}B	7
	4/11 GENERAL NUCLEAR DATA FOR REACTORS - II	7
	Fission cross section measurements:	7
	Studies of the p-wave neutron strength function	8
	Neutron cross sections of ^{107}Ag and ^{109}Ag	9
	Neutron scattering measurements on ^{239}Pu	9
	The measurement of alpha, eta and the fission cross sections of ^{239}Pu	11
	Determination of ^{240}Pu resonance parameters	11
	Total cross section measurements on Ba isotopes	11
	PDP-4 data processor	12
	4/12 INTEGRAL DATA MEASUREMENTS	13
	The two blocks experiment	13
	Neutron spectra in heavy water/ordinary water mixtures	16
	Spectra in poisoned D_2O using a neutron chopper	17
	Time dependent neutron spectra in water	18
	Measurements of fast neutron spectra in materials	20
	Calibration of detectors for fast neutron spectra measurements	22
8	FUNDAMENTAL AND BASIC RESEARCH	23
	8/28 NUCLEAR STRUCTURE AND DYNAMICS	23
	PULSED VAN DE GRAAFF ACCELERATOR (IBIS)	23
	Studies of various (^{3}He,n) reactions	23
	The (^{3}He,n) reaction on ^{17}O and ^{18}O	24
	5 MV VAN DE GRAAFF GENERATOR	25
	The channelling of ions in single crystals	25
	Isobaric spin mixing and the decay of analogue resonances	27

CONTENTS (cont'd)

Project No.		Page No.
	Decay of the 2^-, 3^- analogue states in ^{90}Zr to $^{89}Zr_{g.s.}(9/2^+)$ and $^{89}Zr_{1st\ exc.}(1/2^-)$ states via the (p,n) reaction	28
	12 MeV TANDEM GENERATOR	28
	Experiments relating to pure Fermi decays and theories of weak interactions	28
	I - ft value for the decay $^{10}C(\beta^+)^{10}B^{**}$	28
	II - The threshold for the reaction $^{14}N(p,n)^{14}O$	29
	III - The ft value for the decay $^{35}Ar(\beta^+)^{35}Cl$	29
	Accurate measurement of the relative efficiency of Ge(Li) detectors	29
	A study of isobaric analogue states in ^{121}Sb	30
	Decay of isobaric analogue states to highly excited states of ^{118}Sn	31
	Isobaric analogue states observed in the $^{90}Zr(p,p')^{90}Zr$ reaction	33
	$^{56}Fe(d,d')^{56}Fe$ reaction at $E_d = 11.5$ MeV	34
	DWBA calculations and the 3.12 MeV state in ^{60}Ni	34
	Nuclear lifetimes by the Doppler shift attenuation method	35
	Energy loss of heavy ions in matter	35
	45 MeV ELECTRON LINEAR ACCELERATOR	37
	Energy spectra of photoneutrons from heavy nuclei	37
	50 MeV PROTON LINEAR ACCELERATOR (S.R.C.)	39
	Analysis of data from the (p,d) reaction on the even isotopes of tin	39
	I - Occupation numbers in the d-shell	39
	II - D.W.B.A. calculations	40
	Optical model research programme: elastic scattering of 30 MeV protons	42
	SYNCHROCYCLOTRON	42
	Measurement of C_{NN} for p-p scattering at 143, 98 and 73 MeV using a polarized target	42
	Radiation damage phenomena in polarized targets	43
	Polarization and differential cross sections in p-p scattering at 98 MeV	43
	Neutron yield from high energy proton and deuteron bombardment of lead	44
	NIMROD EXPERIMENTS	45
	Investigation of the decay of the f^o-meson	45
	The decay of long lived neutral K-mesons (K^o_L) into two neutral pions	45
8/2	MISCELLANEOUS STUDIES IN PHYSICS	46
	Mössbauer effect:	46
	I - The study of Fe Si alloys	46
8/28	II - The study of absorbers with ultrasonic vibration	46
	III - Hyperfine field of ^{57}Fe in hemin	46

CONTENTS (cont'd)

Project No.		Page No.
	Radio pulses associated with extensive cosmic-ray showers	47
	A cooled image intensifier system for astronomical spectroscopy	48
	Cherenkov radiation in the atmosphere: U.V. experiments	49
	Absorption of high-energy γ-rays in interstellar and intergalactic space	49
	MISCELLANEOUS TECHNIQUES	49
	The preparation of lithium-drifted germanium detectors	49
	The preparation of silicon surface-barrier detectors	50
	Ion implantation in semiconductors	50
	ACCELERATOR OPERATION AND MAINTENANCE	51
4/11	Cockcroft-Walton 0.5 MV generator	51
2/5	3 MeV pulsed Van de Graaff accelerator (IBIS)	51
4/11	5 MV Van de Graaff generator	52
8/28	12 MeV tandem generator	52
3/11	45 MeV electron linear accelerator	52
8/28	Synchrocyclotron	53
8/28	Synchrocyclotron improvement project	54
	REPORTS, PUBLICATIONS AND CONFERENCE PAPERS	60

Fellows, Temporary Research Associates and Attached Staff In Nuclear Physics Division

From 1st November 1965 - 30th April 1966

Dr. A. Asami	Attached	Japan Atomic Energy Research Institute, Tokai-Mura.
Dr. M. Asghar	Attached	Department of Nuclear Physics, Oxford University.
Prof. S. W. Barnes	T.R.A.	
Dr. I. M. Blair	Fellow	
Dr. W. N. Charman	Fellow	
P. J. Clements	Attached	Oxford University.
Dr. W. M. Currie	Fellow	
K. Gul	Attached	Oxford University.
A. V. Hewitt	Attached	Oxford University.
Dr. A. P. Jain	T.R.A.	
Dr. J. G. Jenkin	Fellow	
Dr. R. K. Jolly	Fellow	
Dr. C. H. Johnson	Attached	Oak Ridge National Laboratory.
Dr. B. T. Lawergren	Fellow	
Dr. D. B. McConnell	Fellow	
Dr. I. V. Mitchell	Fellow	
C. M. Newstead	Attached	Department of Nuclear Physics, Oxford University.
Dr. B. H. Patrick	Fellow	
Dr. R. S. Preston	T.R.A.	
Mrs. S. Ramavataram	T.R.A.	
P. T. O. Reivari	Attached	Institute of Technology, Helsinki, Finland.
Dr. A. K. Sen Gupta	T.R.A.	
Dr. R. B. Taylor	Fellow	
Dr. R. E. Van de Vivjer	Attached	Natuurkundig Laboratorium der Rijkuniversiteit, Ghent, Belgium.
Dr. R. B. Weinberg	Attached	Columbia University, U.S.A.
Dr. C. D. West	Fellow	
M. Wigan	Attached	Physics Department, Oxford University.
Dr. P. Wydler	Attached	Eidg. Institut für Reaktorforschung, Würenlingen, Switzerland.

NUCLEAR PHYSICS DIVISION

Division Head: Dr. E. Bretscher

Groups

Neutron Spectra and Nuclear Physics - I

Dr. M. J. Poole

Nuclear Physics - II and Nuclear Photo-effect

Dr. E. R. Rae
Mr. N. J. Pattenden
(acting group leader)

Tandem Generator

Dr. Joan M. Freeman

5 MV Electrostatic Generator and Cockcroft-Walton HT set

Dr. G. A. Jones

IBIS (3 MeV) pulsed Van de Graaff

Dr. A. T. G. Ferguson

Charged Particle Spectrograph

Mr. D. L. Allan

Proton Physics (50 MeV P.L.A.)

Dr. P. E. Cavanagh

Synchrocyclotron

Dr. B. Rose

High Energy Physics

Dr. W. Galbraith

Mossbauer Effect

Dr. T. E. Cranshaw

Scientific Assistants Training School

Mr. J. G. Robins

NUCLEAR DATA FOR FAST REACTORS

(IBIS 3 MeV pulsed Van de Graaff accelerator: A. T. G. Ferguson)

Elastic and inelastic neutron scattering from ^{239}Pu (D. A. Boyce, P. E. Cavanagh, C. F. Coleman, G. A. Gard, J. C. Kerr and J. F. Turner)

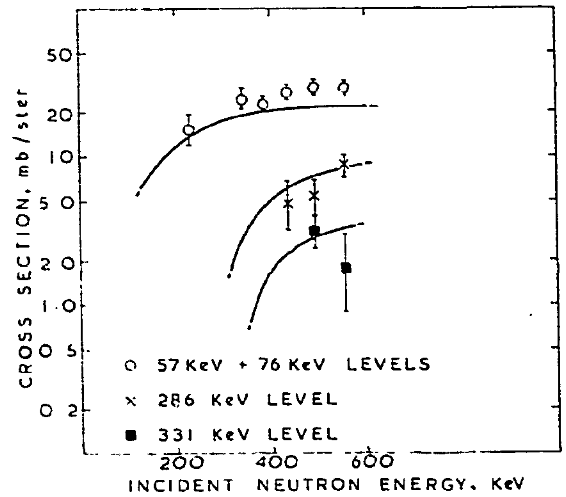

Fig. 1. Inelastic scattering of neutrons from ^{239}Pu; excitation curves for 90° differential scattering. Full lines are from the K.F.K. 120 compilation assuming isotropic scattering.

The observations at 90° of inelastic neutron scattering from ^{239}Pu reported earlier(1) have now been extended in incident neutron energy range up to 1.5 MeV. The data obtained on inelastic scattering are not yet fully analysed. The cross sections extracted so far are shown in Fig. 1 where they are compared with values obtained from the K.F.K. 120 compilation* on the assumption of isotropic angular distributions.

Measurements have also been made on the differential elastic scattering of neutrons from ^{239}Pu at roughly equal lethargy intervals over an energy range 100 keV to 1.5 MeV, in an angular range 20° to 130°. These results have not yet been analysed.

GENERAL REACTOR TECHNOLOGIES AND STUDIES

GENERAL NUCLEAR DATA FOR REACTORS - I

(Nuclear Physics - I: M. J. Poole)

Fission cross section measurements (G. D. James, D. A. J. Endacott)

I - The fission cross section of ^{239}Pu from 4 eV to 25 keV

(a) Assessment of error

Two independent measurements of the ^{239}Pu fission cross section, one made with a cadmium filter and the other with a B_4C filter, have been reported previously(2). The discrepancy between these measurements (2.5% on average), was greater than would be expected from the assigned internal error in each measurement (0.8%). A search for the cause of this discrepancy has shown that it is largely eliminated by computing a fission cross section from each experimental run (the cadmium results for instance comprise six such runs) and combining these cross sections to form a weighted mean. (The results from one experimental run were rejected because they were consistently low). After treating the data in this way, the average discrepancy between the results obtained with a cadmium filter and those obtained with a B_4C filter is reduced from 2.5% to 1.1%, a value consistent with the assigned (internal) error.

---

(1) Nuclear Physics Division Progress Report, AERE - PR/NP9, p.1 (1965).

(2) James G. D. Nuclear Physics Division Progress Report, AERE - PR/NP9, p.1 (1965).

*Tables of neutron cross sections for fast reactor materials published by the Kernforschungszentrum, Karlsruhe.

The greatest contribution to the absolute error in these data comes from the process of normalisation to the data of Bollinger et al[3]. By comparing the values of $\Sigma\sigma_f(E)\Delta E$ (where $\sigma_f(E)$ is the fission cross section averaged over an interval ΔE) over three energy ranges between 6 eV to 16.7 eV it is found that the ratio of the present data to the data of Bollinger et al. varies by 3.1% over this energy interval. This is taken as a measure of the error in normalisation and leads to a final error in the values of the fission cross section averaged over energy ranges E to 2E of 3.3%, comprising 3.1% from normalisation, 1.1% statistical error and 0.47% from the error in the thermal value of the fission cross section.

Having normalised our data to Bollinger's over the range from 6 eV to 16.7 eV, we now compare our cross sections with his over the remainder of the range. By using average values of the cross section over energy intervals E to 2E, the average value of the ratio of the present data to Bollinger's data over the energy range 64 eV to 32 keV was found to be 1.014 ± 0.035. The interval 8 keV to 16 keV was not used in calculating the ratio because it contains two high values of the cross section in Bollinger's data which were assumed to be wrong.

(b) Fluctuation analysis

An analysis of the ^{239}Pu fission cross section over the energy range 20 eV to 24 keV has been carried out, following the method described by Egelstaff[4] to determine the serial correlation coefficient r_k given by the equation

$$r_k(W) = \frac{\text{Cov.}[a_j(W);\ a_{j+k}(W)]}{[\text{Var.}a_j(W).\text{Var.}a_{j+k}(W)]^{1/2}} \qquad (1)$$

in which $a_j(W)$ is given by

$$a_j(W) = \int_{(j-1)W}^{jW} \left[\frac{\sigma_f(E)\sqrt{E}}{\langle\sigma_f(E)\sqrt{E}\rangle} - 1 \right] dE \qquad (2)$$

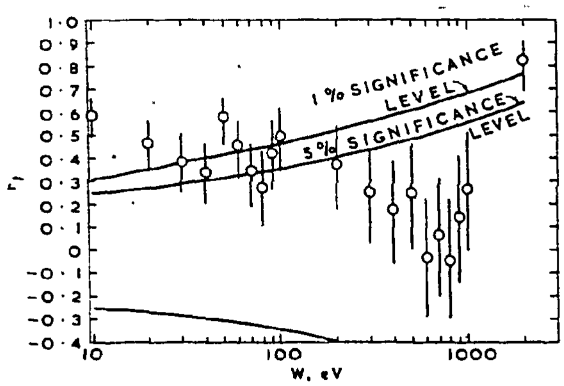

Fig. 2. Correlation coefficient plotted as a function of energy interval for the fission cross section of ^{239}Pu.

Here W is an energy interval over which the cross section is averaged before computing r_k and which has been given values ranging from 10 eV to 2 keV, $\sigma_f(E)$ is the fission cross section at neutron energy E. The upper energy limits used in calculating $r_k(W)$ were determined in such a way that no energy interval W contained less than five data points and varied from 670 eV for W = 10 eV (giving 63 values of $a_j(W)$) to 24 keV for W = 2 keV (giving 10 values of $a_j(W)$. The parameter k was varied from 1 up to half the number of values of $a_j(W)$ available. This analysis confirms the conclusions drawn by Egelstaff from more sparse data on the ^{239}Pu fission cross section. The only significant correlation coefficient is $r_1(W)$. From Fig. 2, which shows $r_1(W)$ as a function of W, it is seen that $r_1(W)$ is above the 1% significance level near W = 10 eV and near W = 50 eV. The ^{239}Pu

(3) Bollinger L. M., Cote R. E. and Thomas G. E. Proceedings of the International Conference on the Peaceful Uses of Atomic Energy (United Nations, Geneva) 15, 127 (1958).

(4) Egelstaff P. J. Nuc. Energy 7, 35 (1958).

fission cross section shows a marked deviation from $1/_v$ dependence near 600 eV which invalidates the use of equation (2) above this energy. This deviation may account for the high value of $r_1(W)$ at $W = 2$ keV.

(c) Multi-level resonance analysis

A computer programme for use on the IBM-7030 has been assembled which can generate a Doppler and resolution broadened R-matrix multilevel fission cross section and which determines the multilevel parameters by a least squares fit to the cross section data. The R-matrix cross section is generated from level parameters by the subroutine REMO (by M. F. James) and the Doppler and resolution broadening is carried out by the subroutine TEMPO (also by M. F. James) using a temperature equivalent to the combined width of the Doppler function and a gaussion resolution function. The true resolution function has been computed independently by a convolution of four functions representing the neutron pulse shape; the timing channel width; the path length uncertainty, for a flight path at 20° to the normal to the water moderator; and the slowing down time uncertainty given by Groenewold and Groendijk[5]. Below 100 eV the resolution function is well represented by a gaussian function. In searching for the best parameters, a STRETCH library subroutine VA02A (by M. J. D. Powell) is used to minimise the function

$$F = \sum_{N=1}^{NP} \left\{ \frac{\sigma_f(N) - \sigma_f'(N)}{\Delta\sigma_f(N)} \right\}^2 , \qquad (3)$$

where NP is the number of data points, $\sigma_f(J) \pm \Delta\sigma_f(J)$ is the measured fission cross section in channel N and $\sigma_f'(N)$ is the broadened R-matrix cross section calculated from level parameters.

Up to now, five levels have been analysed in two separate groups, one containing the 10.96 eV and 11.92 eV levels and one containing the three levels at 14.35 eV, 14.67 eV and 15.47 eV. Figs. 3a,b show the results obtained; the solid line is the R-matrix cross section and the points are the experimental results. The parameters obtained are given in Table I (overleaf). A good fit to the group

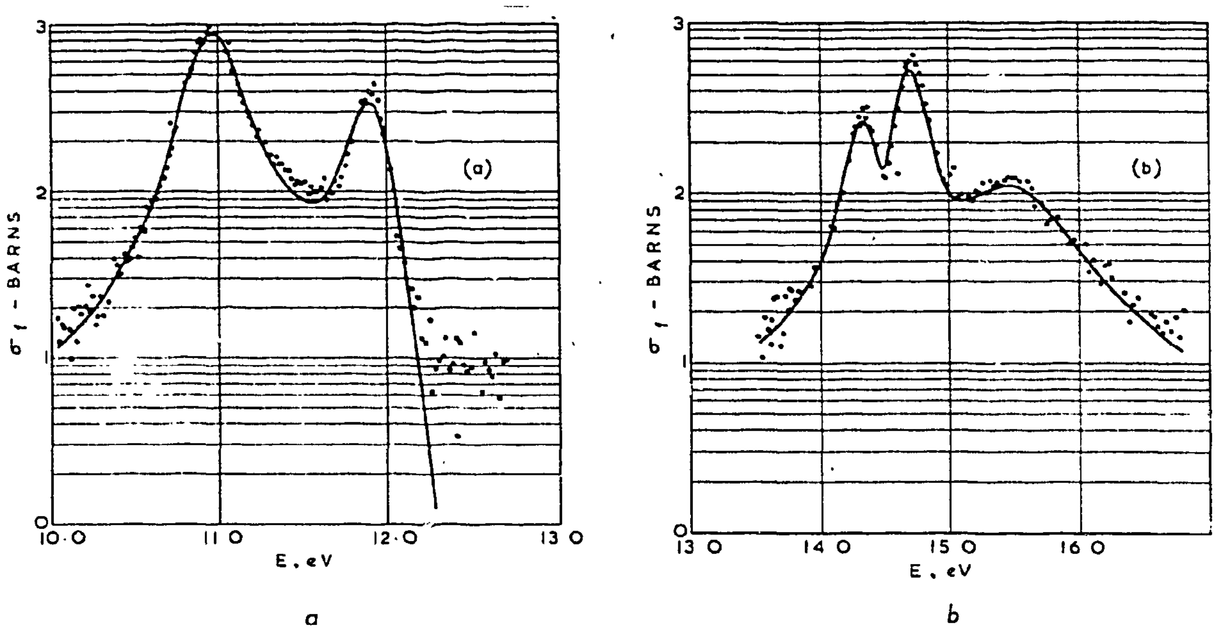

Fig. 3a,b. Multi-level fit (solid line) to the ^{239}Pu fission cross section.

(5) Groenewold and Groendijk, Physica 13, 141 (1947).

TABLE I

R-matrix theory parameters for ^{239}Pu[a]

E_0 (eV)	Γ_n (meV)	Γ_f (meV)	Γ_γ[b] (meV)	J[c]	Relative sign of $(\Gamma_n\Gamma_f)^{1/2}$	No. of data points	F	Requested accuracy
10.93	1.61	168	40	1	+	150	223	3%
11.92	0.60	55.8	40	1	–			3%
14.34	0.61	60.4	40	1	+	120	113	10%
14.7	2.18	19.4	40	1	+			10%
15.42	2.44	876	40	0	–			10%

(a) E_0 is the resonance energy, Γ_n is the neutron width, Γ_f is the fission width, Γ_γ is the radiation width, J is the spin of the compound nucleus and F is given by equation (3).

(b) Assumed values.

(c) Values taken from Sauter and Bowman[7].

of three levels was also obtained using the spin assignment used by Kirpichnikov et al[6]. (J = 0 for the 14.35 eV and 15.47 eV levels and J = 1 for the 14.67 eV level) but this fit took longer to converge. Further work is in progress on the exact resolution function to use with the experimental data analysed here. Until this is complete the parameters of Table I should be treated with caution.

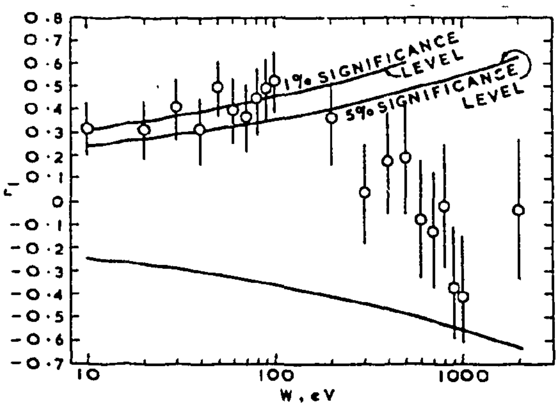

Fig. 4. Correlation coefficient plotted as a function of energy interval for the fission cross section of ^{241}Pu.

II - The fission cross section of ^{241}Pu

(a) Fluctuation analysis

A fluctuation analysis similar to that described above for ^{239}Pu has been carried out for the ^{241}Pu fission cross section and the results are shown in Fig. 4. Again, r_1 is the only serial correlation coefficient that shows any significant correlation and the correlation is greatest near W = 50 eV. The ^{241}Pu fission cross section does not deviate from a $1/v$ dependence and the use of equation (2) is justified throughout the energy range used.

III - The fission cross section of ^{235}U

The fission cross section of ^{235}U has been measured by time-of-flight experiments over

(6) Kirpichnikov I. V., Ignat'ev K. G. and Sukhonichkin S. I. J. Nuc. Energy 18, 523 (1964).

(7) Sauter G. D. and Bowman C. D. Phys. Rev. Letters 15, 761 (1965).

the energy range 1 eV to 30 keV using the neutron booster source with a 0.2 μs electron burst width, $\frac{1}{16}$ μs timing channel widths and a 15 m flight path length. These data are being processed.

Total neutron cross sections (C. A. Uttley, K. M. Diment and C. M. Newstead)

Transmission measurements have been made during this period on both the 300 m and 120 m spectrometers simultaneously by using the ^{10}B overlap filter of the 300 m spectrometer as the detector for the 120 m spectrometer. The pulses from each detector are fed to the same 8 Mc/s tape recorder and and are suitably coded. This procedure enables measurements to be made under good spectrum to background conditions over the energy range 100 eV to 10 MeV. Measurements on two of the nuclei mentioned in the last progress report[8] will be discussed.

Niobium ($^{93}_{41}$Nb)

During the last few years the low energy resonance structure of niobium has been studied using the high resolution time-of-flight spectrometers at Columbia[9] and Saclay[10]. These data have confirmed the earlier ones of Saplakoglu et al.[11] that most of the resonances are weak, and this fact, combined with the relatively high observed resonance absorption integral, suggested that many of the low energy resonances were p-wave and that the p-wave strength function was therefore large. All three groups of workers have determined the p-wave strength function from the measured values of $g\Gamma_n$ for the resonances selected as p-wave resonances. Only in the Saclay work were these resonances positively identified as p-wave resonances. The value of $S_1 = (5 \pm 1)\ 10^{-4}$ obtained recently by the Saclay group is consistent with previous values. In the present experiment the average total cross section from 10 keV to 2 MeV was measured and, in addition, a thick sample high resolution determination was made over the energy range 75 eV to 10 keV. The 'between-resonance' cross section at several energy points over the energy range 90 eV to 3 keV was corrected for resonance and resonance-potential scattering interference effects using the resonance parameters measured by the Saclay group[10]. A low energy potential scattering cross section $4\pi R'^2 = 6.1 \pm 0.2$ barns was obtained, in agreement with the Saclay value of 6.0 barns, and the value $R_0^\infty = -0.14 \pm 0.02$ was calculated from the expression $R' = R(1 - R_0^\infty)$ with $R = 1.35A^{1/3}$ fm. The total cross section from 10 keV to 2 MeV shown in Fig. 5 is fitted by a curve computed on the STRETCH computer using a least squares programme. According to formal resonance theory, the average total cross section for each partial wave ℓ is determined by two parameters - the strength function S_ℓ and the distant level parameter R_ℓ. The most important single parameter is R_0^∞, since it largely determines the s-wave shape elastic scattering cross section which is the most dominant single contribution to the total cross section, at least up to 1 MeV, as can be seen in Table II (overleaf). The value of R_0^∞ determined from the resolved resonance region is fed into the programme and the parameters S_0, S_1, R_1^∞ and S_2 are determined.

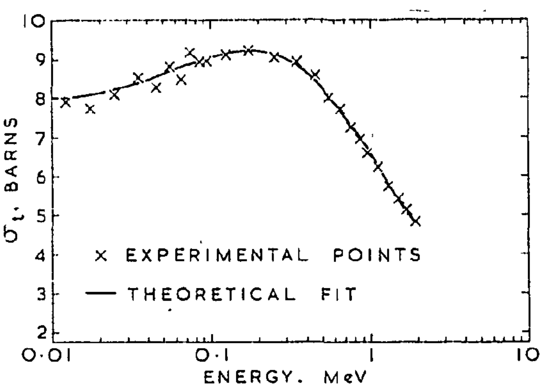

Fig. 5. The total neutron cross section of niobium.

It is assumed that $R_2^\infty = R_3^\infty = 0$, since the d- and f-wave shape elastic contributions (see Table III) are small, and that $S_3 = S_1$. It is clear from Table III, which lists the energy variation of the partial wave cross sections, that the p-wave parameters are largely determined by values of the cross section

(8) Uttley C. A. and Diment K. M. Nuclear Physics Division Progress Report, AERE - PR/NP9, p.2 (1966).

(9) Garg J. B., Rainwater J. and Havens W. W. Jnr. Phys. Rev. 137, B547 (1965).

(10) Le Poittevin G., De Barros S., Huynh V. D., Julien J., Morgenstern J., Notter F. and Samour C. Nuclear Physics 70, 497 (1965).

(11) Saplakoglu A., Bollinger L. M. and Coté R. E. Phys. Rev. 109, 1258 (1958).

TABLE II

Average parameters of Nb

R_o^∞	$S_o \times 10^4$	$S_1 \times 10^4$	R_1^∞	$S_2 \times 10^4$
−0.12	0.23	5.58	0.23	0.76
−0.14	0.17	5.36	0.22	0.92
−0.16	0.11	5.12	0.21	1.11

TABLE III

Partial wave components in the total cross section of Nb

Energy (keV)	S-wave S.E.*	S-wave C.N.*	P-wave S.E.	P-wave C.N.	D-wave S.E.	D-wave C.N.	F-wave S.E.	F-wave C.N.
12.5	6.01	0.63	0.00	1.31	0.00	0.00	0.00	0.00
17.5	5.98	0.53	0.01	1.53	0.00	0.00	0.00	0.00
25.0	5.94	0.44	0.01	1.81	0.00	0.00	0.00	0.00
35.0	5.98	0.37	0.02	2.10	0.00	0.00	0.00	0.00
45.0	5.83	0.33	0.03	2.34	0.00	0.01	0.00	0.00
55.0	5.78	0.30	0.05	2.53	0.00	0.01	0.00	0.00
65.0	5.73	0.27	0.07	2.70	0.00	0.01	0.00	0.00
75.0	5.67	0.25	0.09	2.84	0.00	0.01	0.00	0.00
85.0	5.62	0.24	0.11	2.95	0.00	0.02	0.00	0.00
95.0	5.57	0.23	0.13	3.05	0.00	0.02	0.00	0.00
125	5.43	0.20	0.21	3.27	0.00	0.03	0.00	0.00
175	5.20	0.16	0.36	3.44	0.00	0.04	0.00	0.00
250	4.87	0.14	0.58	3.44	0.00	0.07	0.00	0.01
350	4.46	0.11	0.86	3.25	0.00	0.11	0.00	0.03
450	4.09	0.10	1.09	2.99	0.00	0.15	0.00	0.05
550	3.74	0.09	1.26	2.72	0.01	0.19	0.00	0.07
650	3.42	0.08	1.38	2.48	0.01	0.23	0.00	0.10
750	3.12	0.08	1.47	2.26	0.02	0.26	0.00	0.14
850	2.84	0.07	1.53	2.07	0.03	0.29	0.00	0.18
950	2.59	0.07	1.56	1.90	0.05	0.32	0.00	0.23
1100	2.24	0.06	1.56	1.69	0.07	0.35	0.01	0.30
1300	1.83	0.06	1.52	1.46	0.12	0.39	0.02	0.40
1500	1.49	0.05	1.44	1.28	0.17	0.41	0.03	0.51
1700	1.19	0.05	1.35	1.14	0.22	0.43	0.05	0.61
1900	0.94	0.04	1.24	1.02	0.28	0.45	0.09	0.71

$S_o = 0.17$; $R_o^\infty = -0.14$; $S_1 = 5.36\ 10^{-4}$; $R^\infty = 0.218$; $S_2 = 0.919 \times 10^{-4}$;
$S_3 = S_1 = 5.36\ 10^{-4}$; $R_2^\infty = R_3^\infty = 0$.

*S.E. = shape elastic; C.N. = compound nucleus.

corresponding to energies up to about 600 keV, below which the higher partial waves have little influence. Since the statistical errors on the measured total cross sections are small, an estimate of the errors on the average parameters S_0, S_1, R_1^{∞} and S_2 is obtained from a least squares fit to the data by varying R_0^{∞} by one standard deviation either way. The parameters obtained are given in Table II.

The value of the p-wave strength function S_1 is in very good agreement with those obtained from the analysis of individual resonances and suggests a negligible variation in S_1 over several hundred keV.

Boron ^{10}B (K. M. Diment)

The total cross section of sintered samples of enriched boron has been measured and the data in the energy range 100 eV to 100 keV are plotted in Fig.6. An isotopic analysis of the boron was found to yield 94.58% ^{10}B and a correction to the data below 100 keV has been made for the impurities (0.76% Si, 0.73% C) as well as for the ^{11}B content. The data from 100 keV to 10 MeV have not yet been corrected for the impurities whose cross sections vary rapidly with energy over this range. From Fig. 6 it can be seen that up to ~ 60 keV the total cross section σ_t follows a $^1/_v$ law to within the accuracy of the observations.

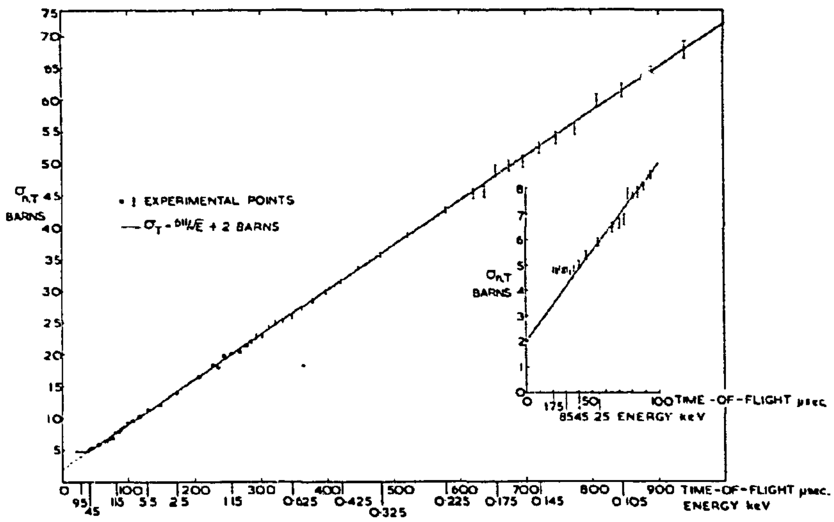

Fig. 6. The total neutron cross section of ^{10}B.

GENERAL NUCLEAR DATA FOR REACTORS - II
(Nuclear Physics - II and Nuclear Photo-effect: E. R. Rae)

Fission cross section measurements (B. H. Patrick and N. J. Pattenden)

The measurement of the fission cross section of ^{235}U was stopped shortly after the end of the period covered by the last report[12], since at this stage the length of the electron burst incident on the "booster" target at the end of the linear accelerator was increased from 130 nsec to 200 nsec[13] and it was expected that this would be the running condition for several months. The resulting change in

(12) Patrick B. H. and Pattenden N. J. Nuclear Physics Division Progress Report, AERE - PR/NP9, p.5 (1966).

(13) Poole M. J. (Private communication).

resolution would otherwise have required that all the previous work on ^{235}U be repeated. Measurements on ^{239}Pu were then begun and it is intended to complete them at the new resolution of 2.5 nsec/m. The work on ^{235}U will be resumed when the electron pulse is returned to its original length.

Three ^{239}Pu samples are being used, with n values ranging from 10^{-3} atoms/barn to 2.4×10^{-2} atoms/barn. The transmission measurements on all the samples have been completed together with more than half of the fission yield measurements. At present the incident neutron spectrum is being measured. The detector for this measurement is a ⅛ in. thick, 2½ in. diameter lithium glass scintillator. The glass is placed in the neutron beam and is viewed from a distance of 2 in. by a 2 in. diameter photomultiplier. An air light guide is used to reduce the effect of neutrons which scatter back from the face of the photomultiplier. Calculations using a Monte Carlo programme written by J. E. Lynn (private communication) have shown that the correction for multiple scattering in the glass is almost constant over the energy range 50 eV to 30 keV. This is important since it is the shape of the spectrum which matters most for this measurement, not the magnitude.

These measurements will be normalized to the lower energy measurements(14) in the 50 eV region.

Studies of the p-wave neutron strength function (C. M. Newstead and N. J. Pattenden)

Transmission measurements made with the 90 metre spectrometer on samples of separated ^{98}Mo and ^{100}Mo(15) of four different thicknesses have been analysed to obtain preliminary values of the neutron and radiation widths. An area analysis method for thick samples (i.e. allowing for appreciable resonance-potential interference and Doppler-broadening), originally developed by Lynn(16) and now rewritten and somewhat modified for the PDP-4 computer, was used.

The data have also been analysed using the Harvey-Atta programma(17) but this programme gives incorrect results for thick samples, apparently because of the insensitivity of the search routine and area function for large $n\sigma$ values. In the case of small $n\sigma$ the self-consistent curves predicted by the Harvey-Atta and PDP programmes are in good agreement. The determination of the radiation widths is, of course, sensitive to the detailed shape of the self-consistent curves, and it has been found necessary to compute the theoretical areas $A_E(\infty)$ rather than interpolate in the area tables(18). Preliminary values of resonance parameters are shown in Table IV.

The preliminary results indicate that the average values of the s- and p-wave radiation widths are different in ^{98}Mo and in ^{100}Mo and that the value used by Pevzner et al.(19) is too large. The values are in better overall agreement with the theoretical calculations of Dovbenko et al.(20) The neutron widths tend to be smaller than those of Pevzner et al.(19) and in better agreement with the maximum likelihood calculations for S_o of Muradyan and Adamchuk(21). The s-wave strength function is found to be $(0.46 \pm 0.4) \times 10^{-4}$ for ^{98}Mo and $(0.5 \pm 0.4) \times 10^{-4}$ for ^{100}Mo. Resonances were assigned as p-wave if no interference was observed. It is intended to confirm these results by performing a further analysis of the transmission data with the Saclay shape programme.

---

(14) Schomberg M. G., Sowerby M. G. and Jolly J. E. This report, p.11.

(15) Newstead C. M. and Pattenden N. J. Nuclear Physics Division Progress Report, AERE - PR/NP9, p.5 (1966).

(16) Lynn J. E. A.E.R.E. Report R 3355 (1960).

(17) Atta S. E. and Harvey J. A. Oak Ridge National Laboratory Report, ORNL-3205 (1961).

(18) Lynn J. E. A.E.R.E. Report R 3354 (1960).

(19) Pevzner M. I. et al. Soviet Physics JETP 17, 191 (1963).

(20) Dovbenko A. G., Zakharova S. M., Kolesov V. E. and Malyshev A. V. Atomnaya Energiya No. 2, 114 (1965).

(21) Muradyan H. V. and Adamchuk Yu V. Kurchatov Report (1965).

TABLE IV

^{98}Mo			
E_R (eV)	$g\Gamma_n$ (eV)	Γ_γ (meV)	ℓ
429.0	0.12 ± 0.02	120 ± 30	1
467.2	0.66 ± 0.06	290 ± 60	0
612.4	0.04 ± 0.007	100 ± 20	1
818.1	0.24 ± 0.05	90 ± 20	1
1526.3	1.37 ± 0.2	280 ± 50	0
2550.5	1.58 ± 0.2	260 ± 50	0
3292	6.4 ± 0.8	250 ± 50	0
9053	45.7 ± 4.0	270 ± 90	0
^{100}Mo			
363.7	0.79 ± 0.14	230 ± 50	0
1069.1	0.29 ± 0.06	80 ± 20	1
1260.9	0.27 ± 0.05	130 ± 30	1
1697.8	0.97 ± 0.1	180 ± 70	1
1938.0	1.25 ± 0.2	240 ± 60	0
3007	3.43 ± 0.6	260 ± 50	0

The s-wave parameters have then been used in conjunction with the higher energy data to obtain the p-wave strength function and distant level parameters as discussed by Uttley et al.[22,23]

Neutron cross sections of ^{107}Ag and ^{109}Ag (M. C. Moxon and A. Asami)

Neutron capture and scattering measurements previously reported[24] indicated that the resonance parameters could easily be obtained from scattering and capture data. In the case of silver, however, lack of knowledge of the isotopic assignment, and the appearance of resonances within the same resolution width for both isotopes, restricted the energy range over which parameters could be obtained. Recently, scattering and capture measurements on separated 10 gram samples of the two silver isotopes (isotopic fraction $\gtrsim$99.5%) have been performed. Figs. 7 a,b (overleaf) show the normalized capture counts per channel versus time-of-flight for ^{107}Ag (a) and ^{109}Ag (b) over the neutron energy range 100 keV to ~ 80 eV. It is hoped that resonance parameters up to ~ 1 keV will be obtained for both isotopes from these measurements by combining them with the scattering data.

Neutron scattering measurements on ^{239}Pu (M. Asghar)

Neutron scattering measurements have been made on a sample of Pu metal 5 cm in diameter and 5.79×10^{-3} atom/b thick, containing about 98% of ^{239}Pu. The detector of the spectrometer[25] was

(22) Uttley C. A. and Diment K. M. Nuclear Physics Division Progress Report, AERE - PR/NP9, p.3 (1966).

(23) Uttley C. A. et al. This report, p.5.

(24) Asghar M., Moxon M. C. and Chaffey C. M. Conference on the study of nuclear structure with neutrons, Antwerp, Paper 65, 1965.

(25) Asghar M. and Brooks F. D. Nuc. Inst. and Methods 39, 68 (1966).

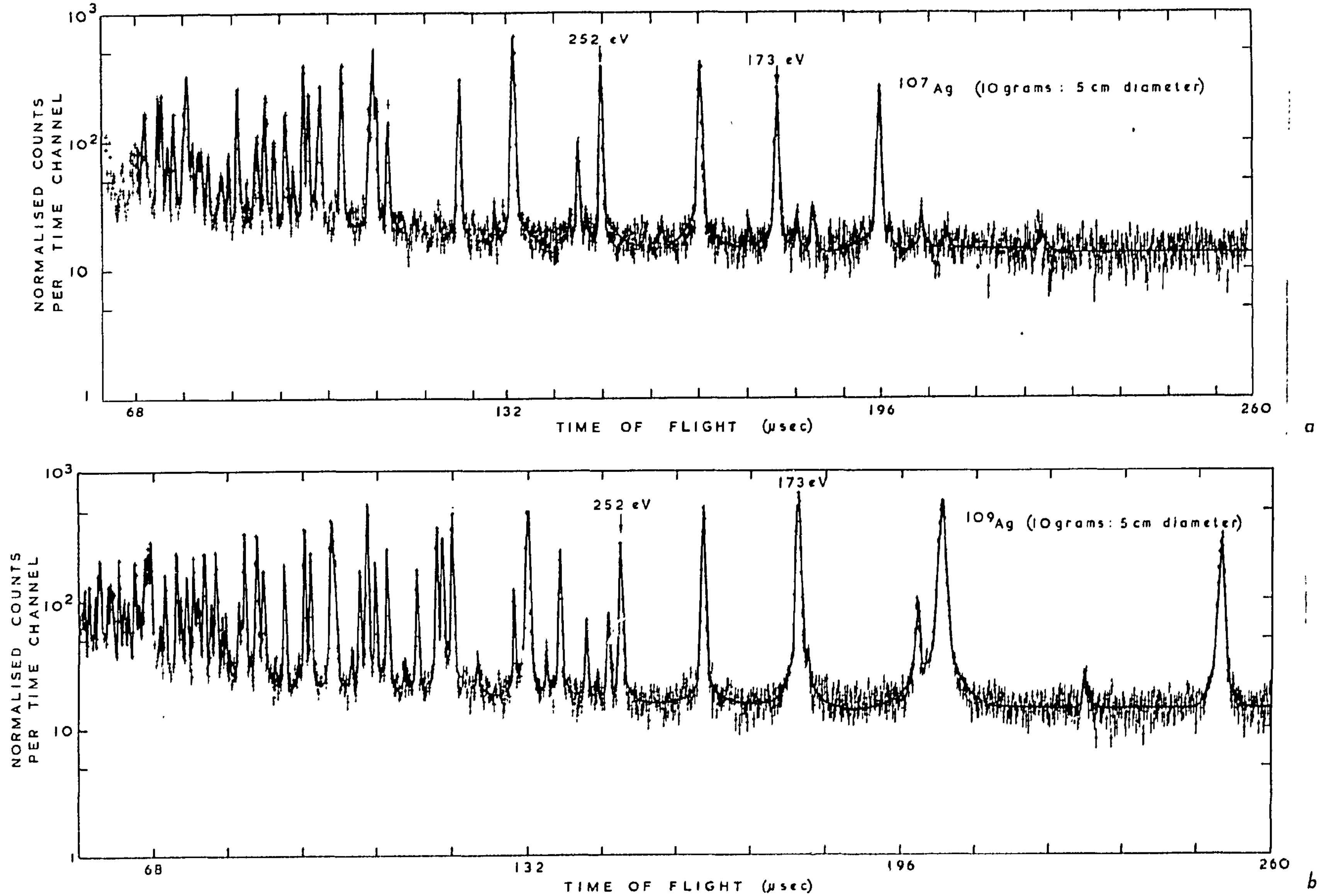

Fig. 7. Normalized capture counts per channel as a function of time-of-flight for ^{107}Ag and ^{109}Ag.

modified to take account of fission neutrons. Resonance scattering areas were determined and combined with published transmission data[26,27] to enable spin assignments of 45 resonances below 300 eV to be made. These measurements have been reported in detail in Report EANDC(UK)70 'S'.

The measurement of alpha, eta and the fission cross sections of ^{239}Pu (M. G. Schomberg, M. G. Sowerby and J. E. Jolly)

Work has continued on the direct measurement of alpha[28] (the ratio of the capture to fission cross sections) for ^{239}Pu as a function of neutron energy. Measurements of the fission neutron yield have been made for three thin ^{239}Pu samples with low ^{240}Pu content, loaned by O.R.N.L., and measurements with the neutron capture detectors will begin shortly. It is not necessary for both kinds of measurement to be made simultaneously provided there is no change in energy resolution.

Measurements of the fission neutron yield have also been made on three thick ^{239}Pu samples and the data from all six samples will be used in a new eta and fission cross section measurement from 10 eV to 2 keV. At present sample transmission and incident neutron spectrum measurements are nearly complete and these will be used in the now modified Stretch computer programme. These measurements will be normalized to the earlier low energy measurements[29] in the 8 eV region.

Determination of ^{240}Pu resonance parameters (M. Asghar, M. C. Moxon, C. M. Chaffey, N. J. Pattenden and J. S. Pratt)

A series of experiments has been undertaken to determine the ^{240}Pu resonance parameters in the energy region from a few eV to about 1 keV. Scattering, capture and transmission measurements are being carried out, and parameters will be obtained by combining the three sets of data using an area analysis method.

Two samples of Pu metal (~ 98% ^{240}Pu), both 7.62 cm diameter but weighing 6.46 and 15.07 g respectively, have been obtained from Los Alamos under the auspices of the EANDC. Scattering yields have been obtained on the 50 m flight path, and capture yields on the 32 m flight path. Transmission measurements are being performed on the 94 m flight path, and should be complete in a few weeks. The detailed resonance analysis will start when the collection of data is complete.

Total cross section measurements on Ba isotopes (R. E. Van de Vijver and N. J. Pattenden)

The range of neutron numbers in the stable Ba isotopes includes at one extreme the 82 neutron closed shell. It has long been known that the mean total radiation width, $\langle\Gamma_\gamma\rangle$, for electric dipole radiation, is of the form[30]

$$\langle\Gamma_\gamma\rangle \propto A^{2/3}\, D_J(U) \int_0^U \frac{E^3 dE}{D(U-E)} \quad ,$$

---

(26) Blons J., Derrien H., Michaudon A., Ribon P. and de Saussure G. International Conference on the Study of Nuclear Structure with Neutrons, Antwerp, paper 163 (1965).

(27) Uttley C. A. International Conference on the Study of Nuclear Structure with Neutrons, Antwerp, paper 98 (1965).

(28) Schomberg M. G., Sowerby M. G. and Jolly J. E. Nuclear Physics Division Progress Reports, AERE - PR/NP8, p.9 (1965); and AERE - PR/NP9, p.10 (1965).

(29) Brooks F. D., Jolly J. E., Schomberg M. G. and Sowerby M. G. Nuclear Physics Division Progress Report, AERE - PR/NP9, p.11 (1965).

(30) Blatt J. M. and Weisskopf V. F. Theoretical Nuclear Physics (John Wiley and Sons, 1952).

where A is the mass number, U is the effective excitation energy of the radiating level, $D_J(U)$ is the spacing of levels of the same spin and parity as the radiating level, and D(U–E) is the spacing to any level (excitation energy E) to which radiation can occur. A level density relationship which includes the effects of closed shells may be inserted in the above expression to predict a variation of $<\Gamma_\gamma>$ with A which agrees qualitatively with observation(31,32). A searching test of the theory is to determine how well its predictions fit measurements of $<\Gamma_\gamma>$ in the immediate vicinity of a closed shell, and this is one of the objectives of this experiment.

The Hg isotopes lie just below the 126 neutron closed shell. It has been observed that the distribution of Γ_γ values appears to be very broad for ^{201}Hg, but not for ^{198}Hg or ^{199}Hg(33,34). This fact is attributed to the large variation in the partial widths for the highest energy transition in ^{201}Hg where these transitions are particularly intense. Similar intense high energy transitions have recently been reported in the ^{135}Ba capture γ-ray spectrum obtained from capture in the 24 eV resonance(35). Cross section measurements with a resolution of 80 ns/m have been reported in the case of natural Ba samples(36). However, it is not practicable to make accurate determinations of Γ_γ for a large number of resonances without using separated isotope samples and superior resolution, since, when many isotopes are present, the observed peaks may contain contributions from resonances in different isotopes. Thus, another objective of the experiment is to determine whether the Ba resonances show a wide Γ_γ distribution.

Samples of about 4 g each of enriched ^{134}Ba, ^{135}Ba, ^{136}Ba and ^{137}Ba were obtained on loan from Oak Ridge National Laboratory, converted into carbonate powder and loaded into special containers suitable for transmission measurements on the 15 m small sample time-of-flight spectrometer. The area of each sample was 0.88 cm^2. A natural $BaCO_3$ sample was also prepared, to provide a means of testing the whole operation.

Preliminary transmission measurements covering an energy range from a few eV to about 1 keV were made on the natural Ba sample, with an optimum resolution of about 18 ns/m. An area analysis of the observed resonances was performed, using the computer program of Atta and Harvey(37). The neutron widths obtained are shown in Table V, where they are compared with the values given in the BNL-325 compilation(38).

Transmission measurements on the separated isotope samples are now being carried out. The collection of data on ^{134}Ba is now complete.

PDP-4 data processor (E. M. Bowey, M. R. Avery, G. D. Spittle and G. B. Dean*

The computer has been operated for 1670 hours during the period of this report, of which one continuous period of 12 hours was devoted to marginal testing of the computer and its peripheral equipment. Peripherals have been the cause of most of the "down time" which has amounted to about 15 hours during normal working hours.

---

(31) Newton T. D. Can. J. Phys. 34, 804 (1956).

(32) Cameron A. G. W. Can. J. Phys. 35, 666 (1957).

(33) Carpenter R. T. and Bollinger L. M. Nuclear Physics 21, 66 (1960).

(34) Bolotin H. H. and Chrien R. E. Nuclear Physics 42, 676 (1963).

(35) Urbanec J., Vrzal J. and Liptak J. International Conference on the Study of Nuclear Structure with Neutrons, Antwerp. Paper 97 (1965).

(36) San K. H., Pikelner L. B., Sharapov E. I. and Sirazhet K. International Conference on the Study of Nuclear Structure with Neutrons, Antwerp. Paper 188 (1965).

(37) Atta S. E. and Harvey J. A. Oak Ridge National Laboratory Report, ORNL-3205 (1961).

(38) Hughes D. J., Magurno B. A. and Brussel M. K. Neutron Cross Sections, Brookhaven National Laboratory Report, BNL-325, 2nd edition supplement 1 (1960).

*Neutron Spectra and Nuclear Physics I Group.

TABLE V

Resonance parameters obtained from a natural Ba sample

E_R (eV)	$2g\Gamma_n^o$ (meV)		Isotope (BNL-325)
	Present data	BNL-325	
24.0	1.96 ± 0.10	2.0 ± 0.1	135
45.6	$(9.1 \pm 2.4)10^{-3}$		
57.0	$(4.4 \pm 0.6)10^{-2}$		
79.6	16.8 ± 1.4	18 ± 2	135
84.9	7.8 ± 1.0	5.5 ± 0.8	135
100.6	7.6 ± 1.5	4.5 ± 1.3	136
103.0	11.2 ± 1.8	15 ± 4	135
220.9	3.6 ± 1.6	2.8 ± 0.9	135
278.9	21.6 ± 5.6	19 ± 4	135
311.4	5.8 ± 3.0	5 ± 2	135
372.2	10.8 ± 3.8	13 ± 5	135
401.2	41 ± 13	20 ± 15	135
414.9	25 ± 5	50 ± 15	137
460.1	7.0 ± 5.6	7 ± 4	135
506.6	32 ± 14	6 ± 4	135
574.0	63 ± 30	27 ± 10	137
643.3	1.6 ± 1.0		

New routines, which provide a more convenient and sophisticated system, have been written to handle data recorded on 1 in. magnetic tape. Circuitry has been designed and installed, and routines have been written, to provide a computer controlled camera facility to enable the display to be photographed.

Two input/output devices, the symbol generator and CRT display, previously only accessible through PDP-4 Machine Language routines, can now be used with FORTRAN programmes. 'Pages' of text are reproduced on the CRT display ~ 50 times faster than with the teleprinter. Graph plotting can also be carried out with FORTRAN programmes.

INTEGRAL DATA MEASUREMENTS

(Nuclear Spectra and Nuclear Physics - I: M. J. Poole)

The two blocks experiment (D. H. Day and J. H. Partridge)

The two blocks experiment is designed to investigate the thermal neutron spectrum as a function of position in a graphite stack containing a plane temperature discontinuity. The experimental equipment, which has been fully described in a previous report[39], consists essentially of two large graphite blocks at different temperatures, separated by crumpled aluminium foil thermal insulation, with provision for the extraction of neutron beams for time-of-flight spectrum measurement.

(39) Day D. H. and Partridge J. H. AERE Report, R 4667 (1964).

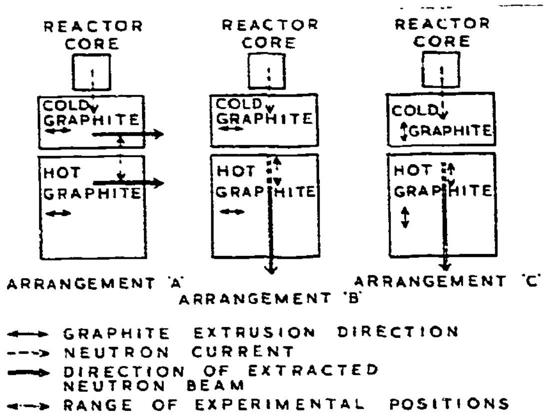

Fig. 8. Experimental geometries.

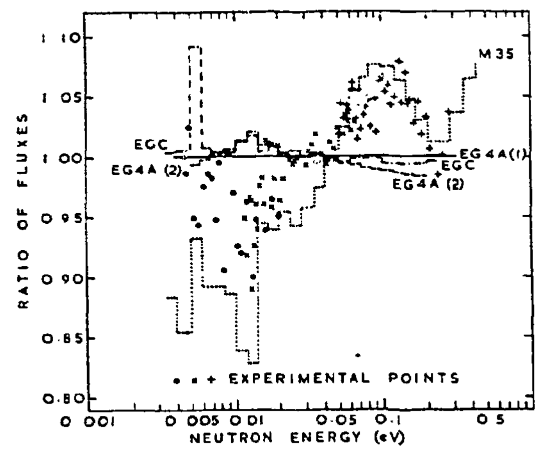

Fig. 9. Ratio of measured and calculated fluxes in graphite at 325°C, 6 cm from the interface with graphite at 35°C. Key to WDSN calculations: EG4A(1) (realistic scattering kernel); EG4A(2) (as above but with allowance for thermal barrier); M35 (heavy gas kernel for atoms of mass 35); EGC (improved version of EG4A).

Measurements have been made using the three different geometries shown in Fig. 8. Spectra measured in arrangement A are those of neutrons taken from points where there are no flux gradients at any energy along the extracted beam direction, and hence these spectra are very close to the isotropic spectra at the points of measurement. Results of this type have already been reported[40,41] for many different distances from the interface, at hot graphite temperatures of 100, 175, 250 and 325°C. Good agreement has been found between the measured spectra and those calculated using the WDSN code and the EG4A scattering kernel. These results are reproduced in Fig. 9, which shows the ratios between measured and calculated fluxes for different scattering kernels. The earlier calculations assumed an infinitely sharp temperature step between the hot and cold regions. New calculations have now been made to take into account the finite size (4 cm) of the thermal barrier by including a third region into the D.S.N. calculations. As the transport mean free path (λ_{tr}) in this region is $\sim$ 100 cm it was not adequate to allow for transverse leakage by the simple addition of a DB^2 term ($D = \frac{\lambda_{tr}}{3}$, B^2 = transverse buckling) to the absorption cross section (Σa) as is done for the other two regions. Therefore the assumption was made that transverse leakage could be handled by using a modified absorption of the form $\Sigma_a^1(E) = \Sigma_a(E) + K\lambda_{tr}(E)$, the value of K being determined empirically by fitting calculated and observed values of total flux in this region. A value of $K = B^2/15$ was found to give the best fit (Fig. 10). The effect on the spectra of the finite interface region is also shown in Fig. 9.

Spectra[41] measured in arrangement B (Fig. 8) have also been reported; the graphite has now been restacked with its extrusion direction turned through 90°, and the same spectra have been measured in arrangement C. Figs. 11 a,b show the results of spectra measured in arrangements B and C, compared with calculated directed spectra from WDSN.

---

(40) Day D. H. and Partridge J. H. Nuclear Physics Division Progress Report, AERE - PR/NP8, p.18 (1965).

(41) Day D. H. and Partridge J. H. Nuclear Physics Division Progress Report, AERE - PR/NP9, p.12 (1965).

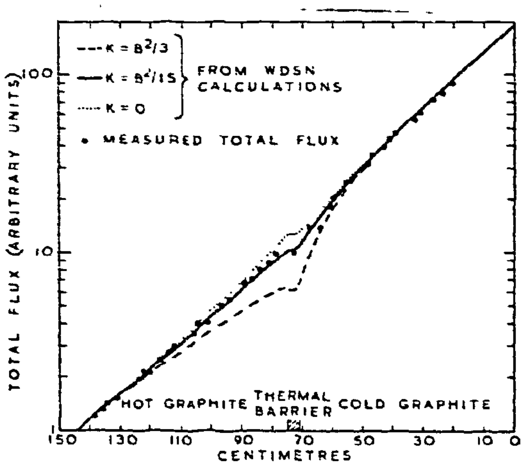

Fig. 10 (above). Total flux distribution with a hot graphite temperature of 325°C.

Fig. 11 (right). Dependence of directed flux on extrusion direction: a) in graphite at 35°C; b) in graphite at 250°C, 12.0 cm from interface with graphite at 35°C.

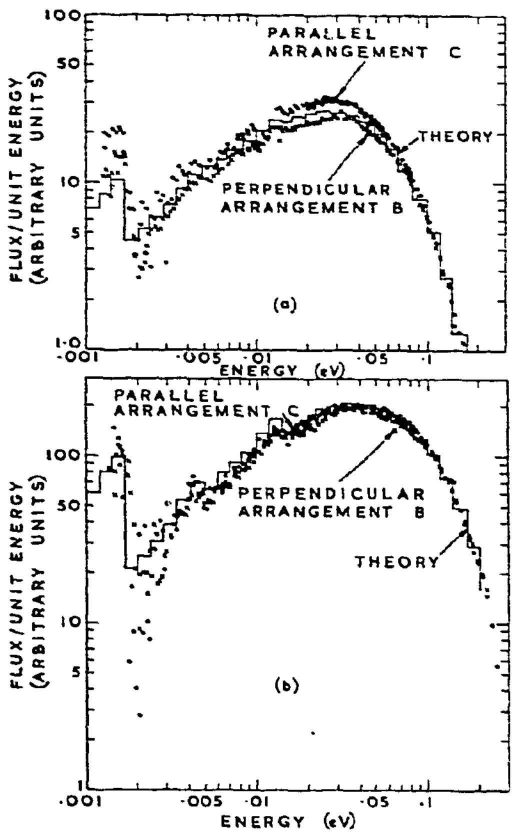

A simple diffusion theory relationship is often used to obtain the directed flux spectrum from the calculated total flux spectrum, viz:

$$F_z(E) = \tfrac{1}{2}\phi(E) - \frac{\lambda_{tr}}{2}\,\frac{\phi(E)}{(z)}$$

where F_z is the directed flux in the z direction and $\phi(E)$ is the calculated flux spectrum. Egelstaff[42] has measured the scattering cross section for neutrons travelling both parallel and perpendicular to the extrusion direction in graphite and the observed differences in spectra are roughly reproduced if these two values are used to obtain two values of λ_{tr} from the above equation. The fact that the difference between spectra measured by extracting beams parallel and perpendicular to the extrusion direction shown in Fig. 11b is much smaller than predicted can be explained partly by the effect of crystal orientation on the cross section at high temperatures and partly by the different behaviour of the flux gradient for this case.

(42) Egelstaff P. A. J. Nucl. Energy, 5, 203 (1957).

Neutron spectra in heavy water/ordinary water mixtures (R. N. Sinclair and P. J. Williams)

Due to the interest in the use of D_2O/H_2O mixtures as moderator in spectral shift reactors, measurements have been made of spectra in a mixture containing 50.55% D_2O and poisoned with various concentrations of cadmium. The experiments were carrried out by the pulsed-source time-of-flight method using exactly the same equipment as has been described for the poisoned D_2O measurements[43]. Two solutions, containing 20.3 g.p.l and 30.4 g.p.l respectively of dissolved cadmium were used, the solution temperature in each case being 290°K. The solutions were prepared by Chemical Engineering Division, A.E.R.E. by dissolving carefully dried cadmium nitrate in a D_2O/H_2O mixture, whose composition had been determined by density measurements.

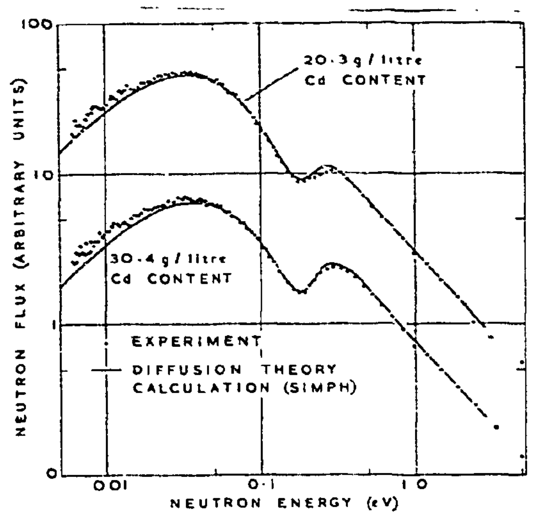

Fig. 12. Neutron spectra in poisoned D_2O/H_2O mixtures.

As a preliminary to the spectrum measurements, flux plots were made for each solution using bare manganese and cadmium gold foils. The results indicated that the spectra were independent of position in the vicinity of the point of observation, so that the solutions may be taken to be "strongly poisoned" and diffusion theory should be adequate to calculate the spectra.

The measured spectra are shown in Fig. 12, together with the results of calculations made using a scattering kernel compounded from the Honeck kernel for bound deuterium[44] and the Haywood kernel for hydrogen[45]. The GAKER code[46] was used to calculate the Honeck bound deuterium kernel. In this model coherent scattering effects are completely ignored; however, in spite of this, it has already been used successfully in this laboratory to calculate time dependent spectra in a tank of pure D_2O[47]. The contributions to the scattering from oxygen was allowed for by assuming it to be a perfect gas of mass 16.

Spectra were calculated in the energy range 0-3 eV. The neutron source for this calculation was the number of neutrons slowing down into this energy region. This number was computed by assuming scattering from a perfect gas for the oxygen and deuterium atoms, and by using an analytical expression to account for the mean kinetic energy of the protons in H_2O for the hydrogen scattering. The experimental and theoretical spectra in Fig. 12 have been normalized to equal neutron loss (absorption plus leakage) over the energy region 0-3 eV. The agreement is not as good as was obtained in earlier comparisons with theory where the measurements were made on mixtures containing heavy water or ordinary water separately, in spite of the fact that the same theoretical models were used. Further calculations will be made using a semi-empirical kernel based on measurements of the inelastic scattering in this mixture[48].

(43) Sinclair R. N. and Williams P. J. Pulsed Neutron Research, Vol. I, IAEA, p. 581 (1965).

(44) Honeck H. Trans. Am. Nucl. Soc. 5, 47 (1962).

(45) Haywood B. C. and Thorson I. M. Brookhaven National Laboratory Report, BNL719, p.26 (1962).

(46) Honeck H. Brookhaven National Laboratory Report, BNL5826 (1961).

(47) Poole M. J. and Wydler P. Proceedings of the I.A.E.A. Conference on Pulsed Neutron Source Measurements, Karlsruhe, 1965.

(48) Day D. H. and Partridge J. H. Private communication.

Spectra in poisoned D_2O using a neutron chopper (P. Wydler)*

Sinclair(43) has already described pulsed source measurements of spectra in D_2O poisoned with boron and cadmium over a range of poison concentrations from 0.98 barns/D atom to 2.60 barns/D atom. Measurements at lower poison concentrations were not possible because the pulsed source method can only be applied to systems with a small die-away time. Accordingly, an experiment to measure neutron spectra in a tank containing 1 tonne of poisoned D_2O using a neutron chopper was set up on one of the irradiation panels of the LIDO reactor. The experimental layout is shown in Fig. 13. It is basically

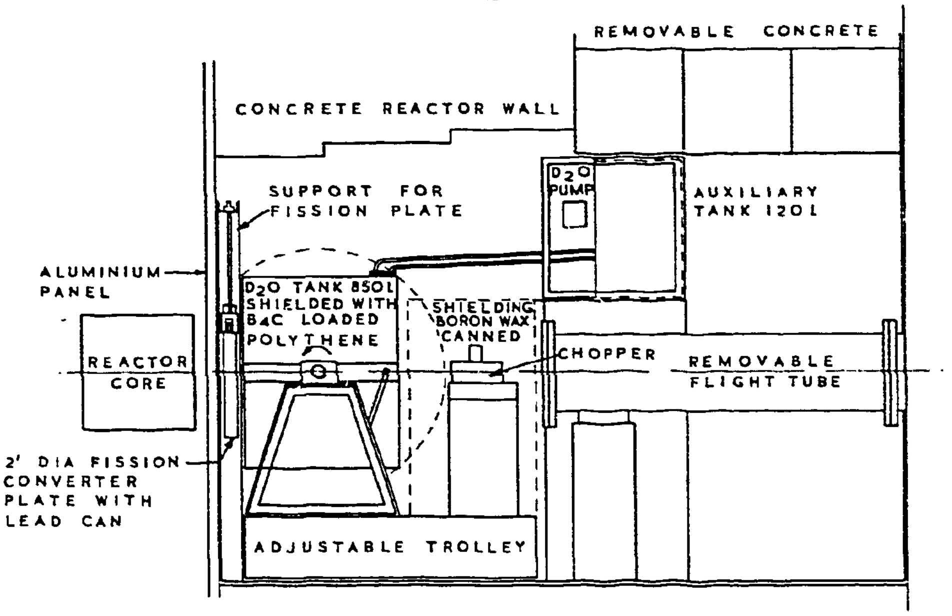

Fig. 13. Experimental arrangement for measuring spectra in poisoned D_2O using a neutron chopper.

similar to the installation used by Coates and Gayther(49) to measure spectra in a heated, graphite-moderated lattice. (In fact much of the same equipment was used). The D_2O tank was cylindrical, 110 cm in dia. x 90 cm in length, and it was placed with one end against the reactor irradiation panel. Between the panel and the end of the tank there was a natural uranium fission plate 1 in. in thickness to convert the mixed reactor spectrum into a basically fast neutron spectrum, so avoiding the necessity of knowing the reactor spectrum when interpreting the experiments. Arrangements were made to extract a beam of neutrons from various positions along the tank axis whose spectrum could be measured with a neutron chopper spectrometer having a resolution of up to 1.2 μs/m. It was also possible to insert detector foils into the tank in order to obtain flux plots.

Experiments have been carried out using Cd poisonings of 0.37, 0.85 and 1.26 b/D atom (measured at 2200 m/sec.), spectra being measured at various axial positions for each solution. Typical spectra are shown in Figs. 14 a,b,c (overleaf). So far no calculated spectra are available; these will be obtained using the WDSN code in slab geometry, and a slowing down distribution obtained from the flux plots as a source.

---

(49) Coates M. S. and Gayther D. B. AERE Report, R 3829 (1966).

*On attachment from Eidg. Inst. fur Reaktorfurschung, Würenlingen, Switzerland.

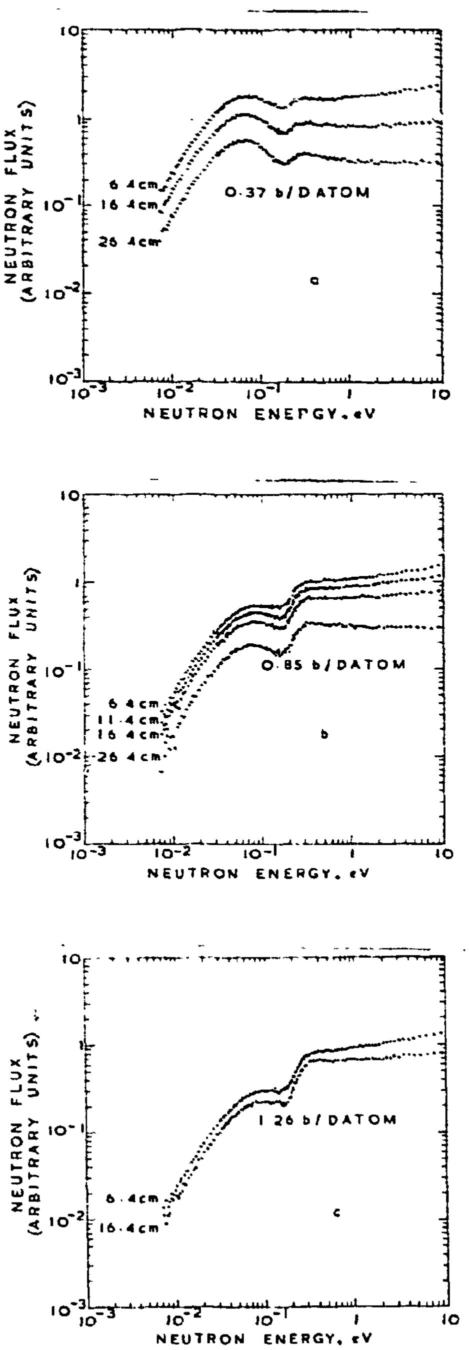

Fig. 14. Neutron spectra in heavy water poisoned with cadmium: a) 0.37 b/D atom measured at three distances from source; b) 0.85 b/D atom measured at four distances from source; c) 1.26 b/D atom measured at two distances from source.

<u>Time dependent neutron spectra in water</u>
<u>(R. N. Sinclair and P. J. Williams)</u>

The chopper technique, which has been successfully used to measure time dependent spectra in graphite(50,51) and in heavy water(52), cannot easily be used for ordinary water because of the very short slowing down and thermalization times involved (~ 10 μsec.). Consequently, an alternative technique has been used in which the moderator is pulsed by the linac and a simple crystal spectrometer is used to allow the time dependence of selected energies to be followed. Several energies, corresponding to different orders, are reflected for each setting of the crystal spectrometer but these are separated in time due to their different times of flight. Provided, therefore, that the flight time is long compared to the neutron lifetime in the moderator, this feature permits observation at several energies simultaneously.

Two experiments are described here. Firstly, a preliminary investigation of the technique using coarse time resolution, and secondly, measurements with improved resolution of the time dependence of the leakage spectrum from a water slab and of the spectrum at the centre of a large water tank.

Fig. 15 illustrates the experimental arrangement for the preliminary investigation. Short pulses of fast neutrons were produced in the uranium target by the pulsed electron beam of the 45 MeV Harwell linac. Neutrons leaving an adjacent polythene moderator (5 cm (thickness) x 14 cm x 14 cm) in a beam with a total angular divergence of 30 minutes of arc were diffracted by a single crystal of nickel. The (2n,0,0) reflections (n is the order of reflection) were observed at a Bragg angle (θ) of 46° by a 3 mm lithium glass scintillation detector 3 mm in thickness. The observed time distribution of detected neutrons (Fig. 16) shows structure which may be assigned to seven orders of reflection, the peaks occurring at times of flight (τ) given by

$$\tau = \frac{1}{n}\,\frac{(2m)}{(h)}\, d_{2,0,0} \sin\theta \text{ , } \mu\text{sec/m} \quad ,$$

where $d_{2,0,0}$ Å is the interplanar spacing of the

(50) Barnard E. and Poole M. J. J. Nucl. Sci. Engng. 17, 513 (1963).

(51) Nicholson K. P. and Poole M. J. J. Nucl. Energy 19, 949 (1965).

(52) Wydler P. and Poole M. J. Pulsed Neutron Research, Vol. I, p.425, I.A.E.A. (1965).

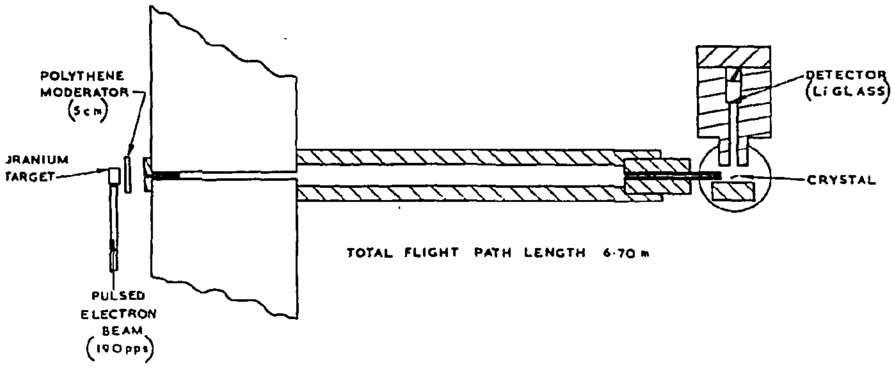

Fig. 15. Experimental arrangement for measurements of time dependent neutron spectra in water using a chopper.

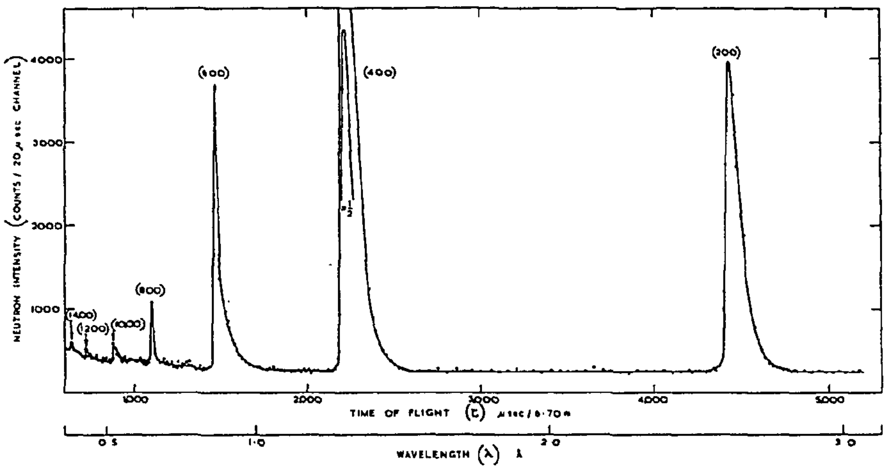

Fig. 16. The time-of-flight distribution of counts observed using a nickel crystal in the arrangement shown in Fig. 15.

{2,0,0} planes, h is Planck's constant and m the neutron mass. The shape of each peak depends upon the time and energy dependent flux $\phi(E,r)$ set up in the moderator, and on the experimental resolution. Even with the coarse resolution of this experiment, a characteristic asymmetric peak shape is apparent due to the relatively rapid growth of the neutron population at a given energy followed by an approximately exponential decrease as neutrons are removed by leakage and absorption.

The accuracy with which a given energy can be selected depends upon the diffraction geometry, and the energy resolution is given by:

$$\frac{\Delta E}{E} = 2 \cot \theta \Delta \theta \quad ,$$

where θ is made up of the divergence of the incident beam and the mosaic spread of the crystal. The time resolution depends on this factor and also on the flight path length. The total width of the time resolution function is given by

$$\Delta t = \tau (L \cot \theta \Delta \theta + \Delta L) \quad ,$$

where L is the total flight path length and ΔL is the maximum path difference for the detected neutrons. (ΔL contains the path difference arising from the finite thickness of the crystal and the uncertainty in the point of detection within the scintillator).

For the experiments using water as moderator the flight path was reduced to 3.1 m and a multi-slit collimator of length 72 in. was designed in order to produce a beam with a total angular spread of 5 minutes of arc. The mosaic spread of the beryllium crystal used in the experiments had been previously measured to be 5 minutes of arc (full width half maximum). This gave an energy resolution of $\Delta E/E = 0.005$ and a time resolution of $0.010\ \tau\ \mu s$.

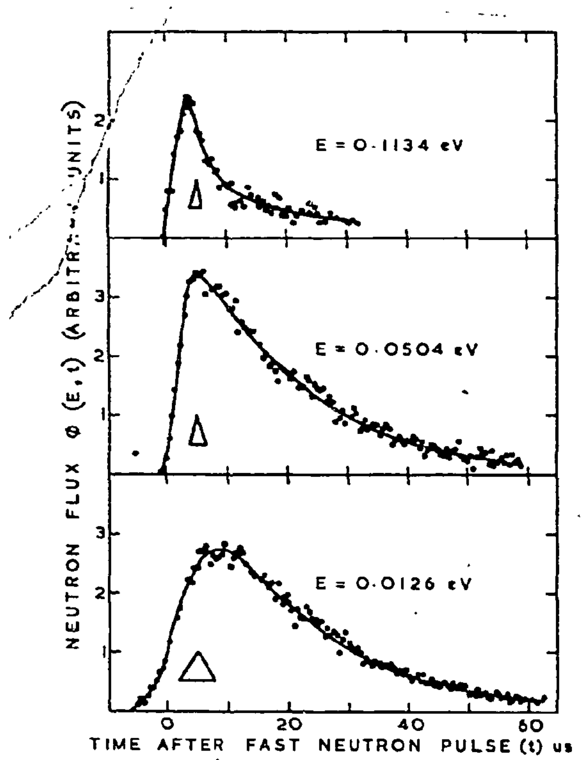

Fig. 17. The time dependence of the neutron flux emerging from a 3 cm x 14 cm water slab for three different neutron energies.

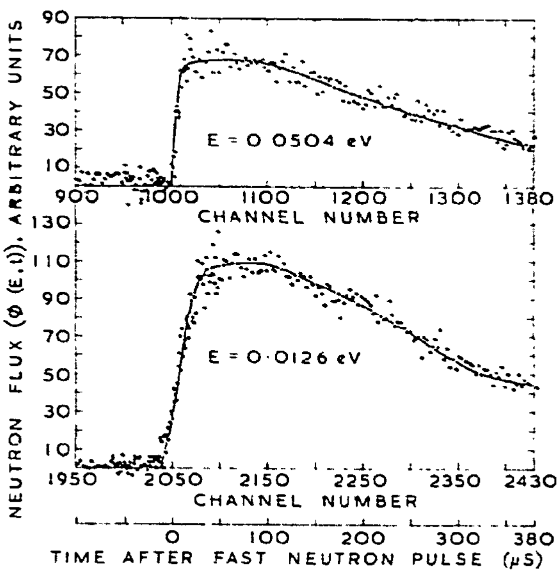

Fig. 18. The time dependence of the neutron flux at two energies emerging from the centre of a large water tank.

In Fig. 17 the time dependence of the leakage flux from the slab of water (3 cm x 14 cm x 14 cm) is illustrated. The three energies correspond to three orders of reflection from the same planes and the distributions were measured simultaneously using 1 μs timing channels. The time origin is derived from the 0.1134 eV distribution where the resolution function (shown) is least significant. The time dependent background was determined by rotating the crystal out of the diffracting position.

Spectra set up in a large tank of water (57 cm x 57 cm x 57 cm) have also been studied. The source was placed in a re-entrant tube 10 cm from the centre of the tank. A beam of neutrons was taken from the centre of the tank by a 2.5 cm probe tube and the history of two neutron energies (Fig. 18) in this beam was observed with the diffractometer described above. In this case the decay of the spectrum is largely due to the loss by absorption.

Time dependent diffusion theory calculations are being made for comparison with the results of this experiment.

Measurements of fast neutron spectra in materials (D. B. Gayther and P. D. Goode)

Measurements have now been completed of the leakage spectrum emerging from a sphere of sodium with a central neutron source. The experimental techniques have been described in earlier reports(53). The source consisted of a cylindrical uranium target bombarded by a pulsed beam of electrons from the

(53) Gayther D. B. and Goode P. D. Nuclear Physics Division Progress Report, AERE - PR/NP7, p.14 (1964).

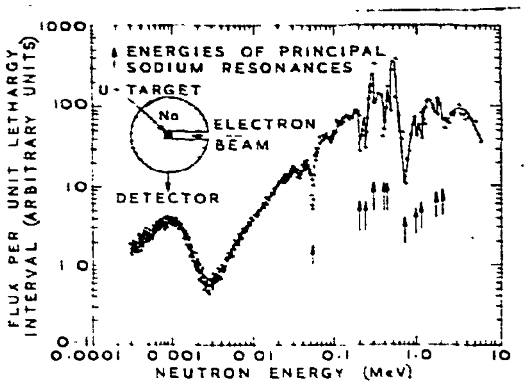

Fig. 19. Leakage neutron spectrum from sodium sphere.

45 MeV linac. The leakage spectra were measured by the time-of-flight method with a 60 m path length, the minimum electron burst width being 100 n sec. The measurement of the neutron source spectrum has been described previously(54). Fig. 19 shows the measured neutron spectrum emerging radially from the sodium sphere. The sodium weighed 372 kg and was contained in an aluminium tank of internal diameter 90.7 cm and wall thickness 0.8 cm. The neutrons whose spectra were being measured passed through a thin "Melinex" window in the tank. The spectrum was measured with two detectors; the ^{10}B plug detector(53) which was used from the lowest energy up to 2 MeV and a plastic,proton recoil detector(54) which was used at energies greater than 200 keV. The two sets of measurements were normalized in the region of energy overlap.

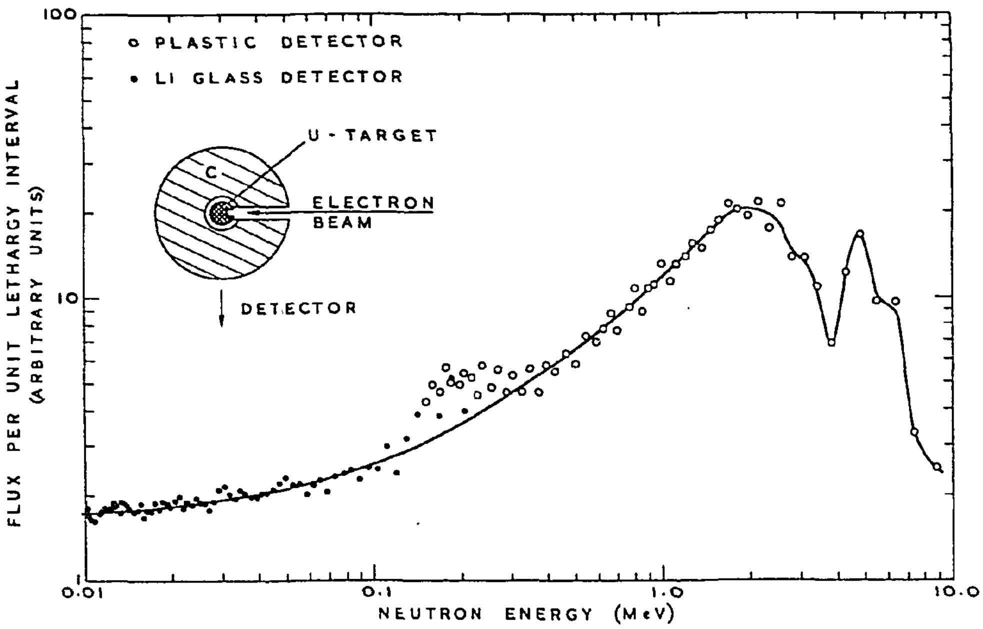

Fig. 20. Leakage spectrum of neutrons from graphite sphere.

Fig. 20 shows a preliminary determination of the leakage spectrum from a graphite sphere. This sphere was 40.6 cm in diameter and a 6 cm diameter natural uranium target was placed in a 10 cm diameter hole at its centre. The measurements were made with a ^6Li glass detector and the plastic detector. The calibration of the efficiencies of these detectors is described below. These detectors do not have a satisfactory energy overlap for normalization of the measurements and the curve shown in Fig. 21 (overleaf) was obtained by using the absolute detection efficiencies of the two counters. The apparent rise in the measurements of the graphite spectrum in the region of 200 keV (Fig. 20) is possibly due to the inaccuracy inherent in the ^6Li glass detector in the vicinity of the (n,α) resonance in ^6Li and

(54) Gayther B. B. and Goode P. D. Nuclear Physics Division Progress Report, AERE - PR/NP9, p.15 (1966).

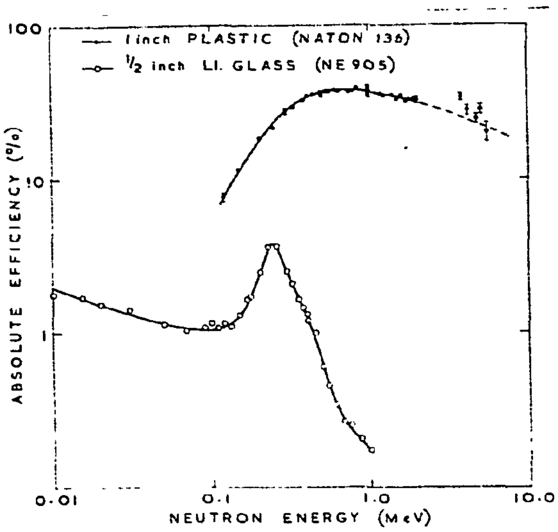

Fig. 21. Measured efficiencies for Li-glass and plastic detectors.

to the uncertainty in detection efficiency of the plastic detector in the region of rapidly falling efficiency near threshold, but the shape is reliable elsewhere.

<u>Calibration of detectors for fast neutron spectra measurements (M. S. Coates, D. B. Gayther, P. D. Goode and D. J. Tripp)</u>

The neutron detection efficiency has been determined for a ^{6}Li glass detector and for a plastic proton recoil detector, using IBIS as a monoenergetic neutron source. The method was described in an earlier Progress Report[53] and is based on a direct comparison with a calibrated Hanson-McKibben long counter. The absolute detection efficiency of the long counter was determined by J. M. Adams using the Harwell spontaneous fission source.

The thickness and diameter of the lithium glass detector (NE 905) were 1.27 cm and 11 cm respectively and it was mounted directly on a 5 in. photomultiplier. In order to reduce the background, the detector pulses were passed through a single channel pulse height discriminator with a 30% width centred on the peak pulse height observed with thermal neutrons. The full width at half maximum of the pulse height distribution observed with thermal neutrons was 27%. With increasing neutron energy, the mean pulse height increases and counts are lost due to the window discriminator being always set with respect to the thermal peak. This is a major contribution to the low detection efficiency of this system for neutron energies approaching 1 MeV. The proton recoil detector consisted of a disk of NATON 136, 2.5 cm in thickness and 12.7 cm in diameter, viewed by a coincidence arrangement of two 2 in. photomultipliers coupled to its back surface by a short perspex light pipe. The results of some of these measurements are shown in Fig. 21. Neutrons in the region of 5 MeV were produced by the $D(d,n)^{3}He$ reaction. Because of the presence of large backgrounds, the results contain some systematic errors and, for this reason, the efficiency is known accurately only up to 2 MeV. The measurements near 5 MeV are to be repeated and it is also intended to make an efficiency determination at 14 MeV.

A full description of the ^{10}B plug detector and its efficiency calibration has already been given[53]. In this detector, γ-rays from the $^{10}B(n,\alpha)^{7}Li^{*}(\gamma)^{7}Li$ reaction are observed in NaI crystals surrounding a ^{10}B plug. The original plug consisted of 774 g of ^{10}B metal contained in a thin walled aluminium container 12.7 cm in diameter. This plug has now been modified by the addition of 741 g of vaseline, which although reducing the efficiency at low energies, results in a considerable enhancement at higher energies. The increase in efficiency at high energies is due to (i) moderating effects in hydrogen which increase the capture probability in the ^{10}B and (ii) increased scattering into the NaI crystals which increases the number of γ-rays arising from inelastic scattering; these γ-rays are also detected and contribute to the counter efficiency. The time uncertainty due to the neutron moderation in the vaseline is considerably smaller than the shortest pulse length (60 n sec.) used in the present measurements. Fig. 22 shows the efficiency of the original ^{10}B plug calibrated on IBIS, the calculated extrapolation to lower energies[53], together with the measured efficiency of the ^{10}B vaseline plug, which was determined by measuring the neutron booster spectrum with each detector and comparing the results.

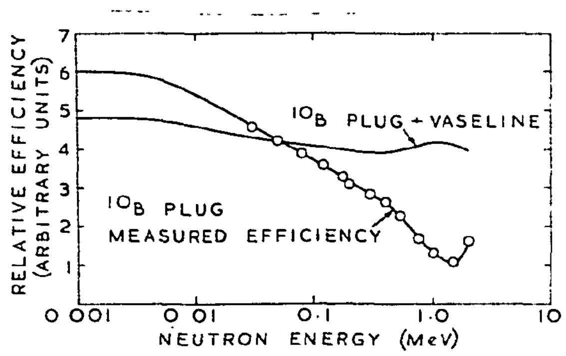

Fig. 22. The effect of additional moderator on the ^{10}B plug detector efficiency.

FUNDAMENTAL AND BASIC RESEARCH

PULSED VAN DE GRAAFF ACCELERATOR (IBIS)

Studies of various (^{3}He,n) reactions (J. M. Adams, A. Adams* and J. M. Calvert*)

Further experiments have been carried out on the study of proton-rich nuclei. In particular, an angular distribution of the neutrons from the reaction ^{24}Mg(^{3}He,n)^{26}Si at 3.0 MeV (Fig. 23 (overleaf)) has been obtained which exhibits a forward peak in spite of the fact that the incident energy is a few MeV below the coulomb barrier.

A study of the energy levels of ^{15}O using the reactions ^{13}C(^{3}He,n)^{15}O and ^{14}N(d,n)^{15}O has yielded angular distributions at 3.0 MeV and excitation functions between 2.0 MeV and 3.0 MeV for most of the ^{15}O energy levels up to 9.0 MeV. Some of these angular distributions exhibit characteristic stripping patterns (Fig. 23).

A DWBA computer programme is being used to analyse the angular distributions that have been measured for the reactions ^{9}Be(^{3}He,n)^{11}C, ^{10}B(^{3}He,n)^{12}N, ^{13}C(^{3}He,n)^{15}O and ^{24}Mg(^{3}He,n)^{26}Si. The programme is based on the theory of Rook and Mitra(55) which assumes that for double stripping the two nucleons are captured into a linear combination of single particle states. Thus the single nucleon form factor, $\psi = \mu/r$ (the radial wave function of the captured nucleon) is replaced by the form factor

$$F = \sum_L (\theta_{11}^L \psi_1^2 + \theta_{12}^L \psi_1 \psi_2 + \theta_{22}^L \psi_2^2)$$

where L ranges over the possible L values for the transition and the θ_{11}^L are parameters. Of the analysis done so far, some of the experimental results agree with this theory better than others (Fig. 23); part of the difficulty may be due to the choice of the ^{3}He optical potentials, about which there is not much information in this energy range.

Some DWBA analysis of the angular distributions obtained from the reactions ^{10}B(d,n)^{11}C and ^{14}N(d,n)^{15}O has been carried out.

---

(55) Rook J. R. and Mitra D. Nuclear Physics 51, 96 (1964).

*University of Manchester.

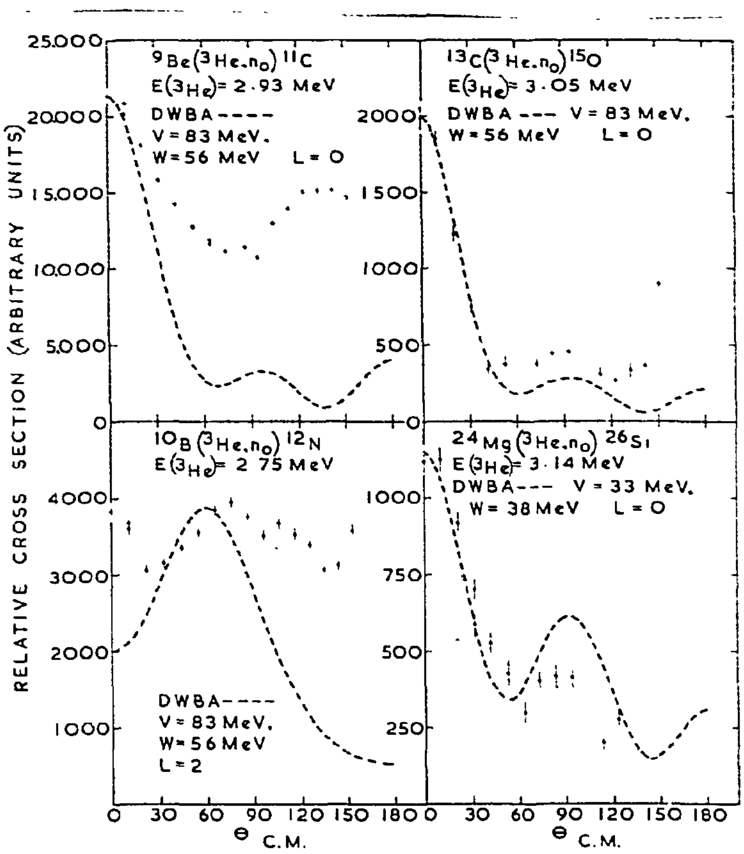

Fig. 23. Angular distributions of (^{3}He,n) reactions.

The (^{3}He,n) reaction on ^{17}O and ^{18}O (B. H. Armitage, K. Gul and B. W. Hooton)

A report of preliminary measurements on the $^{17}O(^{3}He,n)^{19}Ne$ reaction has already been given(56). Subsequently, a high resolution study of this reaction has resulted in the location of eleven neutron groups arising from levels in ^{19}Ne. These data were obtained from measurements with a 100 μg. cm^{-2} W $^{17}O_3$ target (containing 15% ^{18}O) at flight paths of 8 m and 6 m, and at an incident energy of 3.1 MeV. The neutron groups associated with (I) the known triplet of levels close to the ground state(57) and (II) the known triplet of levels near 1.5 MeV(58) were not resolved. Apart from the above (and also a state reported at 2.78 MeV(59)) all the levels in ^{19}Ne shown in Fig. 24 have not been observed previously. There is some doubt at present as to whether a group of neutrons associated with a level at 3.71 MeV in ^{19}Ne is genuine and further work is required to settle this point. It is of interest to note that the apparent close correspondence of levels in ^{19}F and ^{19}Ne is somewhat disturbed if a level

---

(56) Armitage B. H., Gul K. and Hooton B. W. Nuclear Physics Division Progress Report, AERE - PR/NP9, p.19 (1966).

(57) Ajzenberg-Selove F. and Lauritsen T. Nuclear Physics 11, 1 (1959).

(58) Freeman J. M. and West D. Nuclear Physics 38, 89 (1962).

(59) Wesolowski J. J., Anderson J. D., Hansen L. F., Wong C. and McClure J. W. Nuclear Physics 71, 586 (1965).

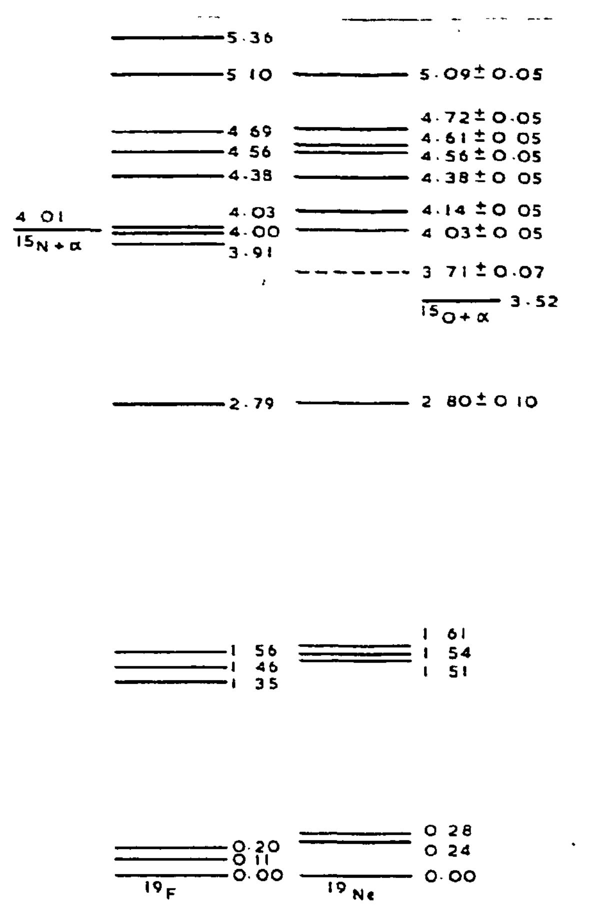

Fig. 24. Energy levels in ^{19}Ne: the excitation energies below 2 MeV are from references[57,58]; the remainder were measured in this work. The existence of a level at 3.71 MeV is doubtful. Levels in the mirror nucleus ^{19}F (references[57,62]) are shown for comparison.

exists at 3.71 MeV in ^{19}Ne. One might suppose, however, that a 3.71 MeV level in ^{19}Ne corresponding to the 3.912 MeV level in ^{19}F would be subject to a Thomas-Ehrmann[60] shift, since the former level lies above the α-dissociation energy while the latter lies just below the corresponding α-dissociation energy in ^{19}F. A more detailed comparison of the level positions in ^{19}Ne and ^{19}F will have to await spin and parity measurements. Preliminary angular distribution measurements have also been made and an analysis of the data in terms of double stripping reactions is in progress.

Particular care had to be taken in the above measurements to ensure that contributions arising from (^3He,n) reactions with ^{18}O and ^{13}C were taken into account. It was necessary to make separate measurements with ^{18}O and ^{13}C targets at several angles of observation.

Measurements have also been made on the $^{18}O(^3He,n)^{20}Ne$ reaction at a flight path of 8 m using WO_3 targets enriched in ^{18}O. More data will have to be taken, however, before the position of levels in ^{20}Ne can be established with any degree of confidence.

Some difficulty was found throughout all this work in obtaining accurate neutron energies from the time spectrum. The method finally adopted was to calibrate the time spectrum with the $^9Be(^3He,n)^{11}C$ reaction, using the accurately known Q-values for the levels in ^{11}C. This technique avoided the necessity of measuring the dispersion of the time-to-pulse height analyser with delay cables. The incident ^3He energy was measured by the method described by Ferguson et al.[61]

5MV VAN DE GRAAFF GENERATOR

The channelling of ions in single crystals (G. Dearnaley and I. V. Mitchell (with R. S. Nelson and B. W. Farmery, Metallurgy Division)).

During the last six months much of the time has been occupied with the design and commissioning of a new system of beam collimation and crystal orientation. Rotation about each of three orthogonal axes can now be made remotely, in steps of $(6 \times 10^{-3})^\circ$, by means of a precision target mount designed

(60) Thomas R. G. Phys. Rev. 88, 1109 (1952).

(61) Ferguson A. T. G., Lawergren B. and Morrison G. C. Nuclear Physics Division Progress Report, AERE - PR/NP8, 22 (1965).

(62) Silbert M. G. and Jarmie N. Phys. Rev. 123, 221 (1961).

by Mr. K. C. Knox. The Van de Graaff beam can be defined to better than 0.01° by a rigidly-mounted set of collimating apertures. With the new system much better reproducibility of beam alignment is now possible. A beam quality of 10^{-4} mm radian has been achieved.

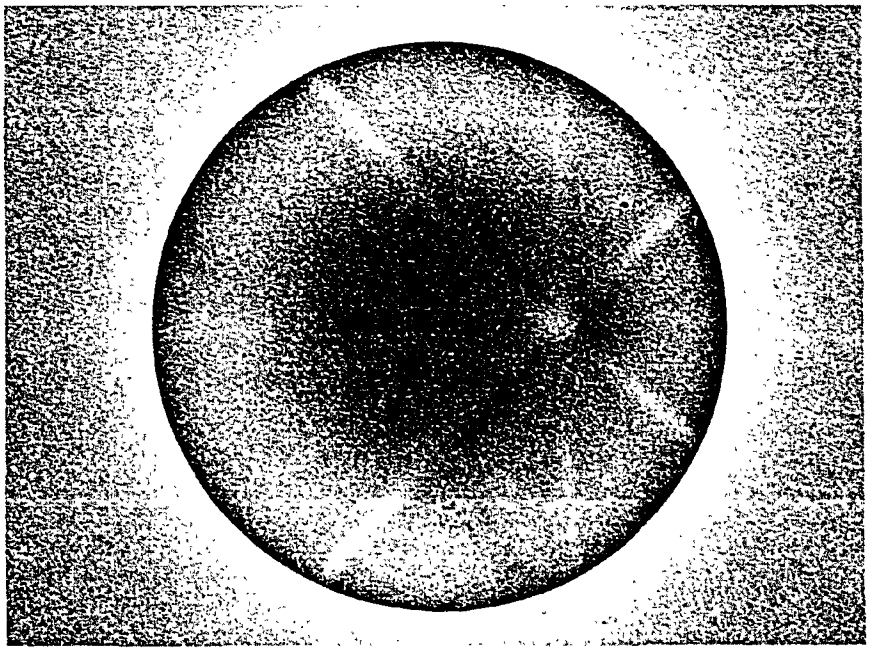

Fig. 25. The channelling of 4 MeV protons through a single crystal of MgO which are travelling near the <100> direction.

The transmission of protons with energies between 1.0 and 4.5 MeV has been studied in thin crystals of silicon, iron and MgO. An X-ray emulsion, mounted behind the target, allows the emerging protons to be recorded photographically. A so far unexplained pattern has been observed when the crystal is misaligned with respect to the beam by about 1° (see Fig. 25): a dark streak appears to one side of each blocking line away from the beam axis. The effect was observed first in MgO, and was tentatively explained by Prof. M. W. Thompson in terms of a build-up of electrostatic charge on the insulating crystal. This would cause a differential deflection of channelled and unchannelled particles. However, the effect did not disappear when the experiment was repeated with a conducting film of aluminium deposited on the rear face of the crystal. Moreover, the effect has now been demonstrated using an iron crystal.

A suggestion[63] that ion focusing occurs in ionic crystals due to the electrostatic charges of ions within the lattice has not been substantiated by further experiments. Very similar effects are observed in MgO and Si when crystals of similar thickness are compared. Such focusing, although physically possible, is now thought to be a second or third-order effect at MeV energies.

In order to achieve some degree of energy sensitivity in the recording photographic emulsion, Nelson has suggested the use of colour film of a type in which the layers which develop to different colours lie at different depths in the emulsion. In Agfa negative colour film, for instance, the surface layer develops to yellow, the next to magenta, and the deepest, lying about 20μ from the surface, develops to cyan blue. Thus protons of energies up to 1.4 MeV will sensitize different layers and so give rise to varying colours on development. Protons of 1.5 MeV channelled along the <110> direction in a 20μ silicon crystal were allowed to enter such an emulsion, and the resulting photograph successfully revealed the higher energy components of the central star pattern in red, while the lower

(63) Nuclear Physics Division Progress Report, AERE - PR/NP9, p.21 (1966).

energy symmetric distribution corresponding to normal transmission appeared in yellow. The technique should be very useful in revealing more information about the energy loss in channelling, and will supplement the more time consuming measurements of energy spectra using collimated detectors.

Isobaric spin mixing and the decay of analogue resonances (Mrs. S. Ramavataram)

The Coulomb mixing of the analogue state with the neighbouring $T_<$ states of the compound system in general arises from

(a) internal mixing;

(b) boundary condition mixing or external mixing.

Theories of isobaric spin analogue resonances[64,65,66] assume that one or the other predominates and make general predictions regarding the decay of the analogue resonances via $T_<$ channels.

According to the Robson theory[64], which assumes external mixing only, the decay of the analogue resonances in $T_<$ channels is governed entirely by the collision matrix element for transitions via the $T_<$ states alone. The branching ratios would then depend on the ratio of the transmission coefficients; size resonances in any particular channel being reflected in large branching ratios.

However, according to theories which assume internal mixing[65,66], the decay of the analogue resonance via the $T_<$ channels would be governed by nuclear structure effects. The essential requirement for a strong transition in any $T_<$ channel would be a good overlap between the configuration of the $T_<$ state mixing into an analogue state and the configuration of the final state in the $T_<$ channel, viz. particle + final nucleus in the appropriate energy state.

The amount of experimental data available at present is rather limited and a systematic study of such decays is lacking. Analysis of the data so far does not give any clearcut indication in favour of either of the two theoretical approaches. For example, the Robson approach has been successful in obtaining good fits to the $^{92}Zr(p,n)$ excitation function[67].

On the other hand, a more detailed investigation[68] of the $^{89}Y(p,n)$ reaction via the 2^-, 3^- analogue states in ^{90}Zr leading to the ground state ($9/2^+$) and the first excited state ($1/2^-$) in ^{89}Zr casts some doubt on the predictions which follow from Robson's theory. The branching ratios observed experimentally cannot be satisfactorily accounted for by transmission factors obtained by optical model calculations[69].

An attempt has been made here to obtain a qualitative description of the results of the $^{89}Y(p,n)^{89}Zr$ reaction[68] under the assumptions of internal mixing. The configurations of the relevant states are obtained on this basis.

---

(64) Robson D. Phys. Rev. 137, B535 (1965).

(65) Jones G. A., Lane A. M. and Morrison G. C. Phys. Letters 11, 329 (1964).

(66) Bloch C. and Schiffer J. P. Phys. Letters 12, 22 (1964).

(67) Robson et al. Phys. Letters 18, 86 (1965).

(68) Mani G. S. and Dutt G. C. Phys. Letters 16, 50 (1965).

(69) Johnson C. H. Private communication.

Decay of the 2^-, 3^- analogue states in ^{90}Zr to $^{89}Zr_{g.s.}$ $(9/2^+)$ and $^{89}Zr_{1st\ exc.}$ $(1/2^-)$ states via the (p,n) reaction (Mrs. S. Ramavataram)

The g-state doublet in ^{90}Y has the configuration:

$$[\pi p_{1/2}(\nu p_{1/2})^2(\nu g_{9/2})^{10}(\nu d_{5/2})]_{2^-,3^-} \quad .$$

Isobaric analogues in ^{90}Zr will contain components (using the arguments of Lane and Soper(70) and also their notation) $\chi_{5/2}$, $\chi_{9/2}$ and $\chi_{1/2}$, where suffixes refer to the orbit in which a neutron is replaced by proton when going from ^{90}Y to ^{90}Zr.

Appreciable transition rates from such an initial configuration to the ground state of ^{89}Zr can be understood if we assume configurations of the type:

$$\left[\{[(\pi p_{1/2})^2(\nu p_{1/2})(\nu g_{9/2})^{10}]\}\{(\nu p_{3/2})^{-1}(\nu d_{5/2})\}\right] ; \left[\{(\pi p_{1/2})(\pi g_{9/2})(\nu p_{1/2})^2(\nu g_{9/2})^9\}\{(\nu p_{3/2}{}^{-1})(\nu d_{5/2})\}\right] ;$$

$$\left[(\pi p_{1/2})(\pi d_{5/2})(\nu p_{1/2})^2(\nu p_{3/2})^{-1}(\nu g_{9/2})^{10}\right] ; \left[\{[(\pi p_{1/2})^2(\nu p_{1/2})(\nu g_{9/2})^{10}]\}\{(\nu f_{5/2})^{-1}(\nu d_{5/2})\}\right]$$

in addition to the simple shell model configurations.

A quantitative examination of these ideas and attempts to take into account coulomb mixing in a more rigorous manner in the analysis of analogue resonances are being considered in collaboration with Dr. A. M. Lane.

12 MeV TANDEM GENERATOR

Experiments relating to pure Fermi decays and to theories of weak interactions (J. M. Freeman and J. G. Jenkin with G. Murray† and W. E. Burcham††)

Although the ft values for transitions between $J = 0^+$, $T = 1$ isobars show considerable consistency in the seven cases which have now been measured with an accuracy of better than 1%, we have found a discrepancy of 1.4% and 6 standard deviations in one case ($^{26}Al^m(\beta^+)^{26}Mg$). This result implies the existence of unknown effects which may seriously influence the value, deduced from the mean ft value, for the weak interaction vector coupling constant, G_V. Some doubt is then also cast on the value of the Cabibbo angle θ_V for non-strange particle decays. It is therefore important to examine the present experimental ft value results carefully, and to investigate other cases, particularly that of $^{10}C(\beta^+)^{10}B^{**}$, the lightest known pure Fermi decay. This is a difficult case since the relevant branch is very weak (~ 1.5%) by comparison with the Gamow-Teller transition $^{10}C(\beta^+)^{10}B^*$.

I - The ft value for the decay $^{10}C(\beta^+)^{10}B^{**}$

The work on this decay, mentioned in the previous progress report(71), has continued and, in particular, further measurements of the energies of the γ-ray transitions from the first and second excited states of ^{10}B, and of the β-decay branching ratio to $^{10}B^{**}$ have been made with an 8 cc Ge(Li) γ-ray detector loaned by Dr. J. M. MacDonald and Mr. J. D. Ridley of Oxford University. Resulting

---

(70) Lane A. M. and Soper J. M. Nuclear Physics 37, 663 (1962).

(71) Nuclear Physics Division Progress Report, AERE - PR/NP9, p.24 (1965).

†University of Manchester.

††University of Birmingham.

values for the energies of the first two excited states of ^{10}B are 718.46 ± 0.20 keV and 1739.9 ± 0.6 keV. Combining these results with the previously measured value for the $^{10}B(p,n)^{10}C$ threshold[71], we obtain for the end-points for the position transitions from ^{10}C to the first and second excited states of ^{10}B the values: 1909.7 ± 2.0 keV and 888.3 ± 2.0 keV respectively.

The β_2^+ branching ratio to the second excited state of ^{10}B has been obtained from the relative yields of 1022 and 718 keV γ-rays following the ^{10}C decay, use being made of a relative efficiency curve for the Ge(Li) detector as described elsewhere in this Progress Report[72]. An upper limit of 0.05% for a branch β_3 to the third excited state of ^{10}B has also been obtained. In this way the β_2^+ (Fermi transition) branch has been found to be $(1.551 {}^{+0.026}_{-0.037})$ per cent of ^{10}C decays. Combining this result with previous measurements of the total half-life of ^{10}C gives the β_2^+ branch a partial half-life of $(1252 {}^{+30}_{-21})$ sec, and the ft value for the Fermi decay becomes $(2980 {}^{+75}_{-55})$ sec, which includes a radiative correction of 1.9% and a K-capture correction of 0.3%. This result is about 4% and 2 standard deviations lower than the mean (3123 ± 7) sec obtained for decays involving nuclei with higher Z. This difference is in the same sense as for $^{26}Al^m$. Further work to reduce the error on the ^{10}C result is planned.

II - The threshold for the reaction $^{14}N(p,n)^{14}O$

Measurements of the threshold for this reaction are being made by the same method as that used at Harwell for other cases relevant to the study of pure Fermi beta decays. This will allow a more direct comparison of the $^{14}O(\beta^+)^{14}N^*$ decay with the other decays.

III - The ft value for the decay $^{35}Ar(\beta^+)^{35}Cl$

This transition, between mirror $3/2^+$ states, involves a Gamow-Teller as well as a Fermi decay. However the Gamow-Teller matrix element in this case is quite small; its ratio to the Fermi matrix element has been obtained through an asymmetry measurement for the decay of polarized ^{35}Ar by Commins et al.[73] An accurate ft value measurement thus offers the possibility of an estimate of the magnitude of the vector coupling constant G_V, which can be compared with the values deduced from $0^+ \rightarrow 0^+$ transitions. We are making measurements of the threshold for $^{35}Cl(p,n)^{35}Ar$, to determine the β^+ end-point. A new radiothorium pot has been installed to provide a ThC′ α-particle source for the proton energy calibration.

Accurate measurement of the relative efficiency of Ge(Li) detectors (J. M. Freeman and J. G. Jenkin)

Ge(Li) γ-ray detectors, because of their very good resolution, offer the possibility of precise measurements of γ-ray yields, provided the total-energy-peak efficiency can be accurately determined for the given experimental geometry. Calculations of this efficiency are difficult because (i) multiple events following Compton scattering make a significant contribution to the total-energy-peak, (ii) wall effects are large, (iii), the geometry, particularly with accelerator experiments, is not precisely defined, (iv) the photoelectric and Compton absorption coefficients are not known to better than a few per cent.

In many experiments only relative γ-ray yields are required. We have devised a method (largely empirical) for obtaining a relation for the relative efficiency covering the γ-ray energy range 500-1500 keV for any given Ge(Li) detector in a specific geometry, with an accuracy of about 1%.

Use is made of sources for which the relative emission rates of pairs of γ-rays are precisely known, viz ^{22}Na, ^{60}Co, ^{46}Sc and ^{50}Mn. Details of the decay schemes involved and the method used to extract the ratios of the total-energy-peak yields are given elsewhere[74]. In each case the measured peak ratio

---

(72) Freeman J. M. and Jenkin J. G. This page.

(73) Calaprice F. P., Commins E. D. and Dobson D. A. Bull. Am. Phys. Soc. 10, 424, AB2 (1965).

(74) Freeman J. M. and Jenkin J. G. Report, AERE - R 5142 (1966), also Nuclear Instruments and Methods (in course of publication).

divided by the known emission ratio gives the efficiency ratio for the counter for the two radiations. To determine the shape of the efficiency curve which fits these ratio measurements, use is made of the semi-empirical formula:

$$\epsilon \propto \tau + \sigma A \exp(-BE_\gamma) ,$$

where τ and σ are the photoelectric and Compton absorption coefficients, for which the *relative* values of Davisson and Evans[(75)] have been found the most satisfactory. The constants A and B in the formula are obtained by using two of the measured efficiency ratios. The other two ratios are then used to check the consistency of the relation.

Considerable confidence in the reliability of the method was gained from the consistency of the results obtained with two Ge(Li) detectors of quite different dimensions, for which the relative contributions to the total-energy peak from the photoelectric and multiple Compton processes were markedly different.

A study of isobaric analogue states in ^{121}Sb (D. L. Allan, G. A. Jones, R. B. Weinberg and R. B. Taylor)

An investigation of the isobaric analogue states in ^{121}Sb has been carried out by studying the elastic and inelastic scattering of protons by ^{120}Sn. Excitation functions for the elastic scattering and inelastic scattering to the first excited state of ^{120}Sn(2^+, 1.17 MeV) and the first 3^- level in ^{120}Sn (2.39 MeV) have been measured over the incident energy range 7.36 to 10.3 MeV (c. of m.). The results are shown in Fig. 26. The resonances observed in the elastic scattering are analogues of the low lying states of ^{121}Sn. The resonances at 7.48 and 7.53 MeV are the analogues of the ground and first excited states of ^{121}Sn respectively. The resonances at 8.62 and 8.92 MeV are analogues of the $d_{5/2}$ states of ^{121}Sn at 1.12 and 1.40 MeV, while the resonances at 10.08 and 10.20 MeV are probably analogues of the $f_{7/2}$ states at 2.59 and 2.69 MeV. Apart from the resonances observed in the elastic channel, there are two other resonances which are seen only in the 2^+ inelastic channel. These are the resonances at 8.40 and 9.78 MeV and they are evidently analogues of the 0.94 and 2.29 MeV levels in ^{121}Sn (the positions of the ^{121}Sn levels cited above are taken from the work of Schneid et al.[(76)]).

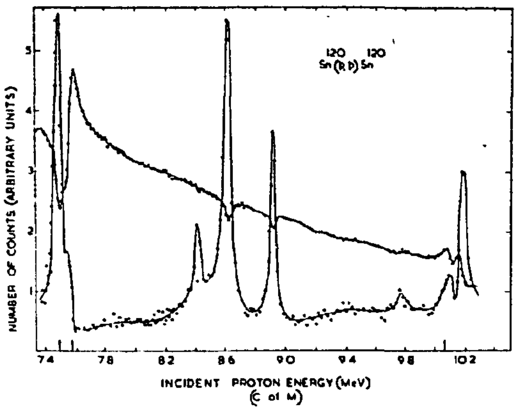

Fig. 26. Excitation functions for proton elastic scattering and proton inelastic scattering to the 2^+ first excited state of ^{120}Sn. The arrows indicate energies at which resonances were observed in the reaction ^{120}Sn(p,p')^{120}Sn*(3^-,2.39 MeV).

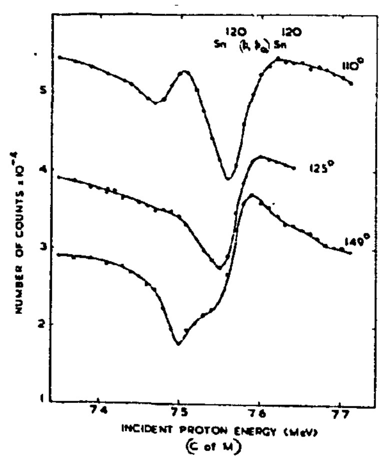

Fig. 27. Excitation functions for the elastic scattering of protons by ^{120}Sn.

(75) Davisson C. M. and Evans R. D. Rev. Mod. Phys. 24, 79 (1952).

(76) Schneid E. J., Prakash A. and Cohen B. L. (To be published).

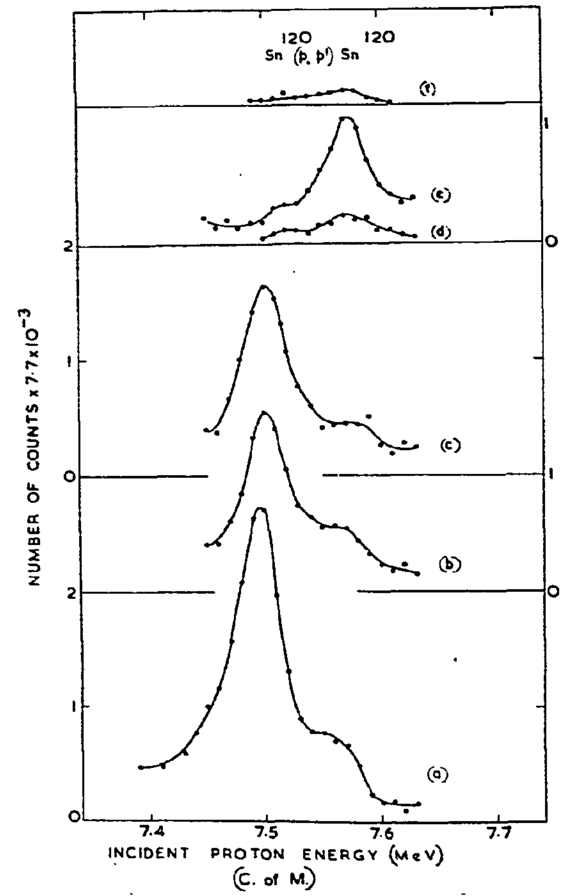

Fig. 28. Excitation functions for the inelastic scattering of protons from ^{120}Sn leading to the following states of ^{120}Sn: a) 2^+, 1.17 MeV; b) 3^-, 2.39 MeV; c) an unresolved triplet of states, 2.83 - 2.96 MeV; d) 0^+, 1.87 MeV; e) 0^+, 2.63 MeV; f) 4^+, 2.18 MeV. The 2^+ excitation curve was measured at 149°; all the others were measured at 110°.

Figs. 27 and 28 show the excitation curves in the region of 7.5 MeV in more detail. The curves for elastic scattering (Fig. 27) clearly show two resonances, the lower of which must be a d-wave resonance since it is not seen at $\theta = 125°$; it is presumably the $d_{3/2}$ ground state of ^{121}Sn[77]. The other resonance is the analogue of the $s_{1/2}$ state of ^{121}Sn lying 50 keV above the ground state. In ^{121}Sn there is also an $h_{11/2}$ state very near this low-lying doublet, but its exact excitation energy is uncertain. The inelastic scattering data (Fig. 28f) indicate that the level is either very weak or degenerate with the $s_{1/2}$ level.

One interesting feature of the ^{120}Sn data is that very few of the resonances correspond to a single particle plus excited core configuration. In the ^{118}Sn + p work, many such resonances were observed[78] whereas, in ^{120}Sn + p, only three resonances at 8.40, 8.92 and 9.78 MeV are observed and all three correspond to a single particle coupled to the ^{120}Sn core excited to the 2^+ state. No resonances were seen which could be attributed to a single particle coupled to the 3^- state of ^{120}Sn. (See also Reference[79]).

Decay of isobaric analogue states to highly excited states of ^{118}Sn (D. L. Allan)

In addition to the experiments reported previously[78,80] in which isobaric analogue resonances were observed in proton elastic and inelastic scattering to the ground and first two excited states of ^{118}Sn (at 1.23 MeV (2^+) and 2.32 MeV (3^-) excitation energy), excitation curves for proton inelastic scattering to about 20 levels in ^{118}Sn with excitation energies between 2.32 MeV and 5 MeV have now been taken. Because of the high density of levels in this range of excitation energy, a charged particle magnetic spectrograph with nuclear photographic plates in the focal plane was used in these measurements. Preliminary results have already been reported[81,82]. As previously, the scattering angle was 90°.

Fig. 29 (overleaf) shows examples of three such excitation curves for levels in ^{118}Sn at excitation energies 3.42, 3.56 and 3.89 MeV, where the numbers 8, 10, 13 refer to the numbers of the proton groups in the spectra shown in References[81,82]. It can be seen that group 10 undergoes very large resonances at 9.98 and 10.28 MeV, group 13 undergoes a strong resonance (actually two closely-spaced resonances) at 10.96 MeV, while group 8 exhibits six strong resonances in the range of incident proton energies

(77) Nuclear Data Sheets, National Academy of Science, National Research Council, Washington 25, D.C.

(78) Allan D. L., Jones G. A., Morrison G. C., Taylor R. B. and Weinberg R. B. Phys. Letters 17, 56 (1965).

(79) Allan D. L., Jones G. A., Taylor R. B. and Weinberg R. B. Phys. Letters 21, 197 (1965).

(80) Allan D. L., Jones G. A., Morrison G. C., Taylor R. B. and Weinberg R. B. Nuclear Physics Division Progress Report, AERE - PR/NP9, 25 (1966).

(81) Allan D. L. Phys. Letters 14, 311 (1965).

(82) Allan D. L. Nuclear Physics Division Progress Report, AERE - PR/NP8, 27 (1965).

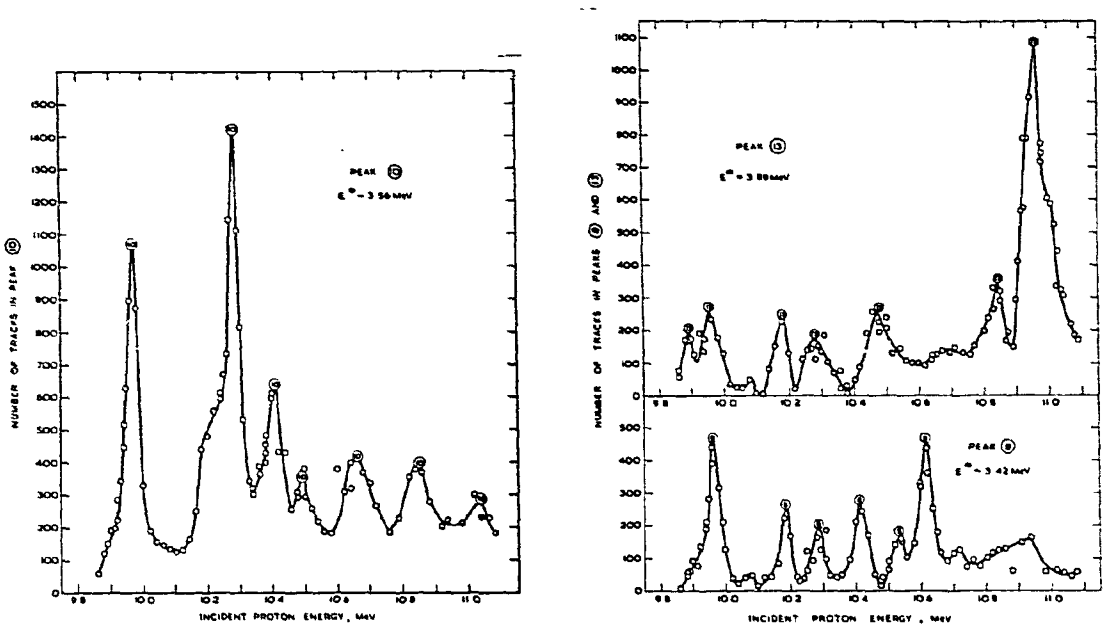

Fig. 29. Excitation curves for the reaction $^{118}Sn(p,p')^{118}Sn^*$ to states of ^{118}Sn at excitation energies 3.42, 3.56 and 3.89 MeV.

represented. Fig. 30a brings together the results for all the excitation curves on the same relative intensity scale; the actual excitation curves are omitted here, only the peaks of each resonance are represented by a symbol giving the reference number (or letter) of each particle group plotted at the appropriate relative intensity (ordinate) and incident energy (abscissa). It can be seen that most of these symbols are clustered around a few discrete vertical lines indicating that the same resonances were observed through many different decay channels. In addition to the results obtained with the magnetic spectrograph, Fig. 30a shows also the relative intensities of the inelastic scattering to the 2^+ and 3^- levels(78,80) reduced by factors of 3 and 5 respectively. The short thick lines near the abscissa scale of Fig. 30a indicate the incident proton energies at which one expects to observe analogues of levels in ^{119}Sn. These energies were obtained by adding the incident energy at which the analogue of the ground state of ^{119}Sn is observed (7.34 MeV(80)) to the excitation energies of ^{119}Sn levels observed(83) in the $^{118}Sn(d,p)^{119}Sn$ reaction. It will be seen that in several cases the expected position corresponds quite closely to the observed position of a resonance. However, there are cases where a ^{119}Sn level observed in the (d,p) reaction is not associated with an analogue resonance and, conversely, there are cases (e.g. the resonance at 10.78 MeV observed through groups 14, 15, 20) where a resonance is observed but no corresponding level was observed in the $^{118}Sn(d,p)^{119}Sn$ reaction. This can be explained by the fact that the levels most strongly excited in the $^{118}Sn(d,p)^{119}Sn$ reaction have configurations with simple connections with the ^{118}Sn ground state configuration, whereas levels with little of the ground state configuration are likely to be missed. This is not the case with $^{118}Sn(p,p')^{118}Sn^*$ reactions; strong resonances can occur when an analogue of a ^{119}Sn level is excited whose configuration has a simple connection with either the (initial) ground state (^{118}Sn) or with the (final) excited state ($^{118}Sn^*$). One may suppose that levels 14, 15, 20 (excitation energy 4-5 MeV) contain little of the ^{118}Sn ground state whereas level 10, whose resonances correspond closely to several ^{119}Sn analogues, is simply related to the ^{118}Sn ground state.

It was originally hoped that comparisons of the energies at which different ^{118}Sn levels resonated would permit conclusions to be made about their configurations. A glance at Fig. 30a shows that such

(83) Allan D. L. (Unpublished, 1965).

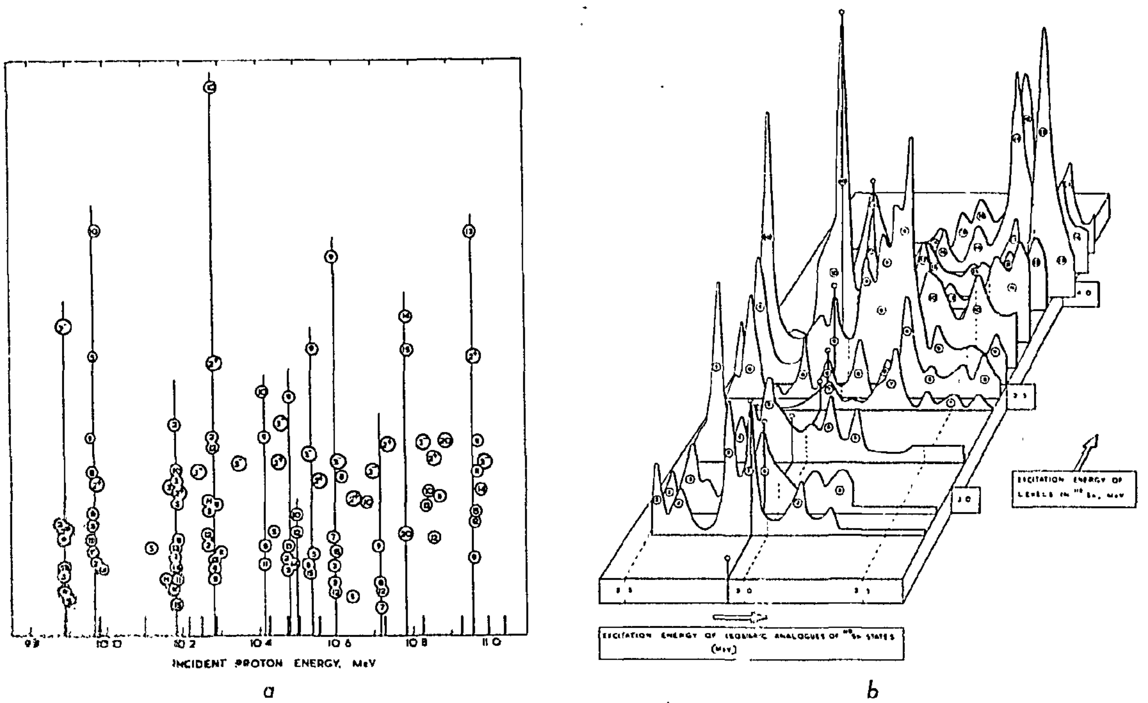

Fig. 30. Analogue state resonances; a) the peaks of each resonance in the excitation curves (e.g. Fig. 29) are plotted on the same relative scale. Vertical lines represent analogue states; short thick lines near abscissa indicate excitation energies of levels in ^{119}Sn plus 7.31 MeV. b) the excitation curves are arranged in accordance with excitation energy of the analogue relative to ground state analogue, and also with respect to the excitation energy of the final state in ^{118}Sn.

relationships are far from simple. The situation is further complicated by the fact that some of the resonances represented by single vertical lines in Fig. 30a are actually unresolved doublets (i.e. analogue state doublets).

Fig. 30b shows the excitation functions plotted with respect to the excitation energies in both ^{118}Sn and ^{119}Sn (= incident energy minus 7.34 MeV). As noted earlier(81,82), there is a tendency for the strongest resonances to occur at roughly similar excitation energies in ^{118}Sn and ^{119}Sn (note: the strongest resonances of levels I and H (excitation energies in ^{118}Sn, 1.74 and 2.03 MeV) and of level 20 (5 MeV) lie off this diagram to the left and to the right, respectively).

Isobaric analogue states observed in the $^{90}Zr(p,p')^{90}Zr$ reaction (G. A. Jones, G. C. Morrison and R. B. Taylor)

The inelastic scattering of protons on ^{90}Zr has been studied in the energy region 6 MeV to 8.7 MeV. The cross sections were obtained by two methods: (a) the measurement of the 2.3 MeV γ-ray from the 5^- (0.8 sec) isomeric level in ^{90}Zr and (b) by directly observing the inelastic proton groups corresponding to 4 levels in ^{90}Zr using a solid state counter. A total of 20 resonances were seen of which 8 were observed to populate the 5^- level in ^{90}Zr either by proton emission directly to this level (1 resonance) or proton emission followed by a γ-ray (7 resonances). The resonances appearing in the 0^+ (1st excited state) and 2^+ (2nd excited state) inelastic channels agree with those seen in the elastic scattering cross section curve measured at Florida State University.

A comparison of these resonances, which correspond to levels in ^{91}Nb and the low-lying levels in the isobaric nucleus ^{91}Zr, shows that (a) the resonances seen in the 0^+ and 2^+ inelastic channels agree very well with the known levels in ^{91}Zr and account for all the known levels; (b) the resonances observed in the 5^- and $(3^-,4^-)$ channels have no corresponding analogue level in ^{91}Zr. This is to be expected as the resonances observed in the high spin inelastic channels are almost certainly due to 2 particle 1 hole analogue states which are difficult to excite in the isobaric nucleus by the (d,p) reaction. If the number of 2 particle 1 hole states is calculated, and we assume that we see only those which decay by emitting a proton with $\ell < 3$, then we expect a total [illegible] resonances in the 5^- and ($4^-,3^-$) channels combined. The face that seven are observed shows reasonable agreement. The extra resonance can be explained as being due either to a more complicated configuration or to a state decaying by emitting an $\ell = 4$ proton.

The results indicate that a more careful investigation of the low-lying levels of ^{91}Zr is needed to find these 2 particle 1 hole states whose analogues are observed as resonances in the ^{91}Nb compound system.

$^{56}Fe(d,d')^{56}Fe$ at $E_d = 11.5$ MeV (R. K. Jolly and A. K. Sen Gupta)

It has been suggested[84] that (t,p) and (d,d') reactions at intermediate bombarding energies lead to the excitation of similar configurations in the residual nucleus. Detailed analyses of the $^{54}Fe(t,p)^{56}Fe$ reaction leading to spin and parity assignments to several states in ^{56}Fe have been completed recently by Cohen and Middleton[85], so it is interesting to compare this information with that obtained from $^{56}Fe(d,d')^{56}Fe$ studies. A detailed correlation of cross sections for the same states excited in the two reactions can be used to understand the nature of states excited in either reaction. Furthermore, detailed shell model calculations of the states in ^{56}Fe are in progress at Oak Ridge National Laboratory[86] so that one will be able to make use of the microscopic form factors inferred from these studies in DWBA calculations of inelastic deuteron scattering cross sections.

An isotopically pure target of ^{56}Fe (1 mg/cm^2) was bombarded by an 11.5 MeV deuteron beam from the tandem generator and the reaction products were analysed with a magnetic spectrograph. Nine energy levels in ^{56}Fe with excitation energies up to 3.90 MeV have been observed with an energy resolution of ~ 20 keV. Angular distributions at 5° intervals have been measured from 20° to 135°. Some preliminary DWBA calculations have been done using a very early version of the ORNL code 'JULIE'.

DWBA calculations and the 3.12 MeV state in ^{60}Ni (A. K. Sen Gupta and R. K. Jolly)

DWBA calculations have been very successful in predicting the shapes and magnitudes of the differential cross sections for the excitation of collective quadrupole and octupole states in even-even spherical nuclei observed via inelastic scattering. It is believed that less strongly excited states (e.g. one particle-one hole excitations) that are reached via a single-step angular momentum transfer process (frequently called single excitations) may also be described equally successfully by DWBA calculations. On this basis, a spin and parity of 3^- was assigned to the 3.12 MeV level in ^{60}Ni from earlier (d,d') reaction studies[87] by one of us (R. K. Jolly).

Recently some controversy has arisen because studies of the $^{61}Ni(d,t)^{60}Ni$ reaction[88] and compound nucleus inelastic proton scattering[89] indicate that the 3.12 MeV level should be assigned spin and parity 2^+. This apparent disagreement gives rise to two questions:

(1) Whether or not there exist two close levels around 3.12 MeV in ^{60}Ni;

(2) *for non-collective* single excitations, whether or not DWBA analyses are reliable enough to predict spins and parities.

---

(84) Cohen B. L. (Private communication).

(85) Cohen B. L. and Middleton R. (To be published).

(86) McGrory J. and Drisko R. M. (Private communication).

(87) Jolly R. K. Phys. Rev. 139, B318 (1965).

(88) Fulmer R. H. and Daehnick W. W. Phys. Rev. 139, B579 (1965).

(89) Mohindra R. K. and Van Patter D. M. Phys. Rev. 139, B274 (1965).

To provide an answer to these questions, we are extending the earlier (d,d′) work[87] using the improved energy resolution ($\approx$ 20 keV) attainable with the magnetic spectrograph at 11.5 MeV bombarding energy. Using a 2 cm position sensitive detector, preliminary studies have been made of the 3.12 MeV group and the collective 2^+ and 3^- groups. A detailed elastic scattering angular distribution has also been measured to provide the optical potential parameters needed for DWBA calculations.

Nuclear lifetimes by the Doppler shift attenuation method (W. M. Currie and C. H. Johnson)

The standard method for determining nuclear lifetimes by the Doppler shift attenuation effect is to record two γ-ray spectra, one with the detector at a forward angle and the other with the detector at a backward angle. To avoid systematic errors which are likely to arise from gain changes in the photomultiplier, it is generally necessary to stabilize with respect to the photopeak of some additional γ-ray group provided by a radioactive source. This reference γ-ray group is recognised by means of β-γ or γ-γ coincidences, and it is suppressed in the final γ-ray spectra.

An alternative method is to use two targets in tandem, the first target having no backing while the second is provided with a backing to stop the recoil ions. Provided the γ-rays can always be uniquely associated with one or other of the targets, a detector placed at 0° will yield two peaks: one fully shifted and one which has suffered an attenuated shift. The separation between these two peaks will be smaller than that achieved by the standard method but, to compensate for this, the counts may be accumulated more rapidly. Also, any given change will affect both peaks in the same way and therefore, provided the gain changes are small, no stabilization should be necessary.

Fig. 31a (overleaf) shows our arrangement for measurements with two targets. The first target is unbacked and does not reduce the beam energy significantly, while the second target has a metal backing appropriate to the measurement being made. The α-particles (or protons etc.) emitted in the reaction are detected in the two annular counters, each of which can detect particles from one target only. These counters can be placed at angles of nearly 0° (as shown) or of nearly 180° to the beam direction if desired. The 3 in. × 3 in. NaI(Tl) detector is placed at 0°, just beyond the Faraday cup.

Measurements of lifetimes in ^{24}Mg are in progress, and other measurements using a 29 cc Ge(Li) detector are planned. In the case of ^{24}Mg, the reaction $^{12}C(^{16}O,\alpha)^{24}Mg$ was used. The first excited state has a well known lifetime which was used to test of the method. Fig. 31b shows fully and partially shifted peaks for the 1.37 MeV γ-ray when the second target had an aluminium backing. The observed separation is in agreement with the known value of the lifetime. Preliminary results have also been obtained for the 4.23 MeV level, and higher lying levels are being examined.

Energy loss of heavy ions in matter (B. H. Armitage and B. W. Hooton)

Measurements have been made of the charge state fractions of sulphur ions traversing gold (i.e. the fraction of sulphur ions with charges 7^+, 8^+, 9^+ etc.) and it has been found that the root mean square charge (Z_r) derived from the measurements differs from the effective charge (Z_e) derived from the relation

$$Z_e^2 = (dE/dX)_S/(dE/dX)_p \quad ,$$

where $(dE/dX)_S$ and $(dE/dX)_p$ represent the energy loss of sulphur ions and protons moving with the same velocity in the same stopping material. Values of $(dE/dX)_S$ were obtained from our own measurements[90] and the $(dE/dX)_p$ data were obtained from Whaling[91].

The results of the charge state fraction measurements made with the broad range magnetic spectrograph are shown in Fig. 32 (overleaf), and the derived values of Z_r for 20 and 30 MeV sulphur

---

(90) Nuclear Physics Division Progress Report, AERE - PR/NP9, p.27 (1966).

(91) Whaling W. Handbuch der Physik 34, 193 (1958).

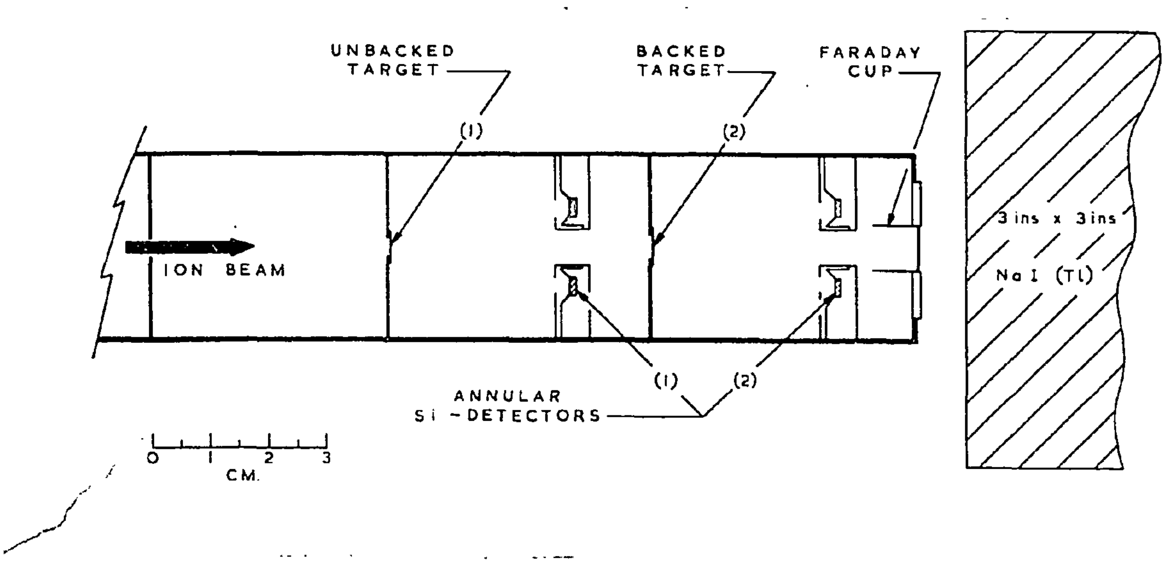

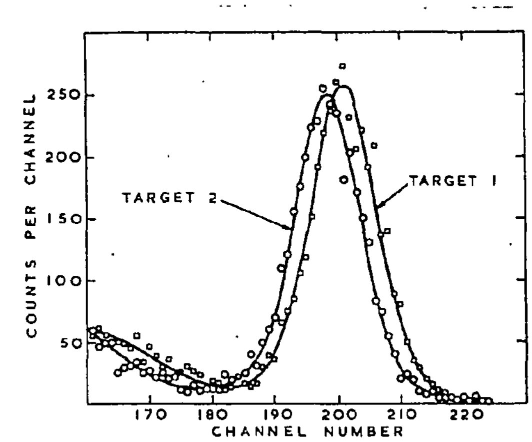

Fig. 31. See: nuclear lifetimes by Doppler shift attenuation method - previous page. Above: experimental arrangement for Doppler shift attenuation measurements. The fully shifted γ-rays from target 1 are measured in coincidence with particle counter 1 and the partially shifted γ-rays from target 2 in coincidence with counter 2; (left) fully (target 1) and partially (target 2) shifted photo-peaks for the 1.37 MeV state in ^{24}Mg excited in the reaction $^{12}C(^{16}O,\alpha)^{24}Mg$.

* * * * * *

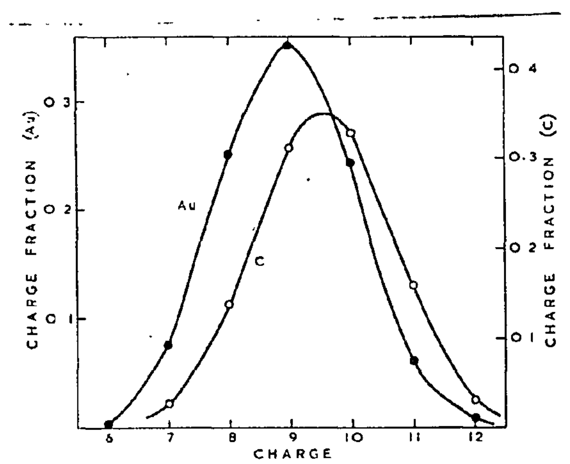

Fig. 32. Charge distribution of 20 MeV sulphur ions in carbon and gold.

ions in gold are given in Table VI. A significant difference is observed between Z_r and Z_e at both energies. This result is in agreement with Booth and Grant[92] who found that Z_r was consistently greater than Z_e for 10-35 MeV chlorine ions traversing gold and aluminium stopping foils.

Booth and Grant[92] observed that the rms charge of oxygen ions was higher in a carbon foil than in a gold one. We have been able to confirm this result with measurements made with 14 MeV oxygen ions. Also, our measurements with 20 and 30 MeV sulphur ions in carbon and gold show a similar dependence of the rms charge on the stopping material. On the other hand, Booth and Grant found that Z_r for chlorine ions in aluminium and gold were almost equal.

(92) Booth W. and Grant I. S. Nuclear Physics 63, 481 (1965).

TABLE VI

Root mean square charges (Z_r) and effective charges (Z_e) for sulphur ions

	20 MeV	30 MeV
	Gold foil	Gold foil
Ze	8.40 ± 0.23	9.53 ± 0.27
Zr	9.2 ± 0.1	10.1 ± 0.1
Z_r/Z_e	1.10 ± 0.03	1.06 ± 0.03
	Carbon foil	Carbon foil
Z_r	9.7 ± 0.1	10.6 ± 0.1

It thus appears that an accurate theory of energy loss will have to take into account variations of electron capture and loss cross sections with the Z of the stopping material.

This work is now being prepared for publication.

45 MeV ELECTRON LINEAR ACCELERATOR

(Nuclear Physics - II and Nuclear Photo-effect: E. R. Rae, N. J. Pattenden)

Energy spectra of photoneutrons from heavy nuclei (D. B. McConnell, B. H. Patrick and E. M. Bowey)

A new series of experiments has been started on the 45 MeV linear accelerator in which the yield of photoneutrons from nuclei with A > 50 is observed for average excitation energies of 25 MeV and 30 MeV, i.e. at energies considerably above the peak of the giant resonance. As is well known, no structure is observed under these conditions due to the high level density. The main component of the yield curve has a statistical origin and this has given rise to the term "nuclear temperature" in the theoretical attempts to describe the energy spectrum. The spectrum is a function of the level density in the daughter nucleus and there have been several attempts to predict the behaviour of the level density as a function of excitation energy and angular momentum[93-96].

In the experiments, the shape of the bremsstrahlung spectrum is first measured for two incident electron energies. This is done by measuring the neutron yield from deuterium by the heavy water - ordinary water difference technique. Figs. 33 a,b (overleaf) show typical neutron spectra from heavy water and ordinary water due to a bremsstrahlung spectrum whose peak energy was 34 MeV. The difference spectrum, due to the neutrons from deuterium only, is shown in Fig. 33c (also overleaf). The successful removal of all resonance structure arising from the oxygen photoneutrons is a good indication of the stability of the linear accelerator mean electron energy and of the reproducibility of the experimental conditions from run to run. The dip in the spectrum around channel 200 is due to absorption by lead and uranium filters placed in the beam to remove γ-rays. Neutron energies are determined by measuring their time-of-flight along a 12 m flight path. The electron pulse has a full width at half height of 20 nsec and timing channels of 2 nsec are used. Using the known photodisintegration cross section of deuterium, a calculated efficiency for the neutron recoil detector, and applying corrections for the lead

---

(93) Le Couteur K. J. and Lang D. W. Nuclear Physics 13, 32 (1959).

(94) Beard D. B. and McLellan A. Phys. Rev. 131, 2664 (1963).

(95) Gilbert A. and Cameron A. G. W. Can. J. Phys. 43, 1446 (1965).

(96) Matchler G. S. Ph.D. Thesis, Mass. Inst. of Tech., Cambridge, Mass., Feb. 1966.

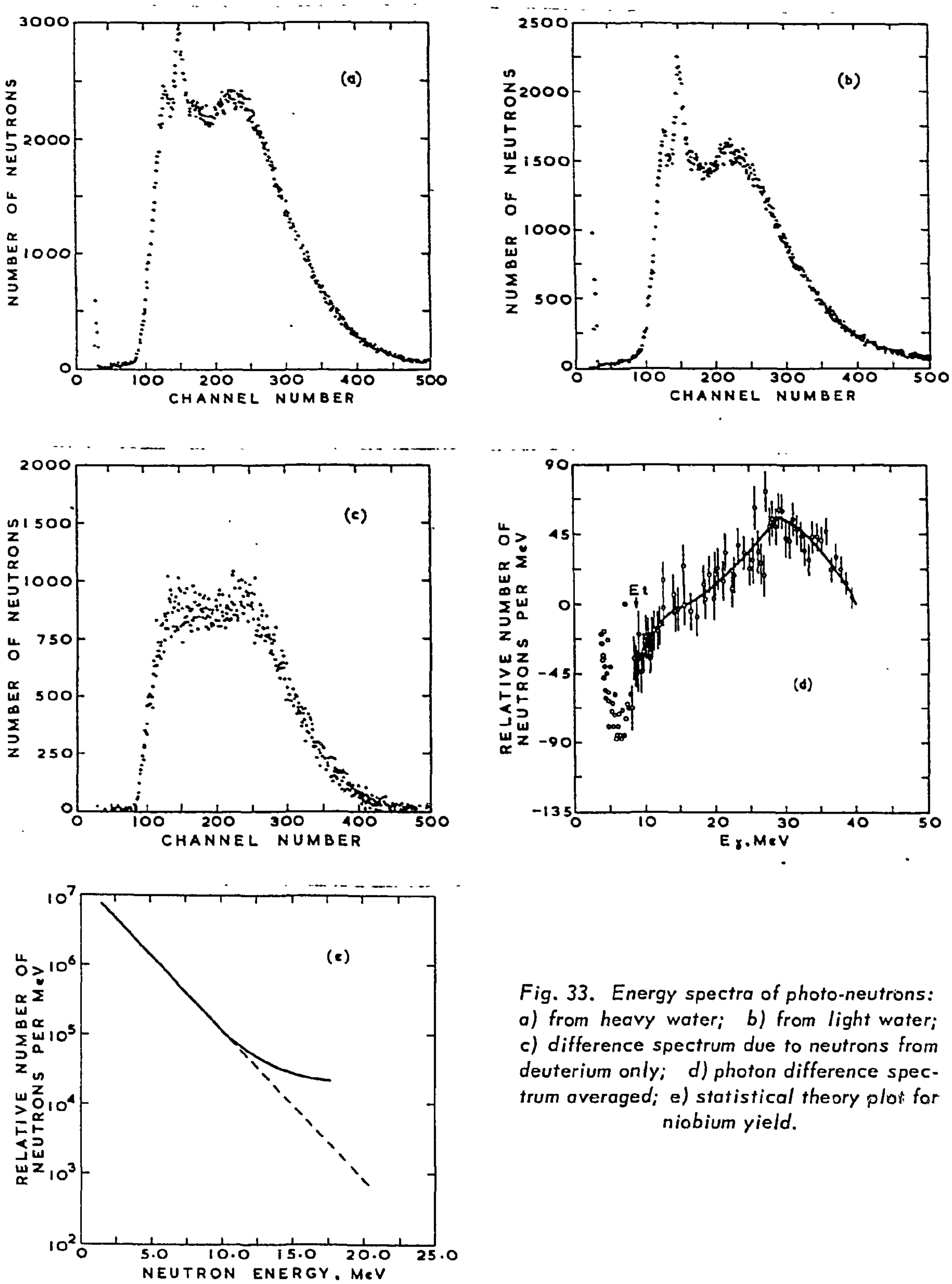

Fig. 33. Energy spectra of photo-neutrons: a) from heavy water; b) from light water; c) difference spectrum due to neutrons from deuterium only; d) photon difference spectrum averaged; e) statistical theory plot for niobium yield.

and uranium filters, the shape of the bremsstrahlung spectrum is obtained. The bremsstrahlung spectra at the two electron energies are subtracted, after suitable normalization, to give an equivalent photon spectrum as shown, for example, in Fig. 33d. Generally, a small negative region exists from the threshhold energy of the element of interest up to ~ 15 MeV. The threshold at 8.8 MeV for niobium is indicated by E_t in Fig. 33d and for each element the normalization is adjusted to make the area of this region small compared to the main positive peak. The errors shown are statistical.

The photoneutron yields from the element being studied are also measured for the two bremsstrahlung spectra. These measurements are performed on a 110 m flight path with 4 nsec timing channels. The yield curves are subtracted using the same normalization as that chosen for the bremsstrahlung spectra. The resulting neutron spectrum is then due to the equivalent photon spectrum, which has a full width at half height of ~ 12 MeV. The elements so far investigated are Fe, As, Nb, In, I and Ta.

Fig. 33e shows the resulting yield curve for niobium, where $N(E_n)dE_n/E_n$ has been plotted as a function of E_n. The curve is nearly linear from 3 MeV to 10 MeV but thereafter it deviates strongly, indicating an increased yield of high energy neutrons.

These results indicate a large "direct" component in the photoneutron spectrum of niobium at excitation energies near 30 MeV. Comparison with the predictions of the statistical model for the "evaporation" spectrum, and of the single-particle model for the direct component, will be made in detail at a later stage after the effects of the choice of normalization factor, energy calibration, and neutron scattering in the target have been fully studied.

50 MeV PROTON LINEAR ACCELERATOR (S.R.C.)

(Proton Physics Group: P. E. Cavanagh)

Analysis of data from the (p,d) reaction on the even isotopes of tin (P. E. Cavanagh and C. F. Coleman)

I - Occupation numbers in the d-shell

The analysis of the (p,d) data has continued. A preliminary determination of the occupation numbers for the $d_{3/2}$ orbit has been made using a method suggested by Cohen[97], in which the sum of the peak (p,d) cross sections for all transitions leading to levels of a given configuration is plotted against the corresponding sum for (d,p) transitions to the same levels, for a series of nuclei. We made the assignment of $d_{3/2}$ for individual levels on the basis of a 'j' dependence of the angular distribution[98] and/or of the $\sigma(p,d)/\sigma(d,p)$ ratios, using the values of Schneid, Prakash and Cohen[99] for the corresponding (d,p) cross sections. If the sum rule given by Yoshida[100] is valid, the points would be expected to lie on a straight line defined by $aU^2 + bV^2 = 1$, where V^2 is the occupation number, U^2 its complement, and a and b are constants. The points shown in Fig. 34 (overleaf) do define such a line reasonably well, suggesting that no important contributions to the $d_{3/2}$ strength have been omitted for any individual nucleus. The intercepts on the two axes give values for a and b, and so enable the occupation number for any nucleus to be determined. The accuracy of the values obtained should not depend to any large extent on the uncertainties involved in the D.W.B.A. calculations of absolute cross sections, but they will be affected by the dependence of the cross sections on the target nucleus mass and on the Q-value of the reaction. These corrections are also obtainable from the D.W.B.A. calculations, but it is hoped that the uncertainties introduced would be less than those arising from an absolute cross section determination. These corrections were not included in the results shown in Fig. 34 (overleaf).

In Fig. 35 (also overleaf) our experimental values for the occupation numbers are plotted as a function of mass number, together with values obtained from the pairing theory calculations of Kisslinger and Sorensen[101], and of Arvieu[102]. In addition, the results of Schneid et al.[99] are plotted with and without Q value corrections. The large discrepancy between our results and those of

---

(97) Cohen B. L. and Price R. E. Phys. Rev. 121, 1441 (1961).

(98) Nuclear Physics Division Progress Report, AERE - PR/NP9, p.29 (1966).

(99) Schneid E. J., Prakash A. and Cohen B. L. (To be published).

(100) Yoshida S. Nuclear Physics 38, 380 (1962).

(101) Kisslinger L. S. and Sorensen R. A. Rev. Mod. Phys. 35, 853 (1963).

(102) Arvieu R. Thesis, Faculty of Science, Paris (Orsay) (1963).

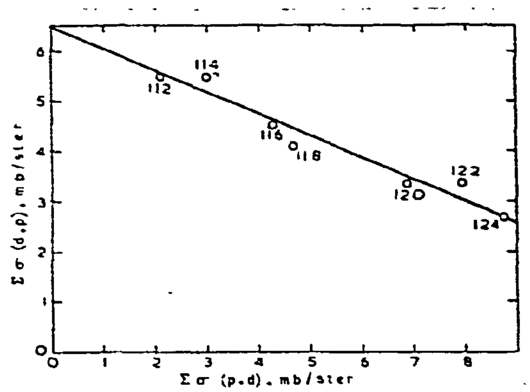

Fig. 34. Cross sections for $d_{3/2}$ levels.

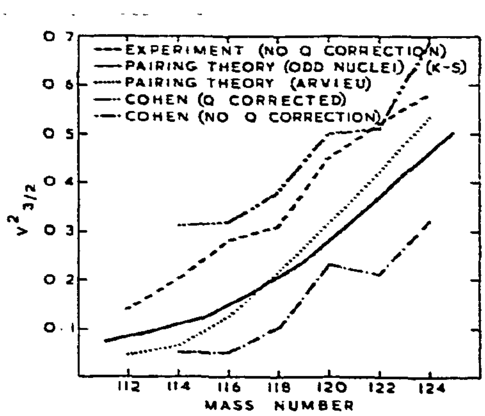

Fig. 35. Occupation numbers as a function of mass numbers.

Schneid et al. (both without corrections) arises because we were able to identify many weak d levels as $d_{3/2}$ which were given $d_{5/2}$ assignments by the above authors. The application of Q-value corrections obtained from conventional D.W.B.A. calculations brings their experimental points up from appreciably below the theoretical curve to a comparable amount above. A similar correction to our data would result in our points lying very far above the theoretical curves.

Single particle energies calculated from quasi-particle energies based on the present $d_{3/2}$ assignments are in much better agreement with theory than the energies derived from the assignments of Schneid et al.[99]

II - D.W.B.A. calculations

Both the $d_{3/2}$ and $d_{5/2}$ data suggest that conventional D.W.B.A. calculations give corrections for the effect of different Q-values on peak differential cross sections which are much too large, and which may even be of the wrong sign. In such calculations the radius parameter for the bound state potential well is arbitrarily kept fixed, and the different Q-values are allowed for by appropriate variations in the well depth. Recently other possibilities have been considered. The view taken here is that variations in the binding energy from the shell model value are brought about by residual interactions which have important short range components. These can be represented as surface interactions, and can be described by adding a variable surface derivative term to the Saxon-Woods potential defining the bound state wave function or, more crudely, by merely varying the radius parameter of the Saxon-Woods potential. We have used this last alternative to account for the range of Q-values spanned by a given configuration.

For these preliminary calculations, a D.W.B.A. programme due to Macefield[103] was used which has no spin-orbit terms and employs a local, zero range interaction. Proton optical model parameters were obtained by fitting the data obtained by Ridley and Turner[104] with a search programme due to Wilmore[105], *in which spin-orbit terms* were omitted. Optical parameters for deuterons were obtained by interpolating and extrapolating the 'deep' well solutions of Perey and Perey[106], fits being obtained also for real radius parameters less than 1.15.

Reasonable fits to the $d_{5/2}$ angular distribution for ^{120}Sn were found for a wide range of the radius parameters for the three real potentials (see Fig. 36), with a range of spectroscopic factors of three to

(103) Macefield B. W. Private communication (1965).

(104) Ridley B. W. and Turner J. F. Nuclear Physics 58, 497 (1964).

(105) Wilmore D. Theoretical Physics Division. (Unpublished).

(106) Perey C. M. and Perey F. G. Phys. Rev. 132, 755 (1963).

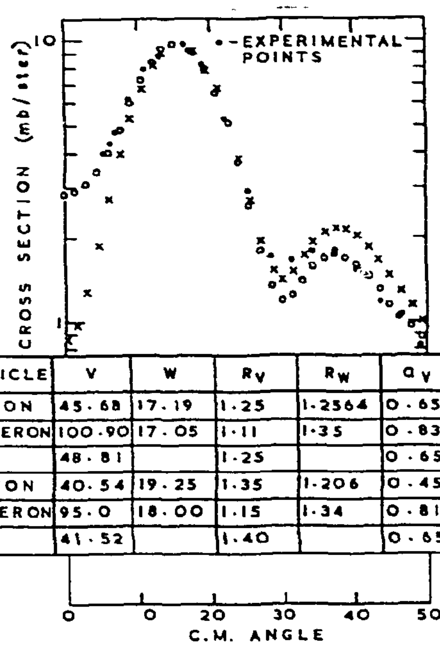

SOLN	PARTICLE	V	W	R_V	R_W	a_V	a_W	S
x	PROTON	45.68	17.19	1.25	1.2564	0.65	0.54	1.03
	DEUTERON	100.90	17.05	1.11	1.35	0.834	0.70	
	B.S.	48.81		1.25		0.65		
o	PROTON	40.54	19.25	1.35	1.206	0.454	0.475	0.46
	DEUTERON	95.0	18.00	1.15	1.34	0.81	0.685	
	B.S.	41.52		1.40		0.65		

Fig. 36. $d_{5/2}$ angular distributions of deuterons from $^{120}Sn(p,d)$.

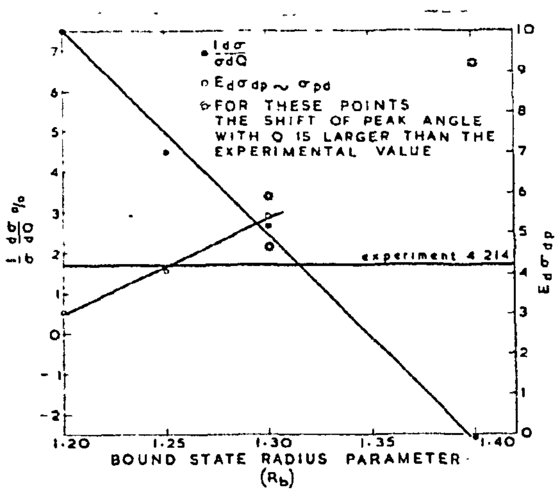

Fig. 37. Calculated peak cross section and Q-variation versus bound state radius parameter.

one. The deuteron optical radius parameter is the main factor controlling the position of the maximum of the angular distribution, though the variation is in the opposite direction to what one might have expected. On the other hand the peak cross section was found to be determined mainly by the bound state radius parameter, as was also its variation with Q. It would be unwise however to generalise from these results.

The peak cross section σ and $(1/\sigma)(d\sigma/dQ)$ are shown in Fig. 37 plotted against the bound state radius parameter, the other radius parameters having been chosen for a reasonable fit. It is possible to eliminate some of the possible combinations by comparison of the shift in the angle of the angular distribution with Q with the experimental value (these are indicated in the Fig. 37).

There is evidence that the $d_{5/2}$ shell is very nearly full[99] for ^{120}Sn; if a range of spectroscopic factors between 80 and 120% is taken to allow for uncertainties due to the omission of spin-orbit terms and of finite range and non-locality corrections from the calculations, we are left with a range of values for the bound state radius parameter between ~ 1.20 and 1.30, a proton radius parameter of 1.25, and a deuteron radius parameter of between 1.07 and 1.15.

The value of $(1/\sigma)(d\sigma/dQ)$ relating to these solutions is (4.5 ± 2.5)% per MeV. The corresponding value from the conventional D.W.B.A. theory, assuming a constant radius parameter, is 14% per MeV. It seems likely therefore that an approach based on a fixed bound state well depth and variable radius parameter may be a more satisfactory one for the particular conditions of shell filling of the tin isotopes. A similar approach is now being made to consider effects due to the variation in isotopic mass.

Optical model research programme: elastic scattering of 30 MeV protons (A. G. Hardacre and J. F. Turner)

Our previously reported elastic scattering data(104) have been supplemented by observations of scattering from ^{112}Sn, ^{114}Sn and ^{124}Sn to provide a set of data for the examination of the isotopic spin component of the optical potential.

These additional observations have been made using the Rutherford Laboratory 180 degree double focusing magnetic spectrometer with sonic spark chamber detection. A limited remeasurement of the scattering from ^{120}Sn made using this equipment is in excellent agreement with respect to angular dependence and absolute magnitude with the earlier observation in which a stack of lithium drifted silicon solid state detectors(104) was used.

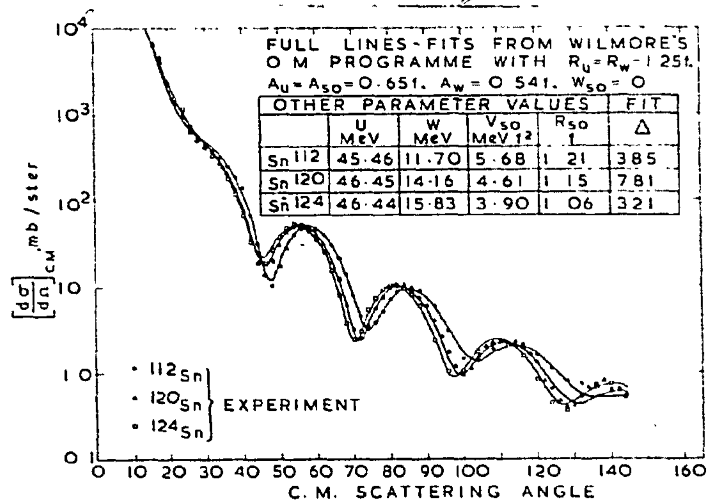

Fig. 38. Elastic scattering of 30 MeV protons from tin isotopes.

The ^{114}Sn data have not yet been analysed. Angular distributions for ^{112}Sn, ^{120}Sn and ^{124}Sn elastic scattering are shown in Fig. 38, where in each case the full lines represent the best fit obtained from Wilmore's optical model search programme using a pure surface absorption term and including a spin-orbit component in the optical potential. Analyses of our earlier data(107) suggest that fits would be improved by the addition of a volume absorption term.

The optical model analysis has not proceeded far enough to provide a measure of the isotopic spin component of the optical potential.

SYNCHROCYCLOTRON

(B. Rose)

Measurement of C_{NN} for p-p scattering at 143, 98 and 73 MeV using a polarized target (T. W. P. Brogden, O. N. Jarvis, J. Orchard-Webb, B. Rose, J. P. Scanlon with M. R. Wigan (University of Oxford))

Results of a preliminary analysis of the data were given in the last Progress Report(108). The detailed multiparameter analysis of the data has now been completed. The major change is in the value

(107) Barrett R. C., Hill A. D. and Hodgson P. E. Nuclear Physics 62, 133 (1965).

(108) Nuclear Physics Division Progress Report, AERE - PR/NP9, p.31 (1966).

of $C_{NN}(90°)$ at 143 MeV, which was previously quoted as 0.91 ± 0.05.

A table of the final results is given below

	Experimental	Predicted	
$[C_{NN}(90°)]_{143\ MeV}$	= 1.00 ± .05	0.97 ± 0.01	Perring
$[C_{NN}(60°)]_{143\ MeV}$	= 0.83 ± .03	0.86	Perring
$[C_{NN}(98\ MeV)/C_{NN}(143\ MeV)]_{90°}$	= 0.69 ± .04		
$[C_{NN}(73\ MeV)/C_{NN}(143\ MeV)]_{90°}$	= 0.25 ± .05		

Radiation damage phenomena in polarized targets (J. Orchard-Webb with M. R. Wigan (University of Oxford))

The decrease in polarization under irradiation of the Harwell polarized proton target has been reported previously[108]. To throw some light on the processes responsible for this reduction in polarization, electron spin resonance (ESR) measurements were made at intervals during a 140 MeV proton irradiation of two Nd-doped L.M.N. crystals. The nuclear counting array used in the measurements of C_{NN} was used to obtain the crystal polarization during each period of irradiation.

The damage to the crystals caused by the 140 MeV protons gave rise to a single well-defined resonance at $g = 2.0054 \pm .0012$, well separated from the $g_{\perp} = 2.72$ of the polarizing Nd centres. The favoured identification for the damage centres is NO_2^{--} [109,110,111]. A measurement of the magnitude of the ESR signal derived from these damage centres showed that less than 10 eV sufficed to form a damage centre. The absolute accuracy of this measurement was severely limited by the non-linearity of the electronics, which were designed merely to monitor the ESR response of a polarized crystal. The ESR data collected are being compared with theoretical models to elucidate the interactions between damage centres, polarizing centres and the crystal that are of importance in the polarizing process.

Polarization and differential cross sections in p-p scattering at 98 MeV (J. P. Scanlon with M. R. Wigan (University of Oxford))

An accurate set of measurements of these quantities comparable with those already reported[112] at 140 MeV is to be made.

The present experiment is being carried out using the same method and counting equipment, the main problem initially being to produce a high quality beam at around 98 MeV energy. Such a beam has now been produced using a polythene energy degrader together with suitable collimation at the point where the initial 143 MeV beam leaves the cyclotron tank. This beam will be used shortly to carry out the polarization measurements.

A liquid hydrogen degrader, which will give the same energy degradation with less multiple scattering of the beam (approx. 0.6° r.m.s. scattering angle), is under construction. This device will be used for the differential cross section measurements, for which purpose it will be placed as close to the scattering target as possible.

---

(109) Bleaney, Haynes and Lewellyn. Nature 179, 140 (1957).

(110) Cunningham J. J. Phys. Chem. 66, 779 (1962).

(111) Pake G. E., Townsend J. and Weissman S. I. Phys. Rev. 85, 682 (1952).

(112) Jarvis O. N., Rose B., Cox G. F., Eaton G. H. and van Zyl C. P. Nuclear Physics Division Progress Report, AERE - PR/NP9, p.33 (1966).

Neutron yield from the high energy proton and deuteron bombardment of lead (D. West and E. Wood)

The yield of neutrons arising in the bombardment of a lead target by protons and deuterons with momenta in the range 0.85 GeV/c to 1.7 GeV/c has been measured using the Birmingham synchrotron. Enriched BF_3 proportional counters were used to measure the thermal neutron distribution in a block of polythene which surrounded the lead target. The dimensions of the target (diameter 10 cm, length 60 cm) were sufficient to contain the great majority of secondary interactions. It was placed at the focus of a beam scattered out of the synchrotron and transported to a remote part of the experimental area in order to reduce backgrounds. The dimensions of the beam profile were 2 cm × 2.3 cm over the region of the target. Beam intensities of about 10^4 particles per burst (100 milliseconds duration) were measured by a pair of scintillators placed in the beam as close to the polythene moderator as possible. Neutron yields were measured relative to that of an Americium-Beryllium neutron source whose intensity is known in terms of the NPL standards to ± 1%. Six channels for neutron counting were used simultaneously with counters placed at radii of 7 cm, 10 cm, 13 cm, 16 cm, 19 cm and 22 cm. Measurements along the axis of the polythene blocks were usually carried out over a length of 140 cm.

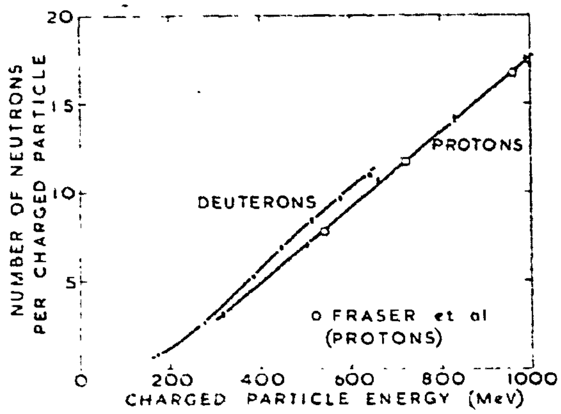

Fig. 39. Neutron yield versus energy for protons and deuterons incident on a lead target, diameter 4 in., length 24 in.

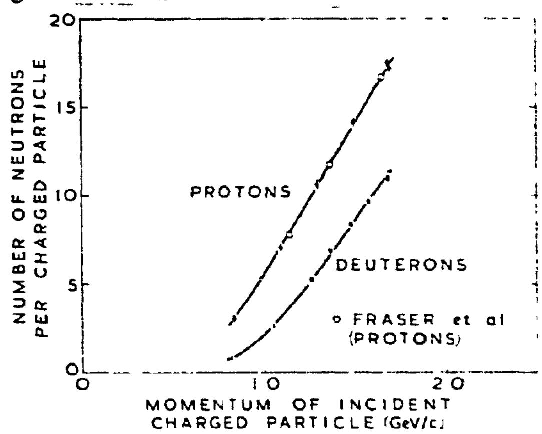

Fig. 40. Neutron yield as a function of momentum of the charged particles.

Our results for protons and deuterons are shown in Fig. 39 together with three measurements (open circles) by Fraser et al.[113] with foils, carried out at Brookhaven using a lead target with the same dimensions as ours. Corrections have been applied to our results for counting losses in the beam detectors (usually about 2%), energy loss along the beam line, mainly in the air and the scintillators (9 to 14 MeV for protons and 14 to 30 MeV for deuterons), neutron backgrounds in the absence of lead (about 0.15 neutrons per incident charged particle independent of particle energy), and neutron leakage into the lead and out of the polythene (total leakage - neutron source, 6.2%; D induced neutrons, 6.8%; p induced neutrons, 6.6%). The errors plotted on the diagram include statistical counting errors and errors arising from the effects of neutron leakage (1%) and background.

The neutron yield from deuterons in the range 300 to 650 MeV is close to that expected on the basis of the most naive of ideas, namely that one more neutron is produced by a deuteron than by a proton of the same energy.

An accelerator with a given magnetic field will be capable of accelerating protons and deuterons to the same momentum and if we wish to consider alternative ions for neutron production we must compare them at the same momentum.

It is therefore also instructive to plot the neutron yields as a function of momentum. This has been done in Fig. 40 where it is apparent that the neutron yield from a deuteron is not more than about ⅔ of that from a proton of the same momentum.

(113) Fraser J. S., Green R. E., Hilborn J. W., Milton J. C. D., Gibson W. A., Cross E. E. and Zucker A. Paper presented at the Annual meeting of the Canadian Association of Physicists, Vancouver B.C. June 10, 1965.

NIMROD EXPERIMENTS
(Synchrocyclotron Group: B. Rose)

Investigation of the decay of the f^0-meson (C. Whitehead and L. Bird in collaboration with groups from Southampton University, University College, London and Rutherford Laboratory)

Since the last progress report further counters have been incorporated into the P3 experiment at the Rutherford Laboratory in order to refine the triggering criterion and this has reduced the number of background triggers to a level compatible with the data handling times.

In recent runs extensive use has been made of the on-line link to the DDP-ORION computer system which is now fully operational in terms of both software and hardware.

In the last run some data were taken and analysis has shown that the geometrical reconstruction of events satisfies the expected criteria and that the kinematical reconstruction, although somewhat less well defined because of low statistics and background events, also shows agreement with the expected performance. Some 45 events consistent with the reaction $\pi^- + p \rightarrow n + \pi^+ + \pi^-$ have been observed in the mass range $\sim$ 1000 MeV to 1500 MeV and further data will be taken to investigate the various angular distributions of events.

NIMROD EXPERIMENTS
(High Energy Physics Group: W. Galbraith)

The decay of long lived neutral K-mesons (K_L^0) into two neutron pions (P. D. Day, W. Galbraith, G. Manning*, A. G. Parham, B. T. Payne, P. H. Sharp and A. C. Sherwood in collaboration with staff of Rutherford Laboratory (RHEL) and C.E.R.N.)

The purpose of this experiment and details of the apparatus have already been given[114]. The data for this experiment were taken at the CERN proton synchrotron machine. A total of over 200,000 spark chamber photographs were obtained, of which some 70,000 correspond to events representing the detection of 4 gamma-rays. Most of these events arise from the normal decay $K_L^0 \rightarrow 3\pi^0$, in which two of the six possible gamma rays have escaped detection. These events constitute the main source of background which might be confused with the two body decay $K_L^0 \rightarrow 2\pi^0$.

In order to obtain some preliminary results, 10% of the photographs have been analysed by hand, including film which contained decays into $2\pi^0$ of the short lived neutral K-meson (K_S^0) regenerated by passing the K_L^0 beam through a carbon absorber. The neutral two pion mode of K_S^0 from regeneration is recognised satisfactorily by our equipment.

Analysis of film to search for the free decay mode $K_L^0 \rightarrow 2\pi^0$ is continuing and further background calculations are being made in a Monte Carlo computer programme which simulates the experiment. The bulk of the film is being analysed on a flying spot CRT machine developed by the Applied Physics Division, R.H.E.L.

---

(114) Nuclear Physics Division Progress Report, PR/NP9, 39 (1966).

*Now at Rutherford Laboratory, S.R.C., Chilton.

MISCELLANEOUS STUDIES IN PHYSICS

Mössbauer effect (T. E. Cranshaw, M. S. Ridout, G. Lang, C. E. Johnson (S.S.P.), P. T. O. Reivari (attached), R. Preston (attached) and A. P. Jain (T.R.A.))

I - The study of Fe Si alloys

Our analysis of the Mössbauer spectra of Fe Si alloys[115] has taken a step forward with the recognition that the Si atoms are not randomly distributed. A repulsive force between Si atoms which forbids the occurrence of Si-Si nearest neighbour pairs seems to account for the observations.

We find that the hyperfine fields at 1st, 2nd and 3rd neighbours of a Si atom are reduced by 7.7, 0.0 and 2.2% respectively. These values seem to account well for the N.M.R. spectra of Fe Si alloys[116], but only the Mössbauer measurements are able to assign the satellite lines to the appropriate neighbour shells.

We have measured the effect of a Si atom on distant Fe atoms (further than 3rd neighbours) by studying the concentration dependence of the hyperfine field and the isomer shift at atoms which have no 1st, 2nd or 3rd neighbour Si atom. The effect on the hyperfine field at distant atoms has the opposite sign to the effect at first neighbours, whereas the isomer shift has the same sign. Thus the radial dependences of the isomer shift and the hyperfine field, or charge density and spin density are different.

II - The study of absorbers with ultrasonic vibration

The splitting of a Mössbauer line by frequency modulation was demonstrated by Ruby et al.[117] In the present work the occurrence of equally spaced sidebands has been used to study the linearity of the apparatus and to obtain a calibration in terms of frequency directly. This information combined with our measurement of the ^{57}Fe hyperfine structure spectrum allows us to determine the ratio μ_1/μ_0 for the excited and ground states of ^{57}Fe. We found this ratio to be 1.710 ± .003, which may be compared with 1.715 ± 0.004 and 1.7135 ± 0.0015 found by Preston et al.[118] and Perlow et al.[119] The frequency found for the ground state splitting is 45.48 ± .04 Mc/s. The frequency found by N.M.R. methods is 45.46 Mc/s[120] showing that the hyperfind fields in domain walls and bulk iron are the same within experimental error.

A sample spectrum is shown in Fig. 41. The relative intensity of the nth satellite line given by a simple theory[121] is $J_n^2\,(x_0/\lambda)$, where x_0 is the vibration amplitude and $2\pi\lambda$ is the wavelength of emitted radiation. The observed intensities do not agree with this theory, and the discrepancy is not yet completely understood.

III - Hyperfine field of ^{57}Fe in hemin

Hemin is an iron-containing compound made by removing the protein molecule from haemoglobin. It is therefore a convenient model compound, the study of which may be helpful in understanding the more complex haemoglobin. Previous work led to the surprising conclusion that the iron in hemin has a hyperfine field very small compared with that in haemoglobin compounds.

---

(115) Nuclear Physics Division Progress Report, AERE - PR/NP7, p.39 (1964).

(116) Rubinstein M. Private communication.

(117) Ruby S. and Bolef, D. Phys. Rev. Letters 5, 5 (1960).

(118) Preston R. S., Hanna S. S. and Heberle J. Phys. Rev. 128, 2207 (1962).

(119) Perlow G. J., Johnson C. E. and Marshall W. Phys. Rev. 140, A875 (1965).

(120) Listner J. O. and Benedek G. B. J. Appl. Phys. 34, 688 (1963).

(121) Abragam A. Comp. rend. 250, 4334 (1960).

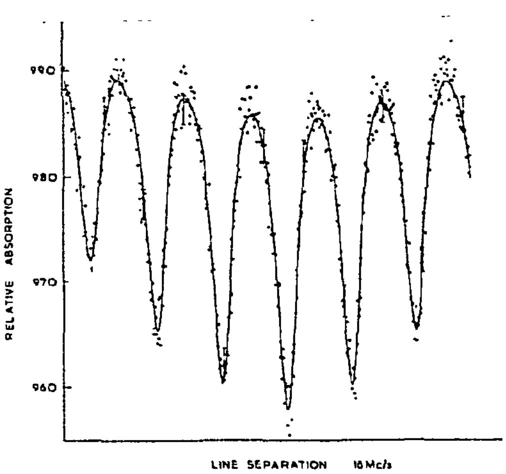

Fig. 41. Frequency modulated spectrum.

We have measured the hyperfine field of ^{57}Fe in hemin with the Mössbauer effect by magnetizing the specimen in large magnetic fields (30 kG) at low temperatures 1.5-4.2°K). The saturation value of the hyperfine field was found to be 480 kG, and the quadrupole splitting was found to be + 0.80 mm/sec. These values disagree with those suggested by earlier work but are close to those found for haemoglobin fluoride HiF(122), which also is in a high spin ($s = \frac{5}{2}$) ferric state. The main difference between the behaviour of the iron in the two compounds therefore seems to arise from the shorter relaxation times in hemin due to the closer iron-iron separations.

Radio pulses associated with extensive cosmic-ray air showers (W. N. Charman, J. H. Fruin, J. V. Jelley (A.E.R.E.), F. Graham-Smith and R. A. Porter (Jodrell Bank, University of Manchester))

As described in the last Progress Report(123), attempts have been made to observe radio pulses from showers at an elevation ~ 15°, following general ideas discussed by N. A. Porter, J. V. Jelley(124) and S. Colgate(125). Various light receivers were therefore set up to detect the showers, these receivers being fully automated with servo-control of the single channel counting rates. It was soon found that at this elevation the genuine shower rate was so low as to be exceeded by the effect of muons in the relatively thick windows of the large photomultipliers; the use of the 'wide-field' light receivers with the 17.5 cm diameter cathodes and the single 150 cm diameter searchlight had therefore to be abandoned. Two 90 cm diameter searchlights were then set up as a coincidence system with 12.5 cm diameter phototubes, to give an acceptance cone of 0.05 steradians centred on an azimuth of 270° and an elevation of 15°. At this elevation, on nights of good low angle sky transparency, the detector counted showers at a rate ~ 0.2 min^{-1}. The radio emissions were detected with a large rhombic antenna(126) designed to have a main lobe with a maximum at an elevation of 12° and a width in azimuth ~ 20°. A bandwidth of 4 Mc/s was used, centred on 45 Mc/s.

Even though the experiment was hampered by exceptionally bad weather, by interference from the nearby electric railway, and by a high susceptibility to other sources of interference, probably associated with the exposed nature of the rhombic antenna, enough information was obtained to suggest that radio emission can be observed from showers at low elevation. Oscillographic displays of the radio and light pulses were photographed simultaneously; from these records it was relatively easy to identify and reject events due to flashes from electric trains.

Some preliminary results of an analysis of about 260 events observed on four clear nights are shown in Fig. 42 (overleaf). The histogram of Fig. 42(a) shows the result of selecting only the largest bandwidth-limited pulse on each trace and for each ¼ μsec time interval integrating the corresponding

(122) Lang G. and Marshall W. Proc. Phys. Soc. 87, 3 (1966).

(123) Nuclear Physics Division Progress Report, AERE - PR/NP9, p.42 (1966).

(124) Jelley J. V. The Ninth International Conference on Cosmic Rays, Paper EAS 26, London, September (1965).

(125) Colgate S. A. The detection of high energy cosmic ray showers by the combined optical and electromagnetic pulse. Unpublished.

(126) Jasik H. Antenna Engineering, Chapter 4.6, McGraw Hill, New York (1961).

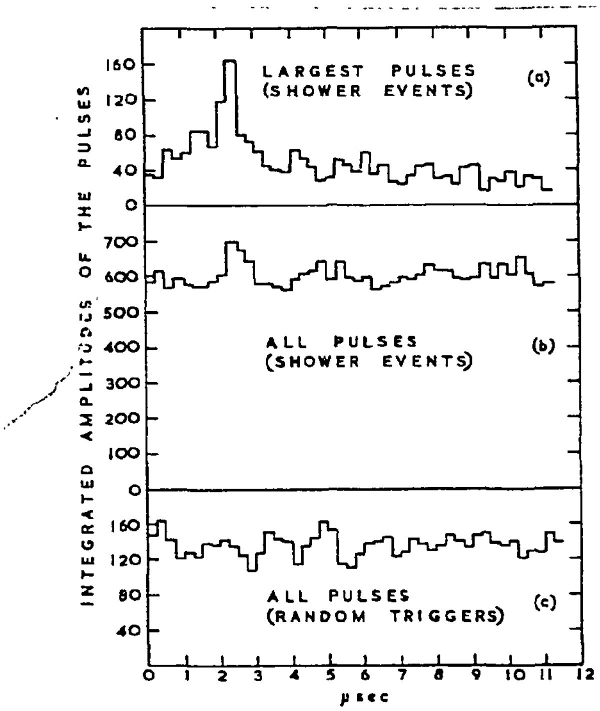

Fig. 42. Histograms of the integrated amplitudes of radio pulses on a 12 μsec time-base triggered by a light receiver.

pulse heights over all traces. By contrast, in Fig. 42(b), the whole of the radio signal on each trace has been taken; while this procedure makes the preferential occurrence of bandwidth-limited pulses at particular positions on the time base rather less noticeable, it does avoid the problem of deciding whether or not a particular pulse is bandwidth-limited. In Fig. 42(c) an analysis similar to that of Fig. 42(b) has been applied to traces obtained by artificial triggering at ½-hour intervals during the observing period. Both Figs. 42(a) and (b) suggest that there is a strong preponderance of radio pulses at a position 2.2 μS along the time base, which on the basis of delay measurements is that expected for radio pulses from showers.

No further experiments are planned in which particle or light detectors will be used to trigger the recording equipment, although it is expected that such devices may still be used to identify radio pulses arising from showers.

A mobile installation using radio only is in the course of design and construction by A.E.R.E. and Jodrell Bank jointly. A multiple coincidence system has been constructed by the Electronics Division. The output from four spaced receivers each equipped with a simple folded dipole, will be displayed on a multi-beam oscilloscope, and the directions from which the radio pulses arrive will be obtained by a timing technique.

A second installation which will also use radio reception only, combined with coincidence techniques, is planned for A.E.R.E. This will operate over a baseline of about 12 km. A search receiver with a wide-band dipole antenna and reflector has been set up at the Chilton site, and the spectrum of background radiation at this site has been scanned over the band 38-88 Mc/s. By day there is prohibitively severe interference from wide-band TV signals but at night the whole band is agreeably clear, with the exception of a narrow-band signal at 75 Mc/s from a local marker beacon, see Fig. 43.

A cooled image intensifier system for astronomical spectroscopy (W. N. Charman, J. H. Fruin, A. V. Hewitt and J. V. Jelley)

A two-week observing session on the Coudé-focus spectrograph of the 20 in. solar telescope at Oxford has given us some astronomical experience. Observations of the H_α and NaD lines in the spectrum of the planet Jupiter were made at a dispersion of 4 mm/Å. No evidence was found of any H_α emission feature associated with a Jovian aurora. A microphotometer analysis of the records yielded much useful information on the astronomical performance of the intensifier system, which was found in general to be in encouraging agreement with that predicted from laboratory tests, and no severe operational difficulties were encountered.

Laboratory measurements of photographic gain, equivalent quantum efficiency, modulation transfer function and other parameters of the system are continuing, and a moving-plate camera to prevent saturation of the recording photographic emulsion is under construction. A programme of measurement of H_γ luminosities of early-type stars(127) is planned for the autumn.

(127) Petrie R. M. Vistas in Astronomy 2, 1346 (1956), Pergamon Press, London.

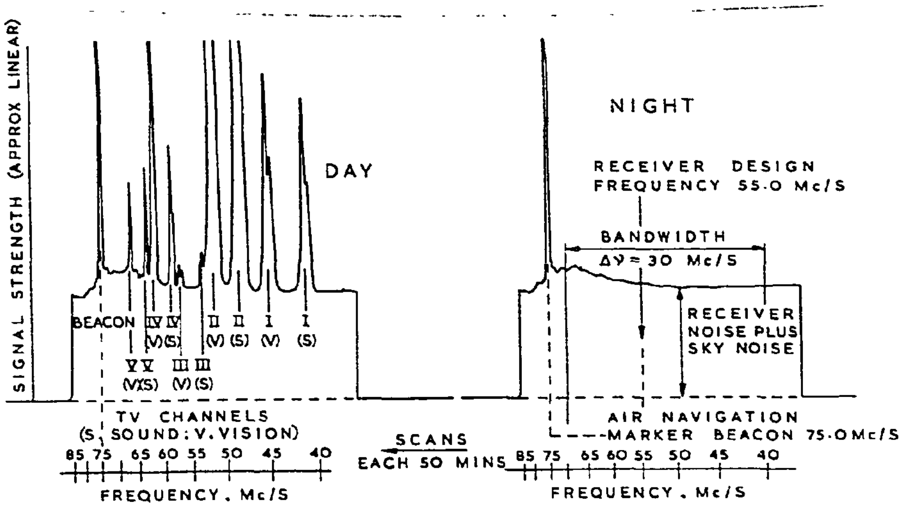

Fig. 43. Day and night scans of the radio spectrum over a band 38-86 Mc/s wide observed at the Chilton (Berkshire) site with westward-looking antenna.

Cherenkov radiation in the atmosphere (W. N. Charman, J. H. Fruin and J. V. Jelley)

U.V. experiments

Work is continuing on the laboratory testing of solar-blind photomultipliers and experiments with the 60 cm mirror system described in the last report.

Absorption of high-energy γ-rays in interstellar and intergalactic space (J. V. Jelley)

The recent discovery[(128)] of a universal microwave radiation field in space has prompted J. V. Jelley[(129)] to consider one particular astrophysical consequence, namely the absorption of high-energy γ-rays by photon-photon pair production. It is found that even over path lengths as short as interstellar distances within the Galaxy this mechanism leads to severe absorption at $\sim 10^{15}$ eV.

MISCELLANEOUS TECHNIQUES

The preparation of lithium-drifted germanium detectors (G. Dearnaley and B. D. Rogers)

During the latter part of 1965 a variety of germanium crystals from suppliers in the U.S.A., U.K., Belgium and France have been tested for the purpose of making large-volume gamma-ray detectors. Results were very variable, but did suggest that British germanium from a 3 in. dia. crystal grown by G.E.C., Wembley, some years ago was very promising. A good lithium ion-drift rate was achieved and the large area obtainable (45 cm^2) makes the drifting of plane slabs, which can be stacked together, a feasible way to achieve detector volumes greater than 100 cm^3. After similarly promising results had been obtained at A.W.R.E. and at Oxford University with this material, steps were taken to interest the group at G.E.C. (now part of A.S.M. Ltd.) in accepting a development contract aimed at improving

---

(128) Penzias A. A. and Wilson R. W. Astrophys. J. 142, 419 (1965), also Roll P. G. and Wilkinson D. T. Phys. Rev. Letters 16, 405.

(129) Jelley J. V. Physical Review Letters 16, 479 (1966), also AERE Report No. R 5121.

germanium for lithium-drifted detectors. It is hoped that A.S.M. Southampton will agree to undertake this work.

The assessment of material using essentially only one set of ion drift equipment proved so lengthy that the decision was made to set up a further five sets, so that several crystals may be drifted simultaneously. A simpler type of thermo-electric temperature control table has been designed, and the array of units should soon be complete.

Staining techniques have revealed that regions of high electric field remain near the n-type electrode of many diodes even after several weeks of drift. A new configuration for the lithium diffusion is shortly to be tried out in which the lithium extends around the edge of the crystal. A masking technique to enable this to be done has been worked out. It is hoped that this structure will render the diodes less sensitive to contamination or adsorption of water during drifting.

The LiCl-KCl eutectic referred to in the last Progress Report[130] as a means of carrying out lithium diffusion has proved very successful in one instance. In other attempts, severe damage (flaking and staining) was caused to the crystal, but a modification to the technique is to be tried out in order to overcome this problem. It is felt that if the method can be perfected it has advantages for both large planar and co-axially drifted detectors.

The preparation of silicon surface-barrier detectors (G. Dearnaley, with M. M. Aslam, Pakistan A.E.C.)

After a hiatus of three years, research is to be undertaken again on this popular form of detector. Several new ideas have developed, and there are problems still to be solved. Attention is focused on (1) methods of protecting the edge of the front contact, where a high surface electric field exists; (2) methods of forming a reliably non-injecting rear contract, by diffusion or by ion-implantation; (3) a neat, simple and effective mounting structure. Discussions with Dr. Aslam have resulted in plans for a new detector preparation procedure.

Ion implantation in semiconductors (G. Dearnaley and M. A. Wilkins)

Studies of the ranges of phosphorus ions injected into silicon crystals are to be made by the technique of forming a surface oxide layer of known thickness, dissolving it, and counting the ^{32}P activity in the sample. A new technique of anodic oxidation has been developed, combining the constant-current forming used by Schmidt and Michel[131], and Davies[132], with the borate anodising solution used by Tannenbaum[133], and Anand[134]. The resulting process combines rapid oxidation with a reproducible thickness of oxide, probably because the voltage is initially low and so does not lead to breakdown while the film is still thin.

The process of ^{32}P precipitation from HF solution, and the preparation of dry samples for automatic beta-counting has been checked, using samples of known relative activities. We are indebted to J. G. Cunninghame and C. Webster of Chemistry Division for their help in this part of the work.

Samples of silicon, cut close to the {110}, plane have been obtained. These will be mounted so as to allow measurements of the ion range at angles close to the principal channel axis in silicon. For annealing specimens after implantation a controlled-temperature furnace has been ordered.

---

(130) Nuclear Physics Division Progress Report, AERE - PR/NP9, p.45 (1966).

(131) Schmidt P. F. and Michel W. J. Electrochem. Soc. 104, 230 (1957).

(132) Davies J. A. et al. Can. J. Phys. 42, 1070 (1964).

(133) Tannenbaum E. Solid-State Electronics 2, 123 (1961).

(134) Anand K. V. Private communication (1965).

Electrical measurements of sheet conductivity in the implanted layer are to be made at successive stages as the layer is stripped away; this is in order to compare the concentration of electrically active phosphorus ions with the total phosphorus content. A four-point probe equipment has been set up and tested, for this purpose.

ACCELERATOR OPERATION AND MAINTENANCE

Cockcroft-Walton 0.5 MV generator (G. A. Jones, F. D. Pilling and E. Sparrow)

		Hours
	Machine experimental hours	640
	Machine experimental hours per week	24
Users:		%
	Nuclear Physics Division	0.3
	Other Harwell Divisions (Chiefly Analytical Chemistry)	71
	Other users (Chiefly Exeter University)	29

3 MeV pulsed Van de Graaff accelerator (D. R. Porter and J. R. Johnson)

Analysis of machine running

	Hours
Running time possible	4020
Time taken by maintenance	1451
Experimental time available	2569
Experimental time taken up	1766

Machine availability = 64%
Experimental usage = 69%

Fault analysis

	Hours lost
Ion source changes and terminal equipment faults	569
Vacuum faults	69
Cooling circuits	80
Electronic faults	85
Control circuits	78
Accelerator tube, charge belt, drive motor and alternator replacement	216
Belt and tube conditioning	169
Fitting of tantalum liners	48
General maintenance	135

The increasing use of helium beams has reduced the average life of ion sources to 200 hours. The reasons for this have been increased wear of the canal and the necessity to fit a new ion source for a helium experiment if the existing ion source had been used on hydrogen or deuterium. Three ion sources fitted with beryllium canals were used with helium but showed no improvement in life over the standard canal with a stainless steel liner.

The accelerator tube was replaced in November by a reconditioned tube. The tube removed had completed 4,888 hours. A subsequent voltage test of the machine without the accelerator tube showed little improvement so a new charge belt was fitted. The belt had been operated for 5,232 hours. Since making these changes the accelerator has spent a considerable proportion of its running time at voltages above 3 MV. Use of the recently installed gas dryer has reduced the humidity of the insulating gas to below 10 parts per million.

Modifications to the cooling system alluded to previously have now been carried out and appear to have reduced the effects of outside temperature fluctuations.

Tantalum liners have been fitted to all accessible parts of the flight tube near the target in order to reduce the radiation background.

5 MV Van de Graaff generator (G. A. Jones, F. D. Pilling and E. Sparrow)

		Hours
	Machine experimental hours	1663
	Machine maintenance and running-in	273
	Machine experimental hours per week	64
Users:		%
	Nuclear Physics Division	43
	Other Harwell Divisions (Chiefly Metallurgy, Analytical Chemistry and Health Physics	51
	Other users (University use)	6

12 MeV tandem generator (J. M. Freeman, P. Humphries and F. D. Pilling)

In the six-month period from November 1965 to April 1966 the tandem experimental running hours have been 2190 of which 81% was used by the Nuclear Physics Division, 7% by other Harwell Divisions (Metallurgy, Chemistry and Solid State Physics) and 12% by Universities (Exeter, Bradford, Cambridge, Manchester and Imperial College). Beams of protons, deuterons, oxygen and sulphur ions have been accelerated and the accelerator tubes have now run for a total of 17,250 hours without signs of deterioration.

About 15% of the available time has been taken up in maintenance and breakdown servicing, the latter through failure of the charge belt motor, for which modification of the bearing housings was required. A change of belt after it had run for 6,754 hours was also required and the foils were changed twice.

45 MeV electron linear accelerator (M. J. Poole, J. R. James and B. Clear)

From 1st November 1965 to 30th April 1966 the accelerator ran for a total of 3050 hours, i.e. 81% of the scheduled operational time and 70% of the time available. For comparison, the corresponding figures for February to October 1965 were 78% and 69%, and for July 1964 to October 1965, 75% and 69%. During the period under consideration, 659 of the hours lost were accounted for by machine faults and 56 hours by experimental requirements. Routine maintenance occupied 554 hours and users outside the Nuclear Physics Division took 40 hours.

Operation into Cells III and IV has been less satisfactory, only 55% of scheduled time being available. A large proportion of the lost time is due to the difficulty of setting up a beam into these cells (cells III and IV operate through a 90° deflection system and are situated at a considerable distance from the accelerator). Some investigation into the cause of this, and into the reason for the low transmission to these cells, has been carried out but no definite conclusion was reached. However, it appears that excessive energy spread, excessive beam divergence and unstable operation due to ripple on the main modulator power lines are all affecting the beam.

During the period, a leak developed in one of the booster target fuel element cans. This section has been removed and a temporary natural uranium target substituted, resulting in a fall in output of a factor 2. Manufacture and testing of new target is expected to be complete by 1st June 1966.

Averaged over the past 24 months, the mean life of type K 352 klystrons has been 3520 hours and that of K 211, 1700 hours. The first K 390 (English Electric 8 MW peak klystron) has been delivered and and is now in the accelerator.

Synchrocyclotron (P. G. Davies)

Analysis of machine running

	Hours	Hours	%	%
Hours in period		4344		100.0
Scheduled maintenance and installation work	1600		36.8	
Holidays and visitors	238		5.5	
	1838		42.3	
Scheduled hours		2506		57.7
Machine not available due to faults and ion source changes	15			0.3
Available hours		2491		57.4

The available hours break down into the following categories:-

	Hours	%
Machine in use	807	32.4
Machine not required	1383	55.5
Machine development work	75	3.0
User setting up	138	5.5
Pumping down the vacuum system	28	1.1
Running up and closing down	60	2.5
	2491	100.0

Machine serviceability was 98.1%

The above analysis is based on a 24 hour scheduled day. In fact, during this period demands for running time were light and running normally did not exceed a fourteen hour day. This partly explains the high ratio of "not required" to "used" time.

Machine users

The following hours were available to individual experimental groups:-

		Hours	%
1.	M. Wigan, J. P. Scanlon (100 MeV p-p)	1228	49.3
2.	Time of flight	454	18.3
3.	Imperial College, London	209	8.4
4.	D. West	72	2.9
5.	Machine development (G. B. Huxtable)	48	1.9
6.	R.C.C. Amersham irradiations	30	1.2
7.	Queen Mary College, London	18	0.7
8.	Time not requested	432	17.3
		2491	100.0

Machine faults

The low running hours in the period again resulted in very few faults.

There were no condenser failures although an opportunity was taken on 1st March 1966 to change the seals while carrying out some modifications to the condenser associated with r.f. tests. The condenser had run for 1200 hours and there was evidence of slight oil leakage.

Some vacuum troubles were experienced in the period due, firstly, to a faulty channel drive which was subsequently modified, and secondly, to an intermittent leak on the Cee stub which caused a number of unexplained failures before discovery.

New shielding wall

The neutron shielding wall at the North end of the pit, mentioned in the previous report, has now been rebuilt. Improved shielding consisting of four feet of steel in the vicinity of the beam paths has been provided and a collimator slot four feet wide and one foot deep has been incorporated.

Re-wiring programme

Some of the wiring on and around the machine is nearly twenty years old and evidence has been found of deterioration of V.I.R. cable. In view of the extension of machine life by the Improvement Project, all old wiring is being inspected and replaced where necessary. This is a long term job and will take up to twelve months to complete.

Liquid hydrogen facilities

These have been improved by enlarging the target testing and filling room and completing the new extraction system. In addition, a compressed air driven jib crane has been installed for lowering hydrogen targets into the stables.

Synchrocyclotron improvement project (P. G. Davies and G. Huxtable)

We have had approval for this project and we plan to close the machine in June 1967 for the improvements to be made. We aim to increase the internal proton beam to 10 microamps at 170 MeV, and to accelerate deuterons to 85 MeV, and to accelerate deuterons to 85 MeV, alpha particles to 170 MeV and ^{3}He ions to 227 MeV. There will be an external beam and we expect the extraction system to have an efficiency of at least 10%. A pulsed neutron beam will be available, and tunnels are being dug to extend the present 27 m flight path to 50 m and 100 m.

In all aspects of this project there is close co-operation with the Engineering Division, who are doing much of the design work and are taking responsibility for most of the construction work.

R.f. system (P. E. Dolley, G. B. Huxtable and W. Spencer)

This is designed to produce a peak voltage of 30 kV at the tip of a dee occupying only 90° of the cyclotron azimuth. The mid-frequency can be set to one of three spot values for acceleration of protons, ^{3}He or alphas and deuterons, and a rotating condenser sweeps the frequency at up to 1600 sweeps per second.

The frequency is selected by opening up varying lengths of re-entrant line inside the inner conductor by means of concentric switches (a, b and c in Fig. 44 (overleaf)).

Protons	24.8 to 20.2 MHz	a, b and c closed
^{3}He ions	16.3 to 14.3 MHz	a, b closed, c open
Deuterons and alpha particles	12.4 to 11.4 MHz	a, b and c open

The resonator is expected to take 25 kW of r.f. power, and an oscillator has been built which should deliver this power easily.

Model tests on the r.f. system have shown that it is satisfactory, and we plan to have it built and ready by next March.

The mechanical design is being done by R. Bint of Engineering Division.

Work associated with r.f. test programme (P. G. Davies)

Engineering support has been provided for G. B. Huxtable in connection with the test programme for the new r.f. system. This work has included:-

(i) Construction of the new oscillator.

(ii) Modifications to the r.f. system model, especially the building of a new condenser model.

(iii) Commissioning of the test resonator and associated H.T. supply transferred from the Variable Energy Cyclotron Group, Rutherford Laboratory.

(iv) Rectification work on the first shorting switch.

New modulator (P. G. Davies and G. B. Huxtable)

A new power supply and modulator to power the r.f. system has been designed and responsibility for building this now rests with the Physics and Electronics Support Group. Work has been done in association with M. J. Lee on detail design.

Ion source (J. P. Scanlon and E. Wood)

The design of the ion source is now being considered. We are thinking about a calutron source capable of producing H, H_2^+, D, ^{3}He and ^{4}He ions. The advantage of such an ion source is that it is capable of producing good beam quality in terms of radial oscillations, thus helping beam extraction if the quality can be maintained during subsequent acceleration.

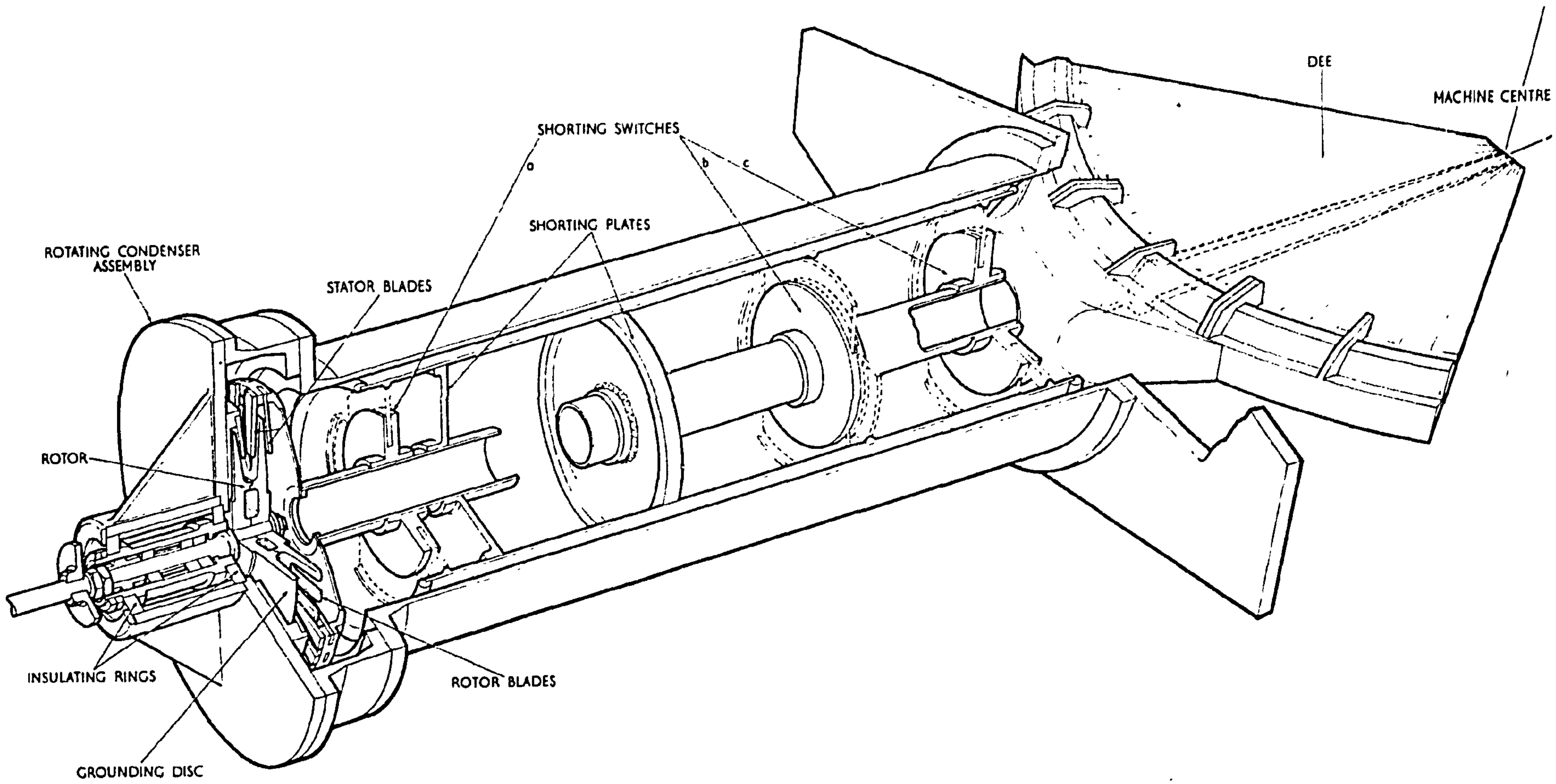

Fig. 44. New dee, line and rotating condenser for synchrocyclotron.

Components are now being manufactured for testing in the existing model magnet, and also for continuing the tests in the cyclotron made previously by P. G. Davies[135]. It is believed that the low bean currents (1/10 μA) obtained previously were due to the fact the ions were only weakly accelerated in their second half-orbit, which prevented them from clearing the ion-source tube. It is hoped that a new system of dee feelers and grid wires will sufficiently increase the accelerating field to avoid this problem which should, in any case, be much less severe when a voltage of 30 kV is available in the improved cyclotron.

The Michigan State University orbit calculation program "Pinwheel" has been modified for use on the A.W.R.E. Stretch computer to obtain details of the initial particle orbits, under various r.f. field conditions.

As it is desired to insert the ion-source axially through a hole in the cyclotron magnet yoke, a test hole will be drilled in the model magnet to study the field disturbance and possible methods of correction.

Programme "Walkabout" (J. P. Scanlon)

When a 90° dee structure is used, the particle orbits, particularly at radii less than 15 in., tend to be displaced from the magnetic centre of the cyclotron, thereby producing radial oscillations. A computer program "Walkabout" is being written to study the displacements of orbit centres and the correction of these with magnetic trim coils. Preliminary estimates indicate that it may not be possible to reduce the radial oscillation amplitude much below 1 inch. These effects have been considered in a slightly different way at CERN[136,137]; the conclusions are similar.

Vertical hole in magnet yoke (P. G. Davies)

Some time has been spent during the period investigating various methods of producing a vertical hole through the magnet yoke to the machine centre. This hole will be used for the ion source in the improved machine. Three methods are being pursued viz: 1) conventional drilling, 2) thermic lancing and 3) plasma cutting. Feasibility studies for all three methods are nearing completion.

Pulsed-neutron equipment (A. Langsford and P. H. Bowen)

In preparation for the synchrocyclotron conversion we have been developing a new system for deflecting the internal proton beam in a single turn to produce a neutron burst. At present the deflection voltage is applied to a pair of electrostatic deflector plates 200 times a second using a spark gap switch. The normal pulse frequency after conversion will be around 1000 p.p.s. with the option of 1400 p.p.s. for high resolution work. At these rates the spark gap switch will be inadequate and we propose to use an 80 kV thyratron switch as a replacement.

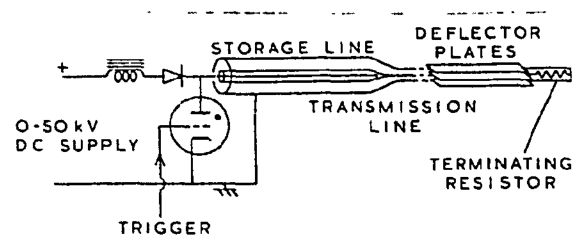

Fig. 45. Schematic diagram of new high voltage deflection system for pulsed neutron work on synchrocyclotron.

Referring to Fig. 45, a storage line is charged to the desired voltage and then discharged by the thyratron. By making the coaxial storage line the first stage of the inner conductor of a coaxial transmission line we share the amplitude of the generated square wave between the two lines. The deflector plates are built into the transmission line and are matched to the impedance of the line. The line is then terminated with a resistive load having the characteristic impedance of the line. Besides

(135) Davies P. G. Nuclear Physics Division Progress Report, AERE - PR/NP9, p.50 (1966).

(136) Kullander S. CERN Report MSC-27/154.

(137) Hedin B. CERN Report MSC-25/193.

being deflected by the electrostatic field, the particles will receive an additional deflection from the magnetic field generated by the current flowing in the plates. The magnetic deflection gives ~ 60% of the total deflection for the 50 Ω system that we are adopting and the consequent reduction in applied voltage will considerably ease insulation problems.

Limited tests of this system have been carried out using a spark gap switch at low frequency. The problem of the terminating resistor, which will have to withstand peak voltages of 40 kV and dissipate up to 3.2 kW, has been solved by using suitably spaced copper electrodes immersed in a copper sulphate solution.

Pulsed neutron beam tunnels (P. G. Davies)

Discussions have been held with New Works Group, Engineering Division, on requirements for the new beam tunnels for use with the improved machine. Designs are now complete and contracts will be placed shortly.

Beam extraction (D. West and T. C. Randle)

Beam extraction from cyclotrons is achieved by inducing the beam to enter a channel in which additional forces, electrostatic and/or electromagnetic, assist in overcoming the effect of the main magnetic field which tends to retain the beam in the machine. We have considered two types of *electrostatic* channel which differ in the principle involved in inducing entry to the channel.

(a) Extraction near $n = 1$ (n is the field index $-\frac{dB}{B}\Big/\frac{dr}{r}$)

The beam escapes from the cyclotron for $n \geqslant 1$ of its own accord. It is merely necessary to ensure that the channel entrance is placed far enough out for the turn-separation of successive orbits to be much greater than the thickness of the septum. The permissible amplitude of radial oscillation is however severely limited. For instance, we have worked out the case for a channel 0.2 in. wide at its entrance, with a septum 0.010 in. thick placed 0.1 in. outside the radius at which $n = 1$. We find only particles having radial oscillation amplitudes up to 0.060 in. would be extracted. One consequence of this is that the extracted beam is very homogeneous in energy, 0.060 in. amplitude of radial oscillation at $n = 1$ corresponds to only 20 keV energy spread. The difficulty of getting the beam past $n = 0.2$ should also be mentioned. Coupling between radial and vertical oscillations requires that the vertical aperture at the radius corresponding to $n = 0.2$ should be twice the maximum amplitude of radial oscillation present. The aperture of the new dee at this radius will permit up to 1.25 in. amplitude of radial oscillation.

(b) Extraction for $n < 1$

The main problem in this case is the small turn-separation, 0.0015 in. when a high duty cycle is used, and the fact that the septum cannot be much thinner than 0.010 in. if it is to withstand the beam. The problem can be overcome by making use of the incoherent radial oscillations present so as to allow a small fraction of the beam to enter the channel at each revolution as its orbit expands. The extraction details depend only slightly on the amount of radial oscillation present. We have worked out the limiting thickness of septum which would just cause all the beam to be lost. Typical values are

$n = 0.44$	Septum thickness for complete loss of beam	0.006 in.
$n = 0.33$	" " " " " " "	0.012 in.
$n = 0.12$	" " " " " " "	0.024 in.

If we take a septum thickness of 0.020 in., for instance, approximately 30% extraction efficiency could be achieved for $n = 0.09$. The energy spread in such a beam would however be about 6 MeV.

The well established regenerative method of beam extraction, in which coherent radial oscillations of the beam ultimately force it into a magnetic channel, typically yields extraction efficiencies of 10% with an energy spread of about 0.5 MeV.

When it became apparent that the expected amplitude of radial oscillation with the modified synchrocyclotron was about one inch, the decision was taken not to use an electrostatic system. The $n = 1$ system would in this case have an extraction efficiency of only 6%. The $n < 1$ system is unattractive because of the large energy spread implied by 1 in. amplitude of radial oscillation. The cost of an electrostatic system is very much greater than the regenerative system and the only point in favour of the $n = 1$ electrostatic system - the narrow energy spread of its extracted beam - was not considered a sufficient justification for the extra expense.

REPORTS, PUBLICATIONS AND CONFERENCE PAPERS

REPORTS

AERE - R 5121	High Energy Gamma Ray Absorption in Space by a 3.5°K Microwave Field. J. V. Jelley.
AERE - R 5142	The Accurate Measurement of the Relative Efficiency of Ge(Li) Gamma-ray Detectors in the Energy Range 500 to 1500 keV. J. M. Freeman and J. G. Jenkin.
AERE - R 5167	Nuclear Bremsstrahlung from 140 MeV Protons. J. A. Edgington (Cambridge) and B. Rose.
AERE - M 1670	Eta and Neutron Cross Sections of ^{235}U from 0.03 to 200 eV. F. D. Brooks, J. E. Jolly, M. G. Schomberg and M. G. Sowerby.

PUBLICATIONS

ALLAN D. L., JONES G. A., TAYLOR R. B. and WEINBERG R. B. Isobaric analogues of the ^{121}Sn ground state triplet. Physics Letters 21, 197 (1966).

ASGHAR M. and BROOKS F. D. Neutron resonance scattering measurements with ^{6}Li glass detectors. Nucl. Instrum. and Methods 39, 68 (1966).

ASGHAR M., CHAFFEY C. M., MOXON M. C., PATTENDEN N. J., RAE E. R. and UTTLEY C. A. The neutron cross sections of thorium and the analysis of the resonances up to 1 keV. Nuclear Physics 76, 196 (1966).

COLVIN D. W. and SOWERBY M. G. Boron pile $\bar{\nu}$ measurements. Physics and Chemistry of Fission, Vol. II, p.25, IAEA, Vienna (1965).

CRANSHAW T. E., JOHNSON C. E. and RIDOUT M. S. The disturbance produce in an iron lattice by Mn atoms. Physics Letters 20, 97 (1966).

DEARNALEY G. and NORTHROP D. C. Semiconductor counters for nuclear radiations. Spon, London 2nd Edition.

EDGINGTON J. A. (Cambridge) and ROSE B. Nuclear bremsstrahlung from p-p and p-d interactions near 140 MeV. Physics Letters 20, 552 (1966).

GALBRAITH W. Pion-nucleon resonances and their effect upon $\pi^{\pm}p$ total cross sections. Proc. Roy. Soc. A.289, 521 (1966).

JARVIS O. N. Analysis of 140 MeV nucleon scattering data for beryllium and carbon. Nuclear Physics 79, 305 (1966).

JARVIS O. N. and COX G. F. Measurement of the absolute differential cross section in proton-proton elastic scattering at 145 MeV. Nuclear Physics 79, 297 (1966).

JARVIS O. N., ROSE B. and TAYLOR A. E. Measurements of proton-nucleus triple scattering parameters near 140 MeV. Nuclear Physics 79, 275 (1966).

JELLEY J. V. High energy gamma ray absorption in space by a 3.5°K microwave field. Physical Review Letters 16, 479 (1966).

LANG G. and MARSHALL W. Mossbauer effect in some haemoglobin compounds. Proc. Phys. Soc. 87, 3 (1966).

LANGSFORD A., BOWEN P. H., COX G. C., HUXTABLE G. B. and RIDDLE R. A. J. A measurement of polarization in neutron-proton scattering in the energy range 20-120 MeV. Nuclear Physics 74, 241 (1965).

LANGSFORD A., DOLLEY P. E. and HUXTABLE G. B. Synchronization of pulses to the phase of a 20 MHz sine wave. Nuclear Instruments and Methods 33, 57 (1965).

MANNING G., PARHAM A. G., JAFAR J. D., Van der RAAY H. B., READING D. H., RYAN D. G., JONES B. D., MALOS J. and LIPMAN N. H. Elastic n-p charge-exchange scattering at 8 GeV/c. Nuovo Cimento X, 40, 167 (1966).

PERLOW G. J., JOHNSON C. E. and MARSHALL W. Mossbauer effect in ^{57}Fe in a cobalt single crystal. Phys. Rev. 140, A875 (1965).

ROSE B. Renormalization of polarization in n-p scattering at medium energies. Physics Letters 20, 86 (1966).

SOWERBY M. G. The ^{10}B(n,α) Branching ratio. J. Nucl. Energy Parts A/B 20, 135 (1966).

IN COURSE OF PUBLICATION

CITRON A., GALBRAITH W., KYCIA T. F., LEONTIC B. A., PHILLIPS R. H., ROUSSET A. and SHARP P. H. Structure in the pion-proton total cross section between 2 and 7 GeV/c. Physical Review.

CRANSHAW T. E., JOHNSON C. E., RIDOUT M. S. and MURRAY G. A. The Mossbauer and N.M.R. spectra of Fe.Si alloys.

FIELDHOUSE P., CULLIFORD E. R., MATHER D. S., COLVIN D. W., MACDONALD R. I. and SOWERBY M. G. Revision of Harwell ^{240}Pu source strength and $\bar{\nu}$ for ^{235}U and ^{252}Cf. J. Nucl. Energy.

DEARNALEY G. Nuclear radiation detection by solid-state devices. Journal of Scientific Instruments.

FREEMAN J. M., JENKIN J. G., MURRAY G. and BURCHAM W. E. ft values of pure Fermi beta decays and the magnitude of the vector coupling constant. Phys. Rev. Letters.

FREEMAN J. M., JENKIN J. G. and MURRAY G. The threshold for the reaction ^{10}B(p,n)^{10}C and the ft values of the superallowed Fermi transition ^{10}C(β^+)^{10}B**. Physics Letters.

JOHNSON C. E. A Mossbauer effect study of the magnetic properties of Fe $Cl_2.2H_2O$. Proc. Phys. Soc. 88.

JOHNSON C. E. Hyperfine field of ^{57}Fe in Hemin. Physics Letters.

LAWERGREN B. The ^{26}Mg(d,n)^{27}Al reactions. Nuclear Physics.

LAWERGREN B. Aluminium 27 and 28. Physics Letters.

SEAMAN G. G., LEACHMAN R. B. and DEARNALEY G. Fluctuation studies of the (α,p) reaction on ^{19}F, ^{23}Na and ^{31}P. Physical Review.

CONFERENCE PAPERS

Invited Papers:

LYNN J. E. Quasi-resonances and the channel theory of neutron-induced fission. Proceedings of the International Conference on the Study of Nuclear Structure with Neutrons. Antwerp 19-23 July 1965, p.125 (1966).

ROSE B. Experimental aspects of nucleon-nucleon scattering and polarization below 1 BeV. Proceedings of the Conference on Intermediate Energy Physics, Williamsburg, Va., February 1966.

Contributed Papers:

Proceedings of the International Conference on the Study of Nuclear Structure with Neutrons, Antwerp, July 1965

LANGSFORD A. High resolution neutron time of flight measurements on sodium and carbon from 0.2 to 140 MeV. Page 529 (1966).

LANGSFORD A. The Harwell 150 MeV synchrocyclotron as an intense pulsed neutron source for nanosecond time of flight studies. Page 562 (1966). (For a list of other papers presented at this Conference see AERE - PR/NP9, p.53).

Proceedings of the Conference on Polarization Phenomena of Nucleons, Karlsruhe, September 1965

JARVIS O. N. Measurement of C_{NN} in 140 MeV p-p scattering using a polarized target.

ROSE B. Measurement of the polarization in n-p scattering in the energy range 20-120 MeV. Page 447 (1966).

Proceedings of the Conference on Intermediate Energy Physics, Williamsburg, Va., February 1966

JARVIS O. N. Measurements of the differential cross section and polarization in proton-proton scattering at 140 MeV.

JARVIS O. N. Measurements of C_{NN} for proton-proton scattering in the 140 MeV region.

Proceedings of the Conference on Isobaric Spin in Nuclear Physics, Tallahassee, March 1966

ALLAN D. L., JONES G. A., MORRISON G. C., TAYLOR R. B. and WEINBERG R. B. Isobaric analogue states of ^{119}Sn and ^{121}Sn. Academic Press Inc. (1966).

Proceedings of DECUS European Seminar, April 1966

BOWEY E. M. and POOLE M. J. FORTRAN programmed output on type 30G display.

BOWEY E. M., AVERY M. R. and McCONNELL D. B. Data analysis systems with the PDP-4 computer in the Neutron Project at Harwell.

Conference on Nuclear Structure and Elementary Particles, Oxford, 30 March-1 April 1966 (The Institute of Physics and the Physical Society)

ALLAN D. L. Decay of analogue states to highly excited states of ^{118}Sn (Paper 54).

ALLAN D. L., JONES G. A., MORRISON G. C., TAYLOR R. B. and WEINBERG R. B. Isobaric analogue states of ^{119}Sn and ^{121}Sn (Paper 55).

ARMITAGE B. H., FERGUSON A. T. G., MONTAGUE J. H. and STARFELT N. Inelastic neutron scattering from ^{235}U (Paper 44).

DEARNALEY G., HOOTON B. W. and JONES G. A. Fluctuations in the $^{31}P(p,\alpha)^{28}Si$ reaction (Paper 59).

EARWAKER L. G. and MONTAGUE J. H. Spin assignments to some levels in ^{11}C (Paper 53).

EDGINGTON J. A. and ROSE B. Measurements of nuclear bremsstrahlung at ~ 140 MeV (Paper 64).

HARDACRE A. G. and TURNER J. F. The isotopic spin term of the nuclear optical potential (Paper 30).

LANGSFORD A., BOWEN P. H., COX G. C., DOLLEY P. E., RIDDLE R. A. J. and SALTMARSH M. J. M. A measurement of the 0° cross section and neutron energy spectrum of the D(p,n)2p reaction with 143.9 MeV and 95.7 MeV protons (Paper 67).

LANGSFORD A. and SALTMARSH M. J. M. Observations of isobaric analogue states by (p,n) reactions in nuclei with mass numbers between A = 27 and A = 238 (Paper 56).

LANGSFORD A. and SALTMARSH M. J. M. Angular distributions of neutrons from $^{7}Li(p,n)^{7}Be$ and $^{9}Be(p,n)^{9}B$ for 94 MeV protons (Paper 66).

LAWERGREN B. Aluminium 27 and 28 (Paper 52).